SYNTHESIS AND EVALUATION OF CATIONIC NANOMICELLES FOR IN VITRO AND IN VIVO GENE DELIVERY

A Dissertation
Submitted to the Graduate Faculty
of the
North Dakota State University
of Agriculture and Applied Science

By

Rhishikesh Subhash Mandke

In Partial Fulfillment of the Requirements
for the Degree of
DOCTOR OF PHILOSOPHY

Major Department:
Pharmaceutical Sciences

April 2012

Fargo, North Dakota

North Dakota State University
Graduate School

Title

Synthesis and evaluation of cationic nanomicelles for in vitro and

in vivo gene delivery

By

Rhishikesh Subhash Mandke

The Supervisory Committee certifies that this ***disquisition*** complies with North Dakota State University's regulations and meets the accepted standards for the degree of

DOCTOR OF PHILOSOPHY

SUPERVISORY COMMITTEE:

Dr. Jagdish Singh

Chair

Dr. Sanku Mallik

Dr. Benedict Law

Dr. Rhonda Magel

Dr. John Ballantyne

Approved by Department Chair:

04/27/2012 — Date

Dr. Jagdish Singh — Signature

ABSTRACT

The goal of proposed study was to contribute towards the development of a nano size, high efficiency and low toxicity non-viral polymeric vector for gene delivery in vitro and in vivo. A series of fatty acid grafted low-molecular-weight chitosan (N-acyl LMWCs) were synthesized, purified and characterized for their physicochemical properties using various analytical techniques such as infrared spectroscopy, elemental analysis and dynamic light scattering. The formulation parameters including pH, sonication duration, and filtration altered the physicochemical characteristics of N-acyl LMWC nanomicelles. The acyl chain length and degree of unsaturation in fatty acids also had an impact on the physicochemical properties and the transfection efficiency of nanomicelles. N-acyl LMWC nanomicelles showed efficient in vitro transfection as visualized and quantified using a reporter plasmid (encoding green fluorescent protein), and therapeutic plasmids (encoding for interleukin-4 and interleukin-10), respectively. The in vitro transfection efficiencies of N-acyl LMWCs with 18:1 and 18:2 grafts (oleic and linoleic acids) were comparable with FuGENE® HD (marketed non-viral vector) but were ~8-fold and 35-fold higher as compared to LMWC and naked DNA, respectively. The in vivo transfection efficiency of N-acyl LMWC to deliver plasmids individually encoding IL-4 and IL-10 as well as a bicistronic plasmid encoding both IL-4 and IL-10 was studied in a multiple, low-dose streptozotocin induced diabetic mouse model. The transfection efficiency of pDNA/N-acyl LMWC polyplexes injected via intramuscular route showed significant improvement ($p<0.05$) over passive (naked DNA) or positive (FuGENE HD) controls. Additionally, a sustained and efficient expression of IL-4 and IL-10 was observed, accompanied by a reduction in interferon-gamma (INF-γ), and tumor necrosis factor-alpha (TNF-α) levels. The pancreas of pDNA/N-acyl LMWC polyplex treated animals exhibited protection from streptozotocin-induced

insulitis and the delivery systems were biocompatible. Histological studies revealed that there were no signs of chronic inflammation at the injection site. The bicistronic plasmid exhibited significantly ($p<0.05$) greater expression of IL-4 and IL-10, and demonstrated the feasibility of bicistronic IL-4/IL-10 plasmid/N-acyl LMWC nanomicelles-based polyplexes as an efficient and biocompatible system for the prevention of autoimmune diabetes.

ACKNOWLEDGEMENTS

Among all the parts of my dissertation, I find acknowledgements to be the most difficult section to write. It's not that I am not grateful to many individuals who have made this journey possible for me. On the contrary, I am indebted by help, support and guidance of so many friends, advisors and family members; that I find it little difficult to name them all in this little section of dissertation. However, this is my feeble attempt to acknowledge some of them here.

First and foremost, I wish to acknowledge my family: my parents, my brother, my in-laws and mostly, my wife, Mayura. They have helped me through this phase of life in every possible way and reaching this milestone would have been impossible without them.

I wish to acknowledge North Dakota State University, for providing me with such a fine environment to study and conduct my research. But more importantly, the University gave me friends. Some of the relationships forged here will last me for this lifetime. I will cherish these fond memories forever.

My sincere thanks go to the Graduate School and Dean Wittrock for the Presidential Fellowship that funded the most of my studies at NDSU. Without this support, it would have been impossible for me to achieve this dream. I also wish to thank National Institutes of Health and the Fraternal Order of Eagles for funding my research.

The College of Pharmacy, Nursing and Allied Sciences, and the Department of Pharmaceutical Sciences will always have a special place in my life. All faculty and staff have been extremely supporting and I know that I will hardly ever meet finer people anywhere in the world. My special thanks go to Janet and Jean, who treated me as a part of their family. I also wish to thank Diana Kowalski from the Library for her help.

Dean Peterson and his staff have always been very friendly and supportive, and I wish to thank them for their help and support.

My graduate advisory committee, Prof. Law, Prof. Magel, Prof. Mallik and Dr. Ballantyne have my heartfelt gratitude. Their expert advice and critical suggestions helped to shape my thought process and were invaluable in my research.

Finally, my sincere thanks go to my major advisor, Prof. Jagdish Singh. He has been my friend, philosopher and guide. Looking back, I realize how big a role he has played in shaping my personality, honing my scientific skills and overall, making me a better person. Over the period of my research at NDSU, he was the one who challenged me when I was being complacent, he was the one who scolded me when I was wrong, he was the one who illuminated my path when I couldn't find the way and he was the one who urged me to walk a few steps more when I was ready to stop. Thank you!

DEDICATION

Dedicated to my parents,

Nilam and Subhash Govind Mandke

and my brother,

Dhananjay

TABLE OF CONTENTS

LIST OF TABLES

LIST OF FIGURES

LIST OF ABBREVIATIONS

% v/v…….Percent volume by volume

% w/v……Percent weight by volume

AAV…….Adeno-associated virus

AFM…….Atomic force microscopy

ANOVA…Analysis of variance

BB…….Biobreeding

CMC…….Critical micellar concentration

CMV…….Cytomegalovirus

DA……Degree of acetylation

DAPI……4',6-diamidino-2-phenylindole

DD……Percent degree of deacetylation

DLS……..Dynamic light scattering

DMSO…..Dimethyl sulphoxide

DNase…..Deoxyribonuclease

DS…….Degree of substitution

EDC……..1-Ethyl-3-(3-dimethylaminopropyl)carbodiimide

ELISA…..Enzyme linked immunosorbant assay

EMEM…..Eagle's minimum essential medium

FBS……Fetal bovine serum

FTIR…….Fourier transform infrared

GAD…….Glutamic acid decarboxylase

GFP……Green fluorescent protein

GPC……..Gel permeation chromatography

H&E……. Hematoxylin-eosin

HEK293…Human embryonic kidney 293

HPLC……High performance liquid chromatography

HRP……..Horseradish peroxidase

i.m…….Intramuscular

i.v……..Intravenous

IACUC…. Institutional animal care and use committee

IDDM…… Insulin dependent diabetes mellitus

IFN-γ…… Interferon-γ

IL-10…….Interleukin-10

IL- 4……..Interleukin-4

IR……. Infrared

LC…….Liquid chromatography

LMWC…. Low molecular weight chitosan

mIL…… Murine interleukin

MLD…….Multiple, low doses

MTT……. 3-(4,5-dimethylthiazol-2-yl)-2, 5-diphenyltetrazolium bromide

Mw……Molecular weight

MWCO….Molecular weight cut-off

N:P ratio…Ratio of nitrogen on the polymer to phosphate groups in DNA

NHS……..N-hydroxysuccinimide

NMR…….Nuclear magnetic resonance

NOD…….Non-obese diabetic

PBS……..Phosphate-buffered saline

pDNA……Plasmid DNA

PEG……..Poly(ethylene glycol)

PEI……Polyethyleneimine

PLA……..Poly(lactic acid)

PLGA……Polylactide-co-glycolide

PLL……..Poly-l-lysine

RI……. Refractive index

RPM…….Revolutions per minute

RT Room temperature

SD…….Standard deviation

SEC……..Size exclusion chromatography

STZ……..Streptozotocin

TAE……..Tris-acetate-ethylenediaminetetraacetic acid

TMB…….3,3',5,5'-Tetramethylbenzidine

TNF-α……Tumor necrosis factor-α

β-gal……..β-galactosidase

1. INTRODUCTION

1.1. Gene Therapy

Gene therapy is defined as the introduction of nucleic acids into cells for the purpose of altering the course of a medical condition or disease (Kay et al., 1997). The idea of inserting a DNA fragment into the cells, where it will be responsible for imparting new functions to the host cell, was first introduced in 1960s (Friedmann, 1992). It represents an exciting field of interest in recent drug delivery, since it is possible to treat/prevent many genetic disorders by simply inserting the correct copy of the defective gene into target cells. It offers multiple opportunities of curing diseases rather than just treating the symptoms of diseases or disorders. Efficient delivery of gene and its subsequent stable expression in vivo is still a major obstacle which needs to be overcome prior to gaining clinical acceptance. Since its inception, gene therapy has progressed steadily and is currently being investigated for treatment of a plethora of conditions. US-FDA has approved two oligonucleotide-based products, namely, Vitravene® (fomvirsen sodium) and Macugen® (Pegaptanib sodium), for treatments of cytomegalovirus (CMV) retinitis and age-related macular degeneration, respectively, while many drug products are in different phases of clinical trials (Sanghvi, 2011). Recent data shows that more than 1500 clinical trials are currently underway in the field of gene therapy as shown in figure 1. A vast majority of these trials target different types of cancers and various viruses are the vectors of choice in these trials. It is interesting to note that more than 60 clinical trials are in the advanced stages (phase III/IV) of completion.

Figure 1 shows the current status of clinical trials in the field of gene therapy distributed according to (A) target diseases, (B) used vectors, (C) phases of clinical trials, and (D) trial locations.

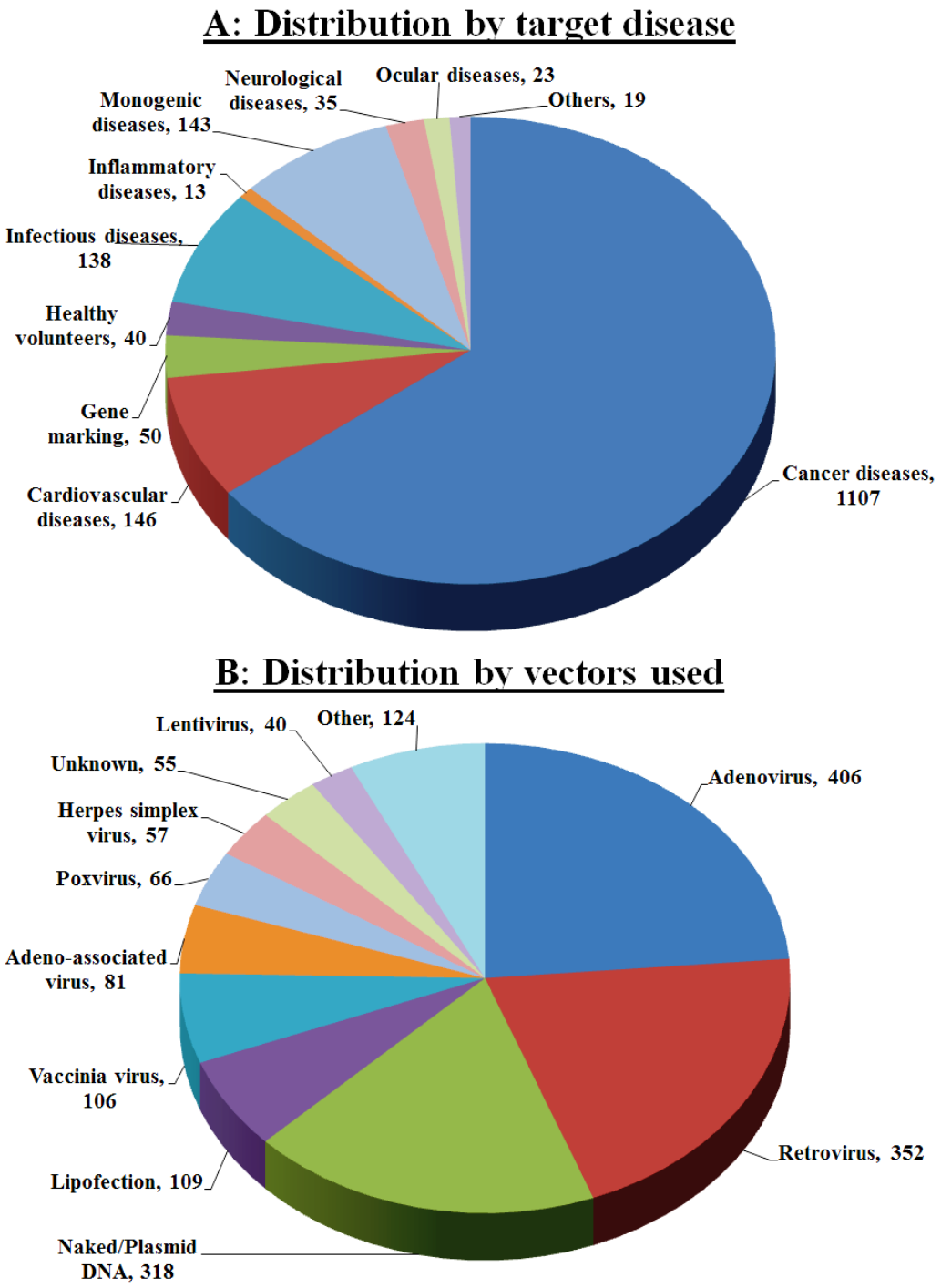

Figure 1(A-B): Current gene therapy trials
(Adapted from J Gene Med 2011, Current as in March 2012, available at http://www.wiley.com//legacy/wileychi/genmed/clinical/)

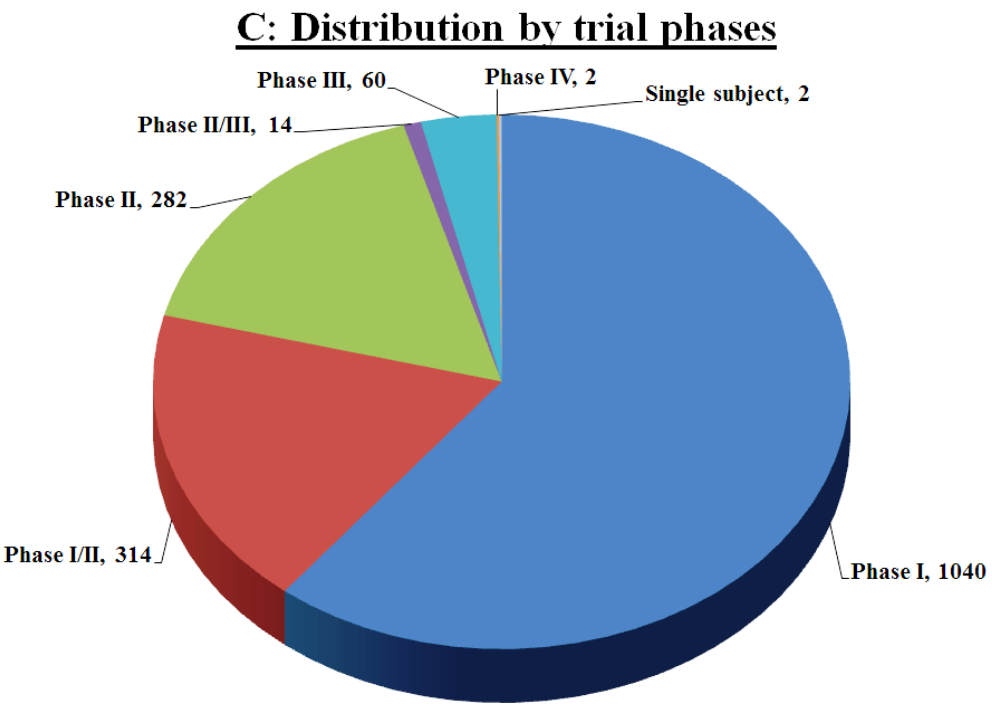

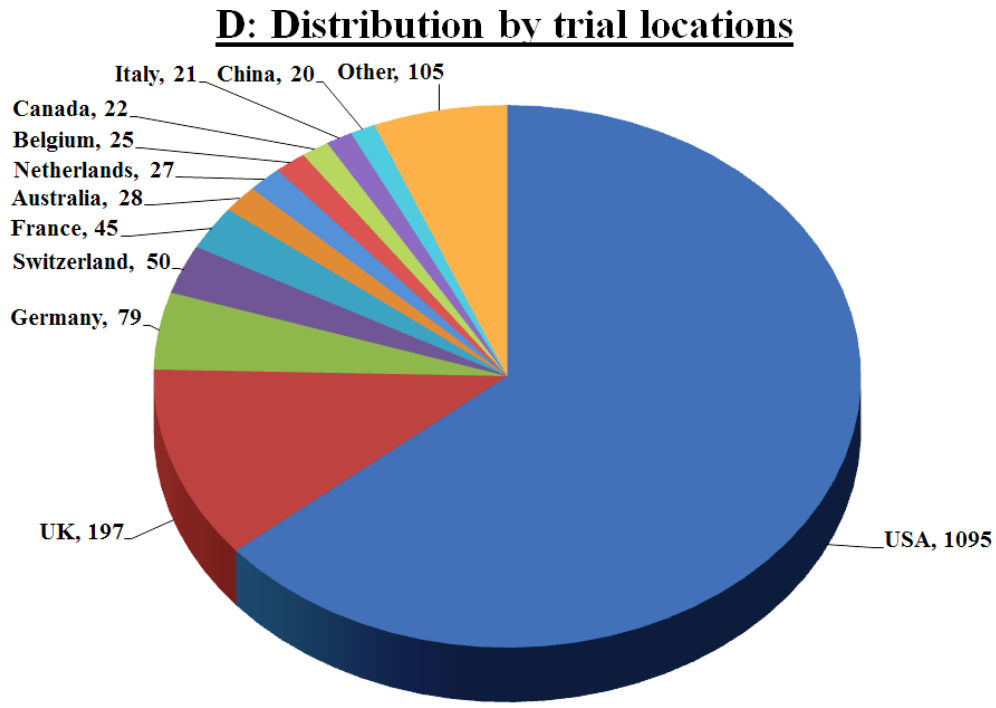

Figure 1(C-D): Current gene therapy trials
(Adapted from J Gene Med 2011, Current as in March 2012, available at http://www.wiley.com//legacy/wileychi/genmed/clinical/)

1.2. Vectors for Gene Therapy

Efficient delivery of gene and its subsequent stable expression in vivo is still a major obstacle which needs to be overcome prior to gaining clinical acceptance. This problem has been succinctly summarized by Dr. Inder Verma as "There are only three problems in gene therapy: delivery, delivery and delivery" (Vivès, 2005). Though naked DNA can be taken up by some cells and tissues during in vitro and in vivo studies, it usually leads to inefficient, transient transfection. Therefore currently, the major strategies to deliver genes of interest are physical insertion and use of various vectors. These vectors are broadly classified as viral vectors and non-viral vectors.

1.2.1. Viral vectors

Viral vectors, as the name suggests, are viruses stripped off their pathogenicity while retaining their ability to transfer and express their genetic cargo efficiently. The viral vectors offer multiple advantages over their non-viral counterparts, including high transfection efficiency, tissue specificity, and genomic integration of delivered genetic material leading to sustained transgene expression. The major types of viral vectors used for gene delivery in clinical trials include adenoviruses, retroviruses and adeno-associated viruses (Figure 1B).

1.2.1.1. Adenoviral vectors

Currently, adenoviral vectors are the most widely used vectors for gene delivery applications in the clinical trials. They offer a critical advantage of delivering double-stranded DNA to the nucleus of the target cells, which can be of dividing or non-dividing nature (Chailertvanitkul and Pouton, 2010). Adenoviruses are non-enveloped viruses containing a double-stranded, linear DNA and are usually associated with relatively mild infections in humans (Smith, 1995). The gene of interest can be inserted in the adenoviral genome after

deleting the E1 gene responsible for virus replication. The main transfection mechanism of adenoviral vectors includes the binding of adenoviral vectors to the extracellular Coxsackie and Adenovirus Receptor (CAR) or CD46, endocytosis into clathrin-coated pits, endosomal escape via the conformational changes and associated partial disassembly of the viral capsid, microtubule-mediated transport to the nucleus and final nuclear binding and uptake of viral DNA by the nucleus (Chailertvanitkul and Pouton, 2010). The adenoviral vectors are usually not integrated into the host genome, but replicate as episomal DNA (Verma and Somia, 1997). The major advantages of adenoviral vectors include their ease of production and ability of episomal DNA transfer to a variety of dividing and non-dividing cells. However, their main disadvantages include a rapid host immune response which can limit the duration of transgene expression and can potentially attenuate the effectiveness of repeat doses, making them unsuitable for treatment of diseases requiring sustained transgene expression (Robbins and Ghivizzani, 1998).

1.2.1.2. Retroviral vectors

Retroviruses are a large class of enveloped viruses in the retroviridae family and contain a single-stranded RNA. Though the application of retroviruses is mostly restricted for non-dividing cells, they offer advantage of integrating the reverse-transcribed viral DNA into the host genome leading to sustained transgene expression (Smith, 1995). The retroviruses are usually not specific for the type of the host cells and usually enter the cells through a cell surface receptor-mediated internalization (Yi et al., 2011). The internalized viral RNA is reverse transcribed into a double-stranded DNA means of the virally encoded pol gene. With the exception of lentiviruses and HIV-1, most of the retroviruses depend upon the disassembly of nuclear envelope during the mitotic processes for the access to nucleus. The double-stranded DNA of the viral origin is then integrated into the host genome in a location-specific (retroviruses) or random

(lentiviruses) manner (Whittaker, 2003). While the retroviruses offer advantages of efficient and sustained transgene expression, they are plagued by concerns about the presence of prooncogenes in viral genome, chances of hostile immune reactions, and insertional mutagenesis (Yi et al., 2011).

1.2.1.3. Adeno-associated viral vectors

Adeno-associated virus (AAV) is a small, non-enveloped virus in the parvoviridae family and contains a single-stranded DNA as its genetic material (During, 1997). It requires a helper virus such as adenovirus or herpes simplex virus for its replication. The cellular entry of the AAV vectors is mediated through cell surface receptors such as heparin sulphate proteoglycan and is enhanced by a variety of co-receptors (Summerford and Samulski, 1998). Post-endocytosis, phospholipase A_2 motif on the N-terminus of the viral VP1 protein is reported to play a major role in its endosomal escape (Daya and Berns, 2008). The nuclear translocation of the viral genome is thought to be mediated using microtubules and the viral replication and sustained expression of transgene depends on the infection by a helper virus (During, 1997). AAV is not associated with any known human infection and offers advantages such as sustained transgene expression in dividing and non-dividing cells, and specific host genomic integration sites. However, its small size and limited payload capacity precludes its application for delivering genes greater than 5.2 kb in size (Robbins and Ghivizzani, 1998).

1.2.2. Non-viral vectors

Due to their several attractive features, non-viral vectors are slowly gaining prominence as the gene delivery vectors of choice for various applications. Though generally these agents are less efficient as compared to their viral counterparts, they offer considerable advantages over viruses. Non-viral vectors are easy to manufacture, generally do not have limitations over their

payload capacity, can be made non-immunogenic, and carry a low risk of insertional mutagenesis (Kay et al., 1997).

The non-viral vectors are broadly classified as physical vectors, which include electroporation, sonoporation, and gene gun, and chemical vectors, which include dendrimers, inorganic nanoparticles, lipoplexes and polyplexes. The physical vectors depend upon the physical insertion of the nucleic acids of interest (usually in the form of a plasmid) directly into the cytosol using electric impulse, ultrasonic waves or small projectiles, while the chemical vectors encapsulate or adsorb the gene of interest and carry it into the host cell (Gao et al., 2007). Each of the non-viral vectors possesses distinct advantages and shortcomings and is discussed below, but the barriers encountered for the non-viral gene delivery essentially remain the same. Figure 2 summarizes the barriers encountered by the chemical non-viral vectors en route to delivery of the genetic cargo to the host cell nucleus (Mandke et al., 2012). The barriers can be enumerated as (1) instability (physical and/or chemical) of the DNA, the vector or the overall delivery systems in the extracellular space due to presence of various charged endogenous molecules and nonspecific nucleases, (2) barriers presented by the cell membrane of the target cell and barriers to the cellular internalization, (3) post-internalization stability of the DNA in the endosomal compartment and subsequent endosomal escape, (4) cytosolic transport of the DNA or the overall delivery system to the nucleus in the presence of cytosolic nucleases, and (5) nuclear entry, localization and expression of the plasmid DNA (Ruponen et al., 2003; Wiethoff and Middaugh, 2003).

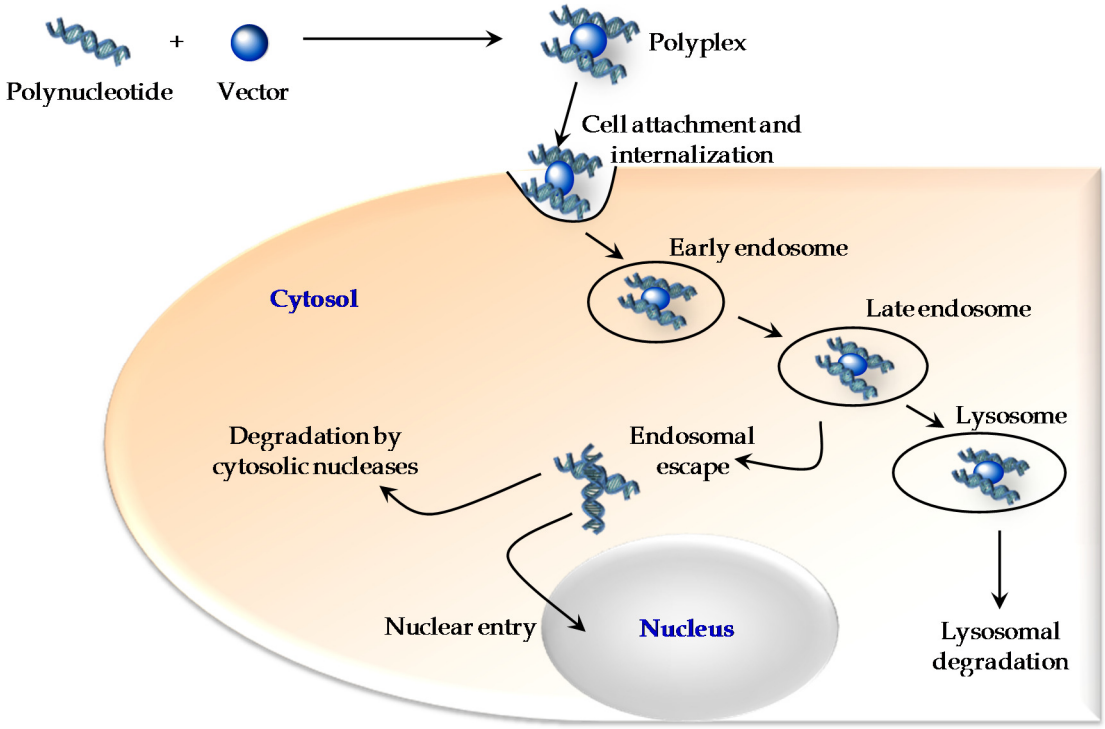

Figure 2: Barriers to the chemical non-viral vector-mediated gene delivery

1.2.2.1. Physical methods for DNA delivery

Electroporation and sonoporation constitute the major physical non-viral methods for DNA delivery into the host cells. Electroporation involves application of high-intensity electric pulses for a short duration to induce a transient permeability in the cell membrane. Such changes in the membrane permeability can be exploited to introduce a large variety of macromolecules in the cells. Over decades, electroporation has been employed to deliver DNA into the cytosol (Medi and Singh, 2008; Wells, 2009). Though initially developed for gene delivery, electroporation has been successfully employed for intracellular delivery of other various moieties for diagnostic and therapeutic applications (Medi and Singh, 2003; Gehl, 2008).

In spite of being a relatively easy and robust method of transfection, the electroporation-mediated transfection efficiency depends on various factors such as length, amplitude and number electric pulse, electrode geometry, type of target tissue, and size of the delivered

plasmid. Moreover, lack of protection for the delivered plasmid renders it susceptible to degradation by intra/extracellular enzymes. Such degradation, combined with requirement of high voltage electric pulses and decreasing transfection with the increase in DNA size constitute major shortcomings of electroporation-mediated gene delivery (Vilquin et al., 2001; Molnar et al., 2004).

Sonoporation is another physical method of DNA delivery, wherein, the target cells are transiently permeabilized using ultrasound to enhance the uptake of various molecules inside the cells. Though the exact mechanism of ultrasound-mediated gene delivery is not completely elucidated, the factors improving the permeability of the target cells are believed to include the reversible pore formation in the cell membranes via the hyperthermia and cavitation effects (Singh and Singh, 1990; Pitt et al., 2004). Various ultrasonically activated gene delivery vectors, including microbubbles and liposomes have been employed for in vitro and in vivo delivery of genes (Koch et al., 2000; Lawrie et al., 2003). However, in absence of chemical vectors or microbubbles, a significant drop in the transfection efficiencies have been observed, which can be attributed to degradation of free nucleic acids due to ultrasound (Peacocke and Pritchard, 1968; Riesz and Kondo, 1992)

1.2.2.2. Lipid-based vectors

Cationic lipids are attractive gene delivery vectors due to various advantages which include ease of fabrication, formulation and reasonably simple transfection methods (Rao and Gopal, 2006). Various cationic lipids have been employed for in vitro and in vivo transfection of mammalian cells. The structures of some representative lipids have been depicted in figure 3. The general structure of cationic lipids has a cationic (amine) head group attached via a linker to aliphatic hydrocarbon chains or other hydrophobic moieties. Depending upon its chemical

structure, these molecules can exist in different structural phases, such as micellar, lamellar or cubic, in an aqueous environment (Wasungu and Hoekstra, 2006). Due to the electrostatic interactions, the cationic lipids spontaneously form complexes with negatively charged DNA and such complexes are termed as lipoplexes. These self-assembling systems can condense the DNA and protect it from degradation by the nucleases and can facilitate endosomal escape of the contenets (Hoekstra et al., 2007).

Cationic lipids can be formulated into liposomes, which, though less efficient than viral vectors, have been increasingly used as non-viral gene delivery agents (figure 1). Various targeting ligands have been employed to impart tissue specificity to the liposomes and studies have shown increased transfection efficiencies by this approach (Guo and Huang, 2011; Nakase et al., 2011). Though various approaches have been employed to improve the efficiency of the liposomes, the question of the delicate balance between the efficiency and toxicity still remains to be addressed (Lappalainen et al., 1994; Tousignant et al., 2000; de la Torre et al., 2009).

1.2.2.3. Polymer-based vectors

DNA, a polynucleotide, is a macromolecule with a high anionic charge density. These properties play an important role in precluding its passage across the biological membranes (Nishikawa et al., 2005). Cationic polymers, via electrostatic interactions, from complexes with DNA (polyplexes), which leads to masking of anionic charge of DNA (facilitating interaction with negatively charged cell membranes), condensation of DNA (improving the hydrodynamic characteristics and protection from nucleases) and endosomal escape. The polyplexes usually have a residual net positive charge, which is critical for their attachment to cell membrane and subsequent cellular uptake (Basarkar and Singh, 2007). Also, most of the cationic polymers used for gene delivery applications have amine groups, which get protonated at acidic pH. When the

polyplex is taken up by the cell into the endosomal compartment, these amine groups get protonated to resist the change in the pH of the endosome and cause the influx of counterions and increase the osmotic load inside the endosomes resulting in endosomal rupture. This phenomenon, known as the 'Proton Sponge' effect was first described by Behr (Behr, 1997). Varieties of natural and synthetic polymers have been known to exhibit this effect and are tried as non-viral vectors with varying degree of success.

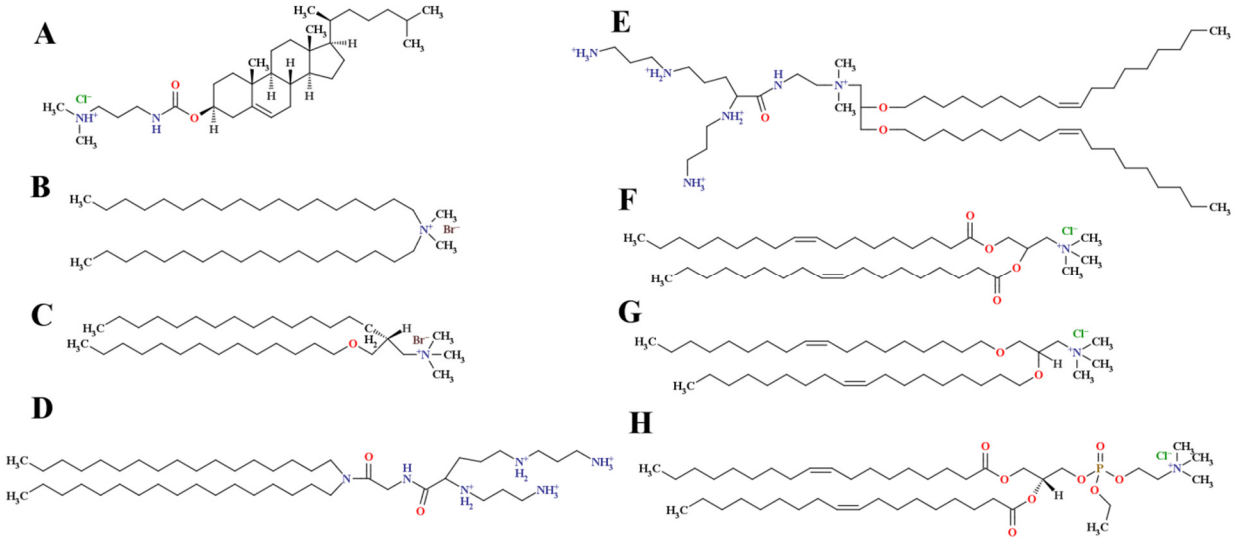

Figure 3: Some of the common cationic lipids used for gene delivery applications (**A**) 3ß-[N-(N',N'-dimethylaminoethane)-carbamoyl]cholesterol hydrochloride (DC-Cholesterol) (**B**) Dimethyldioctadecylammonium (Bromide Salt) (DDAB) (**C**) 1,2-dimystyloxypropyl-3-dimethylhydroxyethylammonium bromide (DMRIE) (**D**) Dioctadecylamido-glycylspermine (DOGS) (**E**) 2,3-dioleoyloxy-N-[2(sperminecarboxamido)ethyl]-N,N-dimethyl-1-propanammonium trifluoroacetate (DOSPA) (**F**) 1,2-dioleoyl-3-trimethylammonium-propane (chloride salt) (DOTAP) (**G**) 1,2-di-O-octadecenyl-3-trimethylammonium propane (chloride salt) (DOTMA) (**H**) 1,2-dioleoyl-sn-glycero-3-ethylphosphocholine (chloride salt) (EPC)

Polyethyleneimine (PEI) is one of the most commonly used cationic polymer and owing to its excellent transfection efficiency, considered as the gold-standard of the non-viral vectors. The transfection efficiency of PEI has been correlated to its various properties such as molecular weight and degree of branching as well as polyplex properties such as N:P ratio and complex size (Thomas et al., 2005). PEI displays a high density of protonable amino groups and

subsequently, excellent buffering ability. It is known to destabilize the endosomes and release the DNA cargo from the polyplexes into the cytosolic compartment, resulting in high transfection efficiencies. PEI, however, is known to be toxic in vitro and in vivo in a dose dependent manner (Moghimi et al., 2005). Various approaches have been tried to build on the excellent transfection efficiency of PEI while reducing its toxicity. Chemical conjugation of PEI with various targeting moieties, steric stabilizers such as polyethylene glycol, and other lipo-polymeric vectors has been reported to improve the toxicological features of PEI (Wang et al., 2010; Yao et al., 2010; Deng et al., 2011; Hashemi et al., 2011).

Poly-l-lysine (PLL) is a cationic, biodegradable polymer synthesized by polymerization of N-carboxyanhydride of lysine (Zhang et al., 2004). PLL is known to condense the DNA into nanoscale polyplexes and promote their cellular uptake. However, its transfection efficiency is lower as compared to PEI, which has been attributed to its inability to destabilize the endolysosomal compartment and subsequent reduction in endosomal escape (Akinc and Langer, 2002). Various conjugation approaches have been successfully tried to improve the transfection efficiency of PLL without compromising its desirable features such biodegradability and high degree of DNA condensation (Zhang et al., 2009b; Sun and Zhang, 2010; Hu et al., 2011; Yu et al., 2011).

Polylactide-co-glycolide (PLGA) and polylactic acid (PLA) are biodegradable polymers extensively studied for delivery of small molecule therapeutics as well as biomolecules (Basarkar et al., 2007; Manoharan and Singh, 2009; Makadia and Siegel, 2011; Tahara et al., 2011; Tran et al., 2012). Structurally, they are polymers consisting of lactic acid and glycolic acid, connected via ester linkages and the physical constructs (such as microparticles and nanospheres) of these polymers exhibit bulk hydrolysis, making them suitable for sustained delivery applications

(Acharya et al., 2010; Makadia and Siegel, 2011). Nanoparticles based on PLGA/PLA have been demonstrated to carry the DNA either entrapped in the polymeric matrix (Ribeiro et al., 2005) or adsorbed on the surface using a cationic surfactant such as E100 (Basarkar et al., 2007), and lead to improved transfection in vitro and in vivo.

1.3. Chitosan as a Non-Viral Gene Delivery Vector

Chitosan is a polysaccharide, comprising of glucosamine and N-acetylglucosamine and is obtained by partial deacetylation of chitin. Chitin (poly (β-(1-4)-N-acetyl-D-glucosamine)) is the structural element in the exoskeleton of crustaceans and fungal cell walls and is estimated to be the second most abundant polymer in the world (Rinaudo, 2006). Chitosan is a generic term applied to chitins which are sufficiently deacetylated to form soluble amine salts. Since the polymerization and deacetylation of chitin are highly variable, chitosan cannot be exactly defined in terms of its chemical composition (Jones and Mawhinney, 2005). The general structure of chitosan is presented in figure 4.

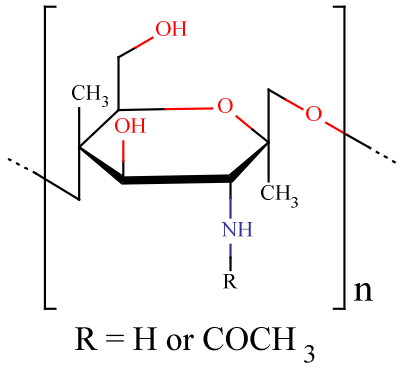

Figure 4: Chemical structure of chitosan

Most of the functional properties of chitosan depend upon its chemical composition, especially its degree of acetylation/deacetylation (DA or DD, respectively), charge distribution and molecular weight. DA, which represents the fraction of acetylated glucosamine moieties (N-

acetylglucosamine), or DD, which represents the fraction of unacetylated glucosamine moieties, are important determinants of the chitosan properties (Rinaudo, 2006). Commercially available chitosan molecular weights can vary from 10,000 to 1,000,000 Da (Jones and Mawhinney, 2005) and play a major role in determining its solubility. Though chitosan is sparingly soluble in water and any other alkaline aqueous solutions above pH 6.5, it is readily soluble in acidic (pH < 6.5) aqueous solutions. This pH dependent solubility of chitosan is widely exploited in its various pharmaceutical applications (Kumar et al., 2004).

Chitosan has a wide range of applications in the diverse fields such as pharmaceutical (Jones and Mawhinney, 2005), food and agriculture (Synowiecki and Al-Khateeb, 2003; Liu et al., 2004), and marine biology (Kurita, 2006). In pharmaceutical industry, chitosan and its derivatives have been used in rapid release (Shiraishi et al., 1990), controlled release (Prabaharan and Mano, 2005; Bhattarai et al., 2006; Colonna et al., 2007), and mucoadhesive formulations (Nafee et al., 2003; Panigrahi et al., 2004), to deliver small molecules (Shiraishi et al., 1990), peptides (Colonna et al., 2007), and genes (Borchard, 2001; Dass and Choong, 2008). Different delivery systems such as films and coats (Panchagnula et al., 2006; Gilhotra and Mishra, 2008), gels (Ganguly and Dash, 2004; Marsich et al., 2008), beads (Dambies et al., 2001), tablets (Nunthanid et al., 2004), microspheres (Genta et al., 1997; Grenha et al., 2007; Ubaidulla et al., 2007), nanospheres (Ding and Xia, 2006; Masotti and Bordi, 2008; Yoksan and Chirachanchai, 2008), and micelles (Zhang et al., 2007; Ye et al., 2008), fabricated using chitosan and its derivatives have been used for these applications.

Chitosan has been extensively studied as a potential gene delivery vector due to its excellent biocompatibility and safety profile with varying degree of success (Mao et al., 2010). At low pH, below its pKa, the primary amines of chitosan backbone are positively charged and

can form complexes with negatively charged DNA by ionic interactions thereby condensing it into small particles and offering protection from DNase I & II degradation (Richardson et al., 1999; Köping-Höggård et al., 2001). The transfection efficiency of chitosan depends on a number of physicochemical properties of chitosan/DNA complexes, such as DNA compaction, size, and zeta potential. These features, in turn, depend on different formulation parameters such as DD, molecular weight, N/P ratio (ratio of positively charged primary amine moieties on chitosan to negatively charged phosphate groups on DNA) and pH of transfection medium (Ishii et al., 2001; Sato et al., 2001; Mao et al., 2010). Moreover, chitosan is amenable to various chemical modifications due to the presence of hydroxyl and amino groups in its structure. These modifications, when carefully controlled, can be used to alter the physical, chemical and biological characteristics of chitosan (Prabaharan, 2008).

The major factors limiting the transfection efficiency of chitosan include its insolubility at physiological pH and its incomplete release of the payload upon reaching the cytosol (Nishimura et al., 1991; Francis Suh and Matthew, 2000; Peng et al., 2009). The insolubility of chitosan has been attributed to microcrystalline domains in the 3-dimensional structure of chitosan due to inter- and intra-molecular hydrogen bonding, while the incomplete release of DNA has been attributed to the high charge density of chitosan backbone. However, this cationic charge density is reported to play an important role in attachment and condensation of negatively charged DNA and its protection from degrading environment. It has been suggested that chitosan, a polyamine with a large number of primary and secondary amine groups, interacts strongly with negatively charged DNA. The strength of these electrostatic interactions as well as insolubility of chitosan at physiological pH have been implicated in incomplete dissociation of

DNA/chitosan polyplexes in the cytosol, thereby reducing its transfection efficiency (MacLaughlin et al., 1998; Kiang et al., 2004).

1.4. Micellar Delivery Systems

Amphiphillic compounds, in a liquid medium, tend to aggregate over a narrow concentration range. Such aggregates, irrespective of their degree of structural organization, are collectively termed as micelles (Martin, 1993). The minimum concentration required to promote the micelle formation in the liquid medium is termed as the 'critical micellar concentration' or CMC. Irrespective of their diverse geometries, micelles exhibit various characteristic properties such as Faraday-Tyndall effect, light scattering, Brownian motion and electrokinetic properties such as electrophoresis and electroosmosis (Bowman et al., 2005). Aqueous dispersions of micelles are routinely used in pharmaceutical formulations to improve the solubility of hydrophobic compounds (Martin, 1993).

The thermodynamically favorable nature of micelles leading to their spontaneous formation, their ability to improve the solubility of various compounds, and their electrochemical properties have attracted the attention of formulation scientists over a long duration and micelle-based delivery systems have been tried to deliver drugs and biomolecules (Croy and Kwon, 2006). Micellar delivery systems have been reported to deliver anticancer drugs and other small molecules (Bontha et al., 2006; Croy and Kwon, 2006; Sawant et al., 2006; Gilmore et al., 2008; Kim et al., 2008; Oh et al., 2009; Park, 2009; Zhang et al., 2009a; Yuan et al., 2011), proteins (Kim et al., 2008; Pelletier et al., 2008; Miller et al., 2009; Zhang et al., 2009a), and siRNA and DNA (Wen et al., 2004; Chao et al., 2007; Wang et al., 2007; Itaka et al., 2009; Choi et al., 2010; Du et al., 2010; Kuo et al., 2010; Zhu et al., 2010). Various targeting ligands have been employed to improve the tissue specificity of micelles (Sawant et al., 2006; Lee et al., 2007; You

et al., 2007; Du et al., 2011). A major shortcoming of micellar systems is the disruption of micelles upon dilution, which is often overcome by chemical shell crosslinking of the micelles. Such crosslinking is often reported to improve the stability of micelles, without significantly compromising their delivery/transfection efficiency (Bontha et al., 2006; Zhang et al., 2007; Choi et al., 2010).

1.5. Diabetes

World Health Organization defines diabetes mellitus as "A metabolic disorder of multiple etiologies characterized by chronic hyperglycemia with disturbances of carbohydrate, fat and protein metabolism resulting from defects in insulin secretion, insulin action or both" (World Health Organization Consultation, 1999). It is broadly classified as Type 1 and Type 2 depending on the absolute or relative deficiency in insulin secretion or response (The Expert Committee on the Diagnosis and Classification of Diabetes Mellitus, 2003).

1.5.1. Type 1A diabetes

Type 1A diabetes, is an endocrine disorder of immunological origin, and is considered as one of the most common chronic disorders. Annually, it affects over 11,000 individuals in US alone, and accounts for ~5-10% of total diagnosed cases of diabetes (Devendra and Eisenbarth, 2003). Though it mainly affects children and adolescents, it has been reported to occur as late as 90 years of age. Therefore, the term "juvenile-onset" is not used anymore to describe this type of diabetes. The requirement of a lifelong treatment, which might prove inadequate, results in deterioration in quality of life of diabetics and put a huge burden on the healthcare systems in US. (The Expert Committee on the Diagnosis and Classification of Diabetes Mellitus, 2003; Craig et al., 2009). Autoimmune diabetes is a multipronged disorder which may lead to cardiovascular complications, retinopathy, neuropathy, and nephropathy.

1.5.1.1. Pathogenesis of Type 1A diabetes

Cell-mediated autoimmunity is primarily implicated in the pathogenesis of Type 1A diabetes. Auto-reactive T cells may exist normally but are restrained by immunoregulatory mechanisms leading to a self-tolerant state. However, when these mechanisms fail, auto-reactive T cells are activated, expand clonally, and cause a series of autoimmune reactions and production of inflammatory cytokines, which results in the destruction of β-cells in the pancreas, and loss of insulin production (Kawasaki et al., 2004). Figure 5 depicts the mechanism of β cell destruction in type 1 diabetes.

Primarily, the inflammation in the pancreas is a T cell-mediated response directed against one or more β-cell markers such as islet cells, insulin, glutamic acid decarboxylase (GAD) and tyrosine phosphatase. In more than 85 % of the diagnosed cases, presence of auto-antibodies for one or more of these markers has been observed along with elevated fasting blood glucose levels. Though diabetogenic seroconversion can occur at the age < 10 years, there is no limiting age factor for development of autoimmunity.

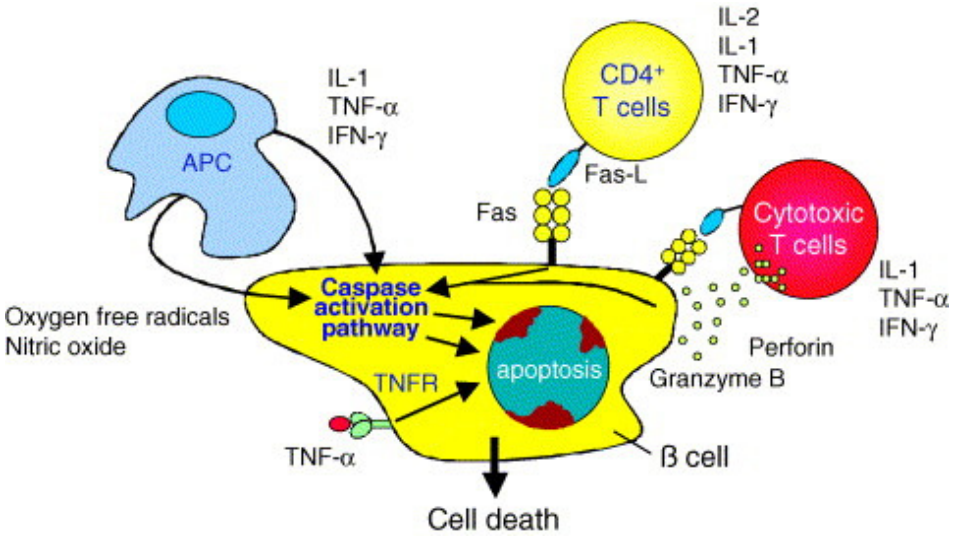

Figure 5: Mechanisms of β cell destruction in type 1 diabetes
(From Kawasaki et al. 2004)

Interestingly, >30% of the young population with type 2 diabetes are known to express anti-islet autoantibodies and would finally move to an active insulin therapy within 3 years (Devendra and Eisenbarth, 2003). Newly diagnosed diabetic patients with insulin deficiency, usually show pancreatic islets invasion by CD8+ T cells and associated β-cell damage. Pancreatic autopsy in these patients indicate mononuclear cell infiltration into the pancreatic islets and a slow destruction of β-cells (Kawasaki et al., 2004). The mechanism of autoimmunity in Type 1A diabetes has been extensively studied using various animal models such as non-obese diabetic (NOD) mice, biobreeding (BB) rats, and multiple low-dose streptozotocin (MLD-STZ)-treated mice improving our understanding of the pathogenic nature of human Type 1A diabetes. Although the precise mechanism of initiation and progression of autoimmunity leading to the destruction of pancreatic β-cells is not yet identified, a broad array of immune cells has been recognized as contributors towards this response. In the NOD mouse, a lymphocytic infiltration of pancreas (insulitis) is followed by β-cell destruction with gradual deficiency of insulin and leads to hyperglycemia. Due to the presence of auto-antigens on the surface of pancreatic β-cells, antigen presenting cells like macrophages and dendritic cells migrate towards the pancreas. Studies showed that these migrating macrophages play as critical role in the progression of autoimmune response in NOD mice and BB rats (Lee et al., 2012). Inactivation of these macrophages offered significant protection against development of diabetes. T cells in these animals lose their ability to differentiate into cytotoxic cells. Macrophage-depleted NOD mice also showed an upregulation of T_H2 response and a downregulation of T_H1 response. CD4+ and CD8+ T cells and B cells usually follow the dendritic cells and macrophages. This insulitis progresses from the vicinity of the islets and eventually invades and destroys the islets. Proinflammatory cytokines such as IL-1, IL-2, TNF-α, and IFN-γ, produced primarily by T_H1

cells play a critical role in the pathogenesis of Type 1A diabetes by causing activation and migration of more inflammatory cells into the pancreas. Moreover, effector T cells also cause β-cell destruction through direct contact with surface ligands such as FasL and membrane-bound TNF-α which induces apoptosis. Cytotoxic T cells also release perforins and granzymes leading to activation of nucleases. All these mechanisms together, either directly or through the induction of caspase pathway, lead to apoptosis of pancreatic β-cells. This β-cell destruction is enhanced by the T_H1 subset of CD4+ T cells and the type 1 cytokines, such as INF-γ, TNF-α and IL-2 which can be effectively suppressed by T_H2 and T_H3 cytokines, such as IL-4, IL-5, and IL-10 (Cox et al., 2001; Devendra and Eisenbarth, 2003; Carter et al., 2005).

1.5.1.2. Diagnosis and prediction of autoimmune diabetes

It has been reported that the expression of two or more autoantibodies (for β-cell markers such as islet cells, insulin, GAD and tyrosine phosphatase) has a strong positive correlation (>85%) with Type 1A diabetes, while the presence of a single autoantibody is usually useful for prediction in >65% of Type 1A diabetes cases (Devendra and Eisenbarth, 2003).

1.5.2. Current therapy for Type 1A diabetes

In Type 1A diabetes, the body's capacity to produce insulin gradually diminishes. So far, the only available treatment of Type 1A diabetes is insulin therapy, either through injection or insulin pumps to mimic the basal and simulated insulin levels. Delivered insulin replaces body's own insulin resulting in restoration of normal or near normal levels of glucose in the blood. However, this therapy is aimed towards management rather than the treatment of the condition. Insulin therapy has to be continued for the entire life of the patient and must be complimented with strict diet control and exercise routine. Moreover, insulin requirement keeps changing over the lifetime of the patient. It is also expensive and has patient compliance issues due to multiple,

daily injections. Though insulin pump can be an effective strategy, it may lead to problems such as pump malfunction/failure and infection at the implantation site. These limitations associated with insulin therapy have led to an intensive research in the development of alternative therapies for type 1 diabetes. Despite the advances in research for novel insulin delivery methods, management of diabetes and associated multiple acute and chronic complications is difficult and expensive. It is reported that there was no impact of low-dose parenteral insulin therapy in delaying the onset of diabetes (Diabetes Prevention Trial--Type 1 Diabetes Study Group, 2002). Therefore, there is a need to develop alternatives of insulin injections for delaying or preventing the onset of Type 1A diabetes. Various novel therapies are currently being investigated to prevent or treat Type 1A diabetes include islet cells transplantation, GAD administration, and cytokine gene therapy.

1.5.3. Experimental therapies for treatment of Type 1A diabetes

1.5.3.1. Islet transplantation

Pancreatic islet transplantation is considered as one of the most promising experimental therapy for treatment of Type 1A diabetes. Numerous clinical trials have been conducted using islet transplantation in combination with immunosuppressive agents. The purpose of islet transplantation is to achieve good glycemic control with minimal side effects. However, so far the results have been disappointing in terms of insulin dependence with only about 10% of subjects being off insulin at one year (Brendel et al., 1999). Moreover, due to immunorejection issues, they have to be maintained on immunosuppressive medication such as tacrolimus, sirolimus, and cyclosporine A for long durations after transplantation, making them more susceptible to infections. Continuing immunosuppressive therapy may also result in serious side effects such as nephrotoxicity, hepatotoxicity, and neurological complications. Recently,

investigators have proposed that surface modification of islets using poly (ethylene glycol) (PEG) can prolong the survival of islets by preventing immunogenic reactions. This study showed that PEGylated islets could survive for a long time in rats with low dose of immunosuppressive therapy with cyclosporine A. However, after the immunosuppressive treatment was discontinued, the islets could not survive for a long time which underlines the need for continuous immunosuppression with islet transplantation. Currently, single donor islet transplantations are being studied to alleviate these problems (Shapiro, 2011).

1.5.3.2. Glutamic acid decarboxylase (GAD)

GAD, a β-cell autoantigen (molecular weight: 65kd), was detected in the sera of Type 1A diabetic patients. Antibodies to GAD65 have been found in 70-75% of Type 1A diabetics compare to 1-2% in healthy individuals (Sanjeevi et al., 1996). Administration of purified GAD protein has been reported to enhance the tolerance of T cell mediated immune response against pancreatic β-cells causing prevention or delay in the development of insulitis and diabetes. Induction of tolerance with the use of GAD also inhibits the immune reactions against other autoantigens on the β-cells. Autoimmune reaction against β-cells can also be prevented by suppressing the expression of GAD in transgenic mice using antisense therapy (Kim, 2011).

1.6. Cytokines

Cytokines are small peptides synthesized and secreted inside the body by activated lymphocytes (lymphokines), macrophages/monocytes (monokines) and cells outside the immune system, and mediate as well as regulate immunity, inflammation, and hematopoiesis. The cytokine action can be autocrine (on the producing cell), paracrine (on neighboring cells), or endocrine (on distant organs). A complex interplay between cytokines is responsible for the pathology of autoimmune diabetes (Tarner and Fathman, 2001; Hill and Sarvetnick, 2002).

1.6.1. Cytokine therapy of diabetes

As discussed earlier, Type 1A diabetes is explained by T_H1/T_H2 balance model. In this case the autoimmunity is caused due to dominance of T_H1 cytokines (IFN-γ, IL-2 and TNF-α); whereas T_H2 cells through their cytokines (IL-4 and IL-10) elicit humoral responses. Restoration of balance between T_H1 and T_H2 cytokines by upregulation of T_H2 cytokine expression can essentially help in prevention of autoimmune diabetes. Administration of an anti-inflammatory cytokine, IL-10, produced by T_H2 population of helper T cells, is known to alleviate the symptoms of various inflammatory and algesic reactions by downregulating the inflammatory cytokine production. Upon systemic administration, IL-10 is known to prevent autoimmune insulitis, however, owing to its short plasma half-life (~2 min), maintenance of sustained plasma levels of IL-10 is challenging.

1.6.2. Cytokine gene therapy: need and applications

Delivery of genes encoding T_H2 cytokines using a viral or nonviral vector has the potential to eliminate these shortcomings by facilitating in situ expression of cytokines. A successful transfection by these systems can result in a sustained expression of these cytokines endogenously, and reduces the need of their repetitive administration. It may also circumvent the problems associated with immune reaction against foreign cytokines. Genes encoding anti-inflammatory cytokines, IL-4 and IL-10 have been delivered to suppress autoimmunity in Type 1A diabetes (Chernajovsky et al., 2004; Li et al., 2008; Basarkar and Singh, 2009; Mandke and Singh, 2012a). Currently, more than 300 clinical trials involving cytokine genes are underway (Figure 1, Adapted from J Gene Med 2011, available at http://www.wiley.com//legacy/wileychi/genmed/clinical/). This fact underlines the level of interest generated by these gene therapies.

1.6.2.1. Interleukin-4 gene delivery

IL-4, a prototypical T_H2 cytokine, has been widely investigated for gene therapy for autoimmune disorders such as experimental allergic encephalomyelitis (EAE), and collagen-induced arthritis (CIA). IL-4 plasmid has been delivered using both viral and non-viral vectors (Kageyama et al., 2004; Wang and Lu, 2010). Expressed IL-4 cytokine helped to inhibit the production of proinflammatory cytokines thereby suppressing autoimmunity. So far, IL-4 gene therapy has achieved mixed success in the treatment of Type 1A diabetes. Delivery of gene encoding IL-4 had been only moderately successful in spontaneously developing Insulin Dependent Diabetes Mellitus (IDDM) in experimental animals. Studies have also showed that i.v. administration of naked IL-4 plasmid was effective only with concurrent IL-10 plasmid administration; but when delivered using a non-viral vector, it showed complete amelioration of the disease (Lee et al., 2002a).

1.6.2.2. Interleukin-10 gene delivery

IL-10 was described in early 1990s (MacNeil et al., 1990) as a cytokine that is produced by T_H2 cell clones and is known to inhibit interferon-γ synthesis in T_H1 clones. IL-10 is a pleiotropic cytokine produced primarily by the T_H2 subset of helper T cells, B cells and macrophages (Figure 2). It induces B cells and mast cells proliferation and differentiation. Its potent anti-inflammatory activity is through the downregulation of the pro-inflammatory cytokines released by activated immune competent cells. Furthermore, it also inhibits monocyte MHC class II molecule, CD23, ICAM-1, and B7 expression leading to inhibition of the ability of the APC to activate the helper T cells. IL-10 is known to inhibit eosinophil survival and IL-4-induced IgE synthesis, while in B lymphocytes it stimulates cell proliferation and Ig secretion. TNF-α and other cytokines stimulate IL-10 secretion, suggesting a homeostatic mechanism

whereby an inflammatory stimulus induces TNF-α secretion, which in turn stimulates IL-10 secretion leading to suppression of TNF-α synthesis. Among the T_H2 cytokines, IL-10 distinctively inhibits cytokine production by mononuclear cells (Borish and Steinke, 2003). It has been previously used for treatment of pain, inflammation and autoimmune diseases such as psoriasis and Crohn's disease (Milligan et al., 2005; Sloane et al., 2009).

These studies indicate that IL-10 might be a good choice for the treatment of T cell-mediated autoimmune diseases including Type 1A diabetes. Production and action of IL-10 is found to be low in both human and animal models of Type 1A diabetes which suggests that the administration of IL-10 can lead to correction of diabetes (Schloot et al., 2002). Since the short half-life (~2 min) limits its use as a therapeutic agent, the IL-10 gene, delivered using viral and non-viral vectors, can be used to prevent or slow down the progression of autoimmune diabetes. It is reported that the IL-10 gene delivered using adeno-associated viral vector resulted in protection of pancreatic islets along with suppression of T cell activation (Goudy et al., 2001). Intramuscular injection of naked plasmid DNA encoding IL-10 also led to prevention of STZ-induced diabetes (Zhang et al., 2003). Additionally, IL-10 gene delivery has also been used for the suppression of autoimmune reaction after pancreatic islet transplantation (Carter et al., 2005).

1.6.2.3. Synergism between IL-4 and IL-10

Studies have showed that administration of chimeric plasmid encoding both IL-4 and IL-10 resulted in synergistic effect in prevention of autoimmune insulitis when administered in the form of polymeric complexes with poly[α-(4-aminobutyl)-L-glycolic acid] (Lee et al., 2003). These complexes were nanoscale in size, non-toxic, biodegradable and exhibited superior transfection efficiency than frequently used gene carrier, Poly-L-Lysine (Lim et al., 2000).

1.7. Statement of the Problem

The proposed research was directed towards the development of a nano size, high efficiency and low toxicity non-viral gene delivery vehicle from chitosan grafted with fatty acids. The fatty acid grafted chitosan based nanomicelles were expected to overcome the major barriers for gene delivery viz. cellular internalization and endosomal escape, and result in improvement in the intracellular gene delivery in order to facilitate the gene expression in vivo.

The hypotheses for the present study were as follows:

1. Soluble, low-molecular weight chitosan, when grafted with fatty acids of varying chain length and unsaturation will form N-acyl LMWC nanomicelles under optimized formulation conditions, and the physicochemical and performance (transfection) aspects of these nanomicelles will be influenced by the type of fatty acid modification. These nanomicelles will be positively charged, which will facilitate the DNA condensation and help to protect DNA from enzymatic degradation. The pDNA/N-acyl LMWC polyplexes will be biocompatible, non-toxic and will efficiently transfect the cells both in vitro and in vivo.

2. The intramuscular delivery of a bicistronic plasmid encoding IL-4 and IL-10 by using pDNA/N-acyl LMWC polyplexes will protect the murine pancreas from streptozotocin-induced insulitis by enhancing the expression of IL-4 and IL-10; and diminishing the serum levels of pro-inflammatory cytokines such as TNF-α and IFN-γ.

To test these hypotheses, following specific aims were planned:

1. To depolymerize and fractionate chitosan to obtain soluble low molecular weight chitosan fraction (LMWC)

2. To derivatize the LMWC with different fatty acids to obtain graft polymers, which self-assemble to form micelle-like structures in aqueous environment

3. To study the effect of formulation variables on size and charge of the polymeric nanomicelles by dynamic light scattering (DLS) and zeta potential measurement, respectively.

4. To test the transfection efficiency of nanomicelles to deliver reporter plasmids in vitro

5. To study in vitro and in vivo biocompatibility of N-acyl LMWC nanomicelles by MTT assay and histological analysis, respectively

6. To study the efficiency of N-acyl LMWC nanomicelles to deliver plasmid encoding Interleukin-4 (IL-4), Interleukin-10 (IL-10), bicistronic plasmid encoding for IL-4 and IL-10, and a physical mixture of plasmids encoding for IL-4 and IL-10, in vivo and its ability to prevent the insulitis due to Type 1A diabetes in multiple, low-dose Streptozotocin (MLD-STZ) induced diabetic mouse model

The overall study was intended to result in a nano-scale, cationic, biocompatible, non-viral vector which can be used to deliver therapeutic plasmids in vivo.

2. MATERIALS AND METHODS

2.1. Materials

The materials used in this study and their sources are listed in Table 1.

Table 1: Materials used in this study and their sources

Material	Supplier
1-Ethyl-3-(3-dimethylaminopropyl)carbodiimide (EDC)	Advanced Chemtech, KY
3-(4,5-dimethylthiazol-2-yl)-2, 5-diphenyltetrazolium bromide (MTT)	Sigma-aldrich, MO
4',6-diamidino-2-phenylindole (DAPI)	Invitrogen, CA
Agarose	MP biomedicals, OH
Arachidic acid	Sigma, MO
Chitosan (DD 85%, Mw 50kD)	Sigma-Aldrich, MO
Contour® glucometer Strips	Bayer healthcare, IN
Contour glucometer*	Bayer, NY
Deoxyribonuclease I (DNase I, bovine pancreatic origin)	Rockland, PA
Eagles Minimum Essential Medium (EMEM)	ATCC, VA
ELISA Max™ kit for IFN-γ	Biolegend, CA
ELISA Max kit for IL-10	Biolegend, CA
ELISA Max kit for IL-4	Biolegend, CA
ELISA Max kit for TNF-α	Biolegend, CA
Ethidium Bromide	EMD, NJ
Fetal bovine serum (FBS)	ATCC, VA

(Continued)

Table 1: Materials used in this study and their sources (Continued)

Material	Supplier
Fluka™ Dextran molecular weight standards	Sigma-Aldrich, Steinheim, Denmark
FuGENE® HD	Roche Applied Science, Mannheim, Germany
gWIZ™ Blank mammalian expression vector	Aldevron, ND
gWIZ™ GFP mammalian expression vector*	Aldevron, ND
gWIZ™ β-gal mammalian expression vector	Aldevron, ND
Human Embryonic Kidney (HEK293) cell line	ATCC, VA
Ketoprofen	Medisca, NY
Linoleic acid	TCI, Tokyo, Japan
Linolenic acid	TCI, Tokyo, Japan
Mica substrate	SPI, PA
MicroBCA protein assay kit	Pierce, IL
Myristic acid	Sigma, MO
N-hydroxysuccinimide (NHS)	Alfa Aesar, Lancashire, UK
Ninhydrin	Alfa Aesar, Lancashire, UK
Normal saline	EMD, NJ
Oleic acid	TCI, Tokyo, Japan
Palmitic acid	TCI, Tokyo, Japan
Penicillin-Streptomycin-Amphotericin B Solution	ATCC, VA
Pentobarbital (Nembutal®) injection	Lundbeck, NJ

(Continued)

Table 1: Materials used in this study and their sources (Continued)

Material	Supplier
Potassium bromide	Sigma, MO
pUMVC3-mIL10 mammalian expression vector*	Aldevron, ND
pUMVC3-mIL4 mammalian expression vector*	Aldevron, ND
pVIVO2-mIL4-mIL10 plasmid	Invivogen, CA
Pyrene	Alfa Aesar, Lancashire, UK
Sephadex® G-50 DNA grade	GE healthcare, Uppsala, Sweden
Sodium nitrite ($NaNO_2$)	Sigma-Aldrich, MO
Spectra/Por membrane tubing (MWCO 8000)	Spectrum Laboratories, CA
Stearic acid	Sigma, MO
Streptozotocin	Enzo Life Sciences, NY
Tris-Acetate-EDTA (TAE) Buffer	Rockland Immunochemicals, PA
Water for injection	Thermo Scientific, MA

* = generous gift from Aldevron, LLC, Fargo.

All other chemicals used in the study were analytical or cell culture grade as applicable. Water used in the study was purified and deionized by a Millipore Direct-Q water purification system (Millipore, MA).

2.2. Animals

Male, 5-6 week old, BALB/c mice were obtained from Harlan, Indianapolis, IN and housed in a pathogen free environment and maintained at 12 h dark and 12 h light cycle. The animals were acclimatized in the facility for a week before starting the study and water was provided *ad libitum* for the entire duration. Standard pelleted rodent food was provided *ad*

libitum for the duration of the study except for the 12 h restriction period prior to measurement of fasting blood glucose levels once every week. The animal studies were performed in compliance with the "Principles of Laboratory Animal Care" (NIH publication #85-23, revised in 1985) with the approval from Institutional Animal Care and Use Committee (IACUC) at North Dakota State University (protocol A10052).

2.3. Plasmids

The gWIZ™ Blank (5.1 kb), gWiz™ β-gal (8.3 kb) and gWiz™ GFP (5.8 kb) mammalian expression vectors encoding for blank (control), β-galactosidase, and green fluorescent protein, respectively, were used in the study. Each plasmid consisted of a proprietary modified promoter, followed by intron A from the CMV immediate early gene and a high-efficiency artificial transcription terminator constructed in a modified plasmid backbone to achieve enhanced levels of transgene expression in mammalian cells. The sizes of pUMVC3-mIL4 and pUMVC3-mIL10 plasmids encoding mouse IL-4 and IL-10 were 4.5 and 4.4 kb, respectively. Both plasmids had a CMV early promoter, rabbit beta-globin polyadenylation signal and kanamycin resistance gene. The pVIVO2-mIL4-mIL10 plasmid had FerH (heavy chain) and FerL (light chain) human ferritin composite promoters with the SV40 and CMV enhancers, respectively. Also, their 5'UTRs were replaced by the 5'UTR of the mouse and chimpanzee EF1α genes and a hygromycin resistance gene was incorporated for clonal selections. The structures of these plasmids are shown on figure 6.

2.4. Experimental Methods

2.4.1. Depolymerization of chitosan

Chitosan (Mw 50 kD, DD 85%) was depolymerized following the method of Mao at al. with modifications (Mao et al., 2004). Briefly, 2% w/v solution of chitosan was prepared in 100 ml of 1% v/v acetic acid. Fifty milliliters of 0.1 M sodium nitrite ($NaNO_2$) was added slowly to chitosan solution and was allowed to react for 2 h at room temperature. The pH of the reaction mixture was adjusted to 9.0 using 2 N sodium hydroxide (NaOH, Sigma-aldrich, MO) and the precipitated LMWC was separated following centrifugation and subsequently freeze dried.

2.4.2. Fractionation and molecular weight determination of LMWC

LMWC was fractionated on basis of its molecular weight using size exclusion chromatography (SEC). A preparative-scale SEC column was prepared using Sephadex G-50 DNA grade and the LMWC was eluted through the column using 1% v/v acetic acid as mobile phase. Complete elution of LMWC was ensured using the ninhydrin test (Prochazkova et al., 1999). Eluted LMWC fractions were collected, lyophilized and subjected to molecular weight determination. Molecular weights of the isolated chitosan fractions were determined using gel permeation chromatography (GPC). An Ultrahydrogel® 250 (Waters, MA) column was used in combination with the Agilent 1120 Compact LC system coupled with an Agilent 1200 series RI detector (Agilent, DE) with 1% v/v acetic acid as mobile phase and Fluka™ dextran molecular weight standards (Mw range $5 \times 10^2 - 5 \times 10^4$ Da). A flow rate of 1 ml/min was used and samples were eluted at 40°C. Data was analyzed using EZChrom Elite™ 3.3.2 software (Agilent, Santa Clara, CA). The major fraction of LMWC was selected for further studies.

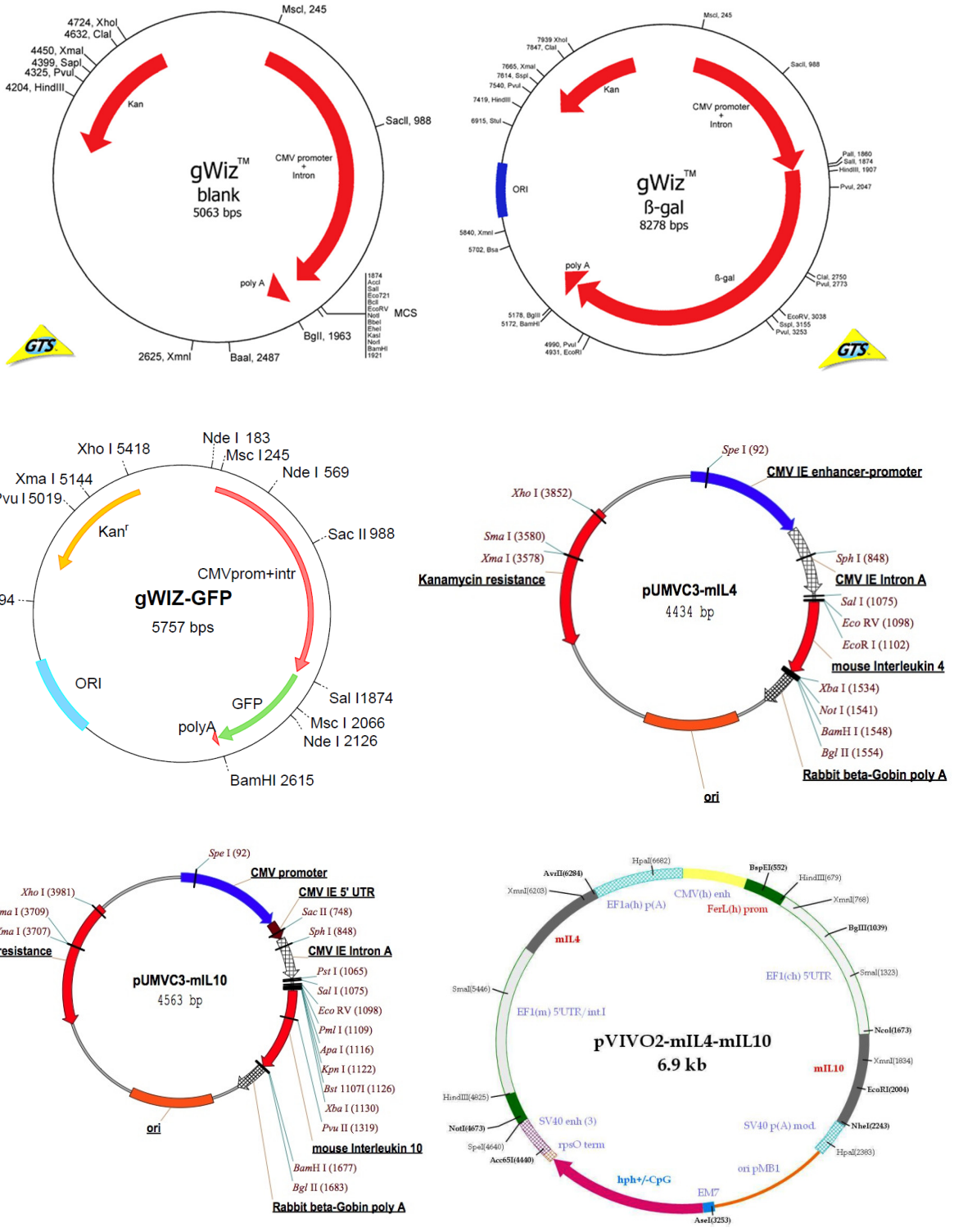

Figure 6: Maps of the plasmids used in this study
(Images reproduced from plasmid suppliers' data)

2.4.3. Synthesis of N-acyl LMWCs

Initially, N-acyl LMWCs were synthesized using tetradecanoic (myristic, 14:0), hexadecanoic (palmitic, 16:0), octadecanoic (stearic, 18:0) and eicosanoic (arachidic, 20:0) acids by EDC-NHS reaction following the method of Hu et al with modifications (Hu et al., 2006). Briefly, 2% w/v aqueous solution of LMWC was heated to 90°C with stirring. A 3% w/v solution of the fatty acid in ethanol was mixed with EDC and NHS and was added continuously to LMWC solution. Reaction was continued for 24 h with constant stirring. The product was filtered, dialyzed using Spectra/Por® membrane tubing for 24 h against water, dried under vacuum, washed with ethanol and lyophilized. The scheme of synthesis is shown in Figure 7. Based on the preliminary transfection efficiency evaluation, C18 derivatives of LMWC were chosen to investigate the effect of increasing unsaturation in the N-acyl groups. Therefore, N-acyl LMWCs were synthesized using unsaturated fatty acids viz. cis-9-Octadecenoic (oleic, 18:1 cis-9), cis, cis-9,12-octadecadienoic (linoleic, 18:2 (n-6)), and all-cis-octadecatrienoic (linolenic, 18:3(n-3)) acids by EDC-NHS reaction.

2.4.4. Structural characterization of N-acyl LMWCs

The N-acyl LMWCs were characterized for their structure using Infrared (IR) spectroscopy. The degree of substitution (DS) of the fatty acyl groups was determined using a reported method (Kasaai, 2008). The results for the degree of substitution were confirmed by elemental analysis using CHNS-932 Elemental Analyzer (Leco, MI).

2.4.5. Determination of critical micellar concentration (CMC) of N-acyl LMWC

N-acyl derivatives of chitosan should self-assemble to form micelle like structures (Yuan et al., 2011). The critical concentration for such micellar assembly was determined using pyrene probe method (Kalyanasundaram and Thomas, 1977). A series of dilutions ranging from 0.002 to

1 mg/ml were prepared for each of the polymers and were mixed with equal volumes of the methanolic solutions of pyrene to obtain a final concentration of 2.0 µM of pyrene. Fluorescence intensities of the pyrene-N acyl LMWC mixtures were recorded using Cary Eclipse fluorescence spectrophotometer (Varian, CA) at excitation wavelength of 310 nm. The ratio of fluorescence intensities of band III to band I of pyrene were plotted against series of concentrations of polymers and the CMC values were determined graphically.

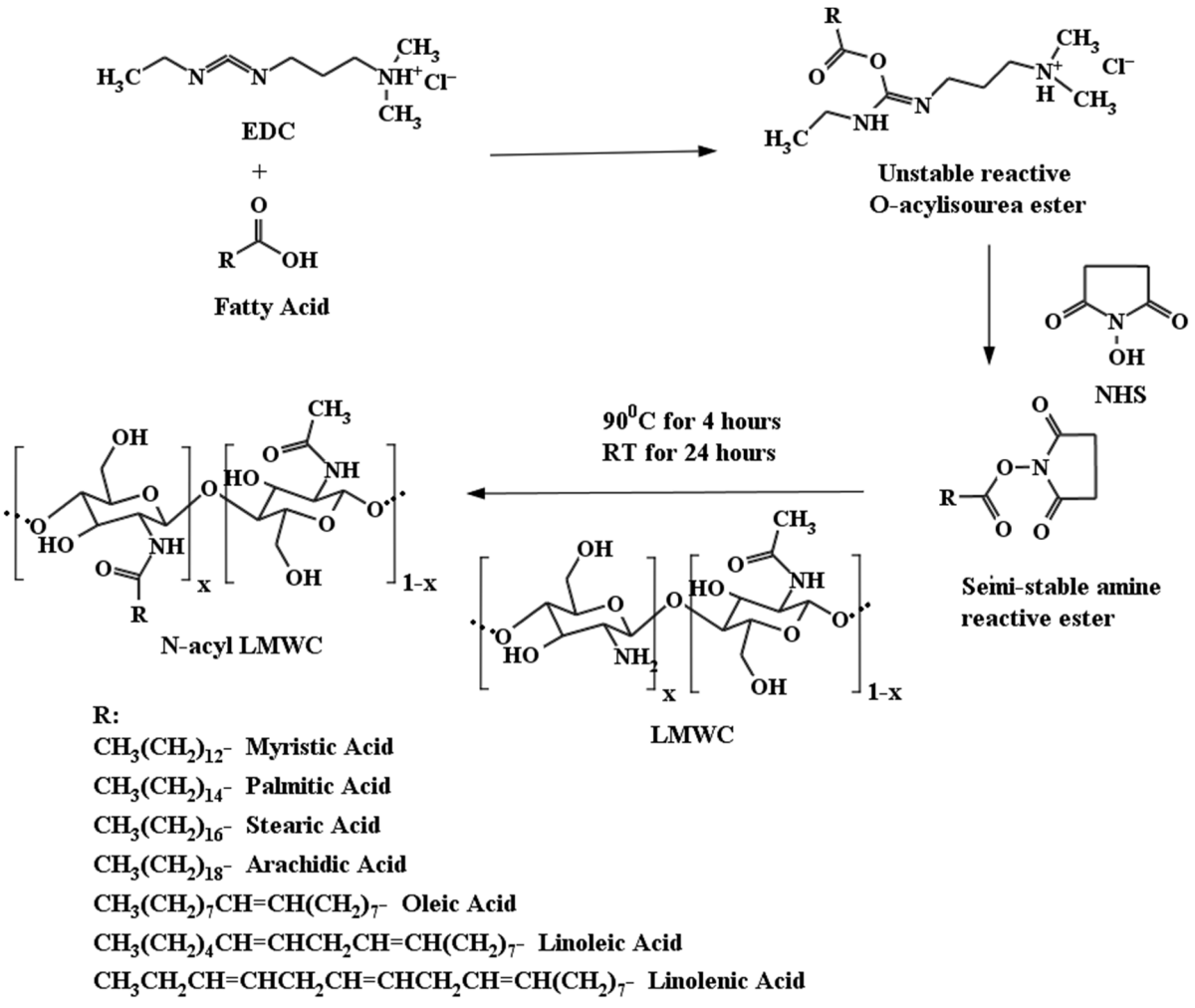

Figure 7: Scheme for synthesis of N-acyl LMWC

2.4.6. Hydrodynamic size, zeta potential, and topological characterization of N-acyl LMWC: effect of formulation parameters

The effect of formulation parameters such as pH, sonication, filtration and DNA addition on the physicochemical properties of N-acyl LMWC nanomicelles was analyzed by various instrumental techniques.

2.4.6.1. Initial hydrodynamic size and zeta potential characterization for N-acyl LMWC

For initial determination of hydrodynamic size and zeta potential, 1% (w/v) aqueous solution of N-acyl LMWC were prepared in deionized water by stirring at 50 RPM for 10 min. The nanomicelles were allowed to stand at room temperature for 30 min and then were subjected to hydrodynamic size and zeta potential analysis using a Zetasizer® Nano (Malvern, PA) dynamic light scattering particle analyzer.

2.4.6.2. Effect of pH on hydrodynamic size and zeta potential of N-acyl LMWC

The effect of pH on the hydrodynamic size and zeta potential of N-acyl LMWC was assessed at pH 5.0, 7.4 and 9.0 using a Zetasizer Nano (Malvern, PA) dynamic light scattering particle analyzer. Depending upon the broad range of pH conditions that a non-viral vector would encounter en route to its internalization and subsequent endosomal escape, the pH conditions were selected. The 1% (w/v) aqueous solution of N-acyl LMWC were prepared in deionized water by stirring at 50 RPM for 10 min and the pH of the solutions was adjusted to 5.0, 7.4 and 9.0 using 0.1 N hydrochloric acid (HCl, Sigma-aldrich, MO) and 0.1 N NaOH as required. Four replicates were used and data was presented as mean ± standard deviation (SD).

2.4.6.3. Effect of sonication on hydrodynamic size and zeta potential of N-acyl LMWC

The effect of sonication and its duration on hydrodynamic size and zeta potential of N-acyl LMWC was studied using a Zetasizer Nano (Malvern, PA) dynamic light scattering particle analyzer. The 1% (w/v) aqueous solution of N-acyl LMWC were prepared in deionized water by stirring at 50 RPM for 10 min and were subjected to sonication at 75 watts and 20 kHz using a probe sonicator (Model 150 V/T, Biologics, Manassas, VA) for durations ranging from 0-7 min. Based on the results of these studies, sonication durations of 0, 1, 3 and 5 min were selected for further investigation and N-acyl LMWC solutions of pH 5.0, 7.4 and 9.0 were studied post-sonication. Four replicates were used and data was presented as mean ± SD. The analyzed solutions were freeze dried and the N-acyl LMWC residues were subjected to structural analysis by IR spectroscopy to detect the structural changes, if any, in the polymer.

2.4.6.4. Effect of filtration on hydrodynamic size and zeta potential of N-acyl LMWC

The sonicated N-acyl LMWC solutions exhibited high polydispersity and hence the effect of filtration on the hydrodynamic size and zeta potential of N-acyl LMWC was also determined. The 1% w/v aqueous solutions of N-acyl LMWC were prepared at pH 5.0, 7.4 and 9.0, and were subjected to sonication at 75 watts and 20 kHz using a probe sonicator (Model 150 V/T, Biologics, Manassas, VA) for 0 (no sonication), 1, 3 and 5 min. These solutions were filtered through a 0.8 µ syringe filter and subjected to hydrodynamic size and zeta potential analysis. Four replicates were used and data was presented as mean ± SD. The recovery of the N-acyl LMWC was measured by filtering a known volume of the solution, freeze drying the filtrate and the amount of N-acyl LMWC in the filtrate was determined by weighing the quantity of residue.

Based on the results of these studies, the aqueous solutions of N-acyl LMWC were prepared by adding N-acyl LMWC in deionized water, stirring at 50 RPM for 10 min, sonicating

the solutions at 75 watts and 20 kHz using a probe sonicator for 5 min to re-disperse the nanomicelles and filtering the solutions through a 0.8 μ syringe filter. The pH of the solutions was adjusted to 7.4 using 0.1 N HCl and 0.1 N NaOH as required. The N-acyl LMWC nanomicelles prepared in this fashion were used in all the further studies and are henceforth referred to as "aqueous solutions of N-acyl LMWC".

2.4.6.5. Effect of DNA addition on surface topology of N-acyl LMWC

Aqueous solutions of N-acyl LMWC (1% w/v) were prepared and gWIZ™ blank plasmid was added to the polymer solution at polymer to DNA weight ratio of 20:1, which corresponded to a N:P ratio (ratio of nitrogen on the polymer to phosphate groups in DNA) of ~ 16.5:1. The samples were placed on freshly cleaved mica plates and were dried under nitrogen overnight. The change in surface topology of N-acyl LMWC nanomicelles before and after addition of DNA was studied visualized a DI-3100 atomic force microscope (AFM, Veeco, MN) in tapping mode using pyramidal cantilevers with a silicon probe having force constant of 2.8 N/m at a scan rate of 2 Hz.

2.4.6.6. Effect of DNA addition on hydrodynamic size and zeta potential of N-acyl LMWC

The effect of DNA addition on the hydrodynamic size and zeta potential of N-acyl LMWC nanomicelles was studied using a Zetasizer Nano (Malvern, MA). Aqueous solutions (1% w/v) of N-acyl LMWCs were prepared and were stirred for 30 min. The hydrodynamic size and zeta potential of the resulting solutions were determined before and after addition of DNA at polymer to DNA weight ratio of 20:1. The storage stability of N-acyl LMWC nanomicelles and N-acyl LMWC/DNA polyplexes was determined after storing them at 4°C and the hydrodynamic size and zeta potential measurements were repeated after 1, 3 and 7 days of storage.

2.4.7. Buffering ability of N-acyl LMWC

To determine the buffering ability of the N-acyl LMWCs, the aqueous solutions of N-acyl LMWCs were titrated against 0.1 N HCl. Aqueous solutions of N-acyl LMWC (1% w/v) were prepared in 0.1 N NaOH and 15 ml of these solutions were titrated against 0.1 N HCl. NaOH solution (0.1 N) without N-acyl LMWC was used as a blank.

2.4.8. Optimization of N:P ratio for transfection efficiency studies

The transfection efficiency of N-acyl LMWC was checked in vitro using HEK293 cells. For initial experiments, HEK293 cells were plated in 24 well plates in 1 ml Eagles Minimum Essential Medium, supplemented with 10% FBS at a cell density of 5 x 10^4 cells/well and allowed to grow for 24 h at 37°C. Aqueous solutions of gWIZ™ β-Gal Mammalian Expression Vector and aqueous solutions of N-acyl LMWCs using myristic, palmitic, stearic and arachidic acid were prepared and mixed with gentle vortexing to obtain the formulations at N:P ratios of 1:20, 1:10, 1:5, 1:1, 5:1, 10:1 and 20:1. The cells were washed with phosphate buffered saline (PBS, pH 7.4) and 100 µl of the formulations, corresponding to 1 µg pDNA/well were then added to each well. At 1 h post-incubation, the cells were washed with PBS again to remove the formulations. Naked DNA was used as a passive control while cells without any treatment were used as negative control to measure the background β-Galactosidase activity. After 72 h, the cells were washed, lysed, and analyzed for β-Galactosidase concentration using β-Galactosidase enzyme assay kit (Promega, WI) as per the manufacturer's protocol. The microBCA protein assay (Pierce, IL) was used to measure total protein content. Milliunits of β-Galactosidase enzyme expressed per mg of protein were measured and based on the results, the optimized N:P ratio of 20:1 was selected for further experiments.

2.4.9. Stability evaluation of the formulations

2.4.9.1. Storage stability of N-acyl LMWC/pDNA polyplexes

The stability of polyplexes formed between gWIZ™ Blank plasmid DNA to N-acyl LMWC solutions was determined at 30 min and 7 days post-preparation using agarose gel retardation assay. Polyplexes were formed by mixing the 1% w/v aqueous N-acyl LMWC solutions and plasmid DNA at N:P ratio of 20:1 and incubated at RT for 30 min before analysis. The polyplexes were stored at 4°C for 7 days and were analyzed again for stability.

2.4.9.2. Structural stability of DNA released from N-acyl LMWC/pDNA polyplexes using DNase protection assay

To assess the ability of N-acyl LMWC to protect the DNA from degradation, DNase protection assay was performed. Polyplexes were prepared as described previously by mixing N-acyl LMWC solutions and plasmid DNA at N:P ratio 20:1 and were allowed to stabilize for 30 min. The polyplexes were then incubated with DNase I for 30 min and the enzyme was deactivated by heating the complexes at 65°C for 5 min. The DNA bound to N-acyl LMWC was released by adding 100 µl of 5% w/v solution of competing polyanion (heparin). The released DNA was subjected to agarose gel electrophoresis to test its integrity.

The agarose gel was prepared at a concentration of 1% w/v in TAE buffer and ethidium bromide was added before setting the gel to visualize DNA. Samples were subjected to electrophoresis at 80 V for 90 min in TAE buffer and DNA migration was imaged using FluorChem 5500 (Alpha Innotech, CA) imaging system.

2.4.10. Determination of in vitro cytotoxicity of N-acyl LMWC nanomicelles

The in vitro cytotoxicity of N-acyl LMWC was tested in Human embryonic kidney (HEK293) cells using (3-(4,5-Dimethylthiazol-2-yl)-2,5-diphenyltetrazolium bromide (MTT) cell viability assay. HEK293 cells were plated in a 96-well plate at a cell density of $5x10^3$ cells/well in EMEM supplemented with 10% FBS. After 24 h of growth, the 100 µl of aqueous N-acyl LMWC solutions, corresponding to 1-2.5 mg/ml of N-acyl LMWC after final dilution, were added to each well. After 24 h of incubation, cell viability was determined by their ability to reduce the MTT to a formazan product by enzyme succinate dehydrogenase. MTT solution (25 µl/well, 5mg/ml) was added to the wells and the plate was incubated at 37°C for 4 h. After 4 h, the media was removed and the formazan crystals formed in the cells were dissolved by adding 150 µl dimethyl sulphoxide (DMSO) to each well and the absorbance was read at 570 nm. The viability of the cells treated with LMWC and N-acyl LMWCs was determined and compared with that of the untreated control.

2.4.11. Visualization of transfection ability of the N-acyl LMWC nanomicelles using confocal microscopy

The ability of the N-acyl LMWC to transfect the cells in vitro and subsequent expression of the proteins was visualized using gWIZ™ GFP mammalian expression vector encoding for GFP. Aqueous solutions of the N-acyl LMWC/pDNA polyplexes were prepared at N:P ratio 20:1. HEK293 cells were plated in polystyrene chamber slide systems (BD Biosciences, MA) at a cell density of $1x\ 10^4$ cells/chamber in 1 ml EMEM, supplemented with 10% FBS and 100 µl of each of the formulations, corresponding to 500 ng pDNA/well were added to wells after 24 h. Untreated cells and naked DNA were used as negative and passive controls, respectively, while LMWC and a commercial transfection agent; FuGENE HD were used as positive controls. The

cells were visualized at 72 h post-transfection using FV300 confocal laser scanning fluorescence microscope (Olympus, NY). A florescent 4',6-diamidino-2-phenylindole (DAPI) nuclear stain was used to define the cell nuclei.

2.4.12. In vitro transfection efficiency of N-acyl LMWC nanomicelles loaded with pDNA

For preliminary studies, HEK293 cells were plated in 24 well plates in 1 ml EMEM supplemented with 10% FBS at a cell density of 5 x 10^4 cells/well and were allowed to grow for 24 h. Aqueous solutions of gWIZ™ β-Gal mammalian expression vector and N-myristoyl, N-palmitoyl, N-stearoyl and N-arachidoyl LMWC were prepared and mixed with gentle vortexing to obtain the formulations at N:P ratio of 20:1. The cells were washed with PBS (pH 7.4) and 100 µl of the formulations, corresponding to 1 µg pDNA/well were then added to each well. At 1 h post-incubation, the cells were washed with PBS to remove the formulations. Naked DNA was used as a passive control while cells without any treatment were used as negative control to measure the background β-Galactosidase activity. After 24, 48, and 72 h, the cells were washed, lysed, and analyzed for β-Galactosidase amount using β-Galactosidase enzyme assay system (Promega, WI) as per the manufacturer's protocol. The microBCA protein assay (Pierce, IL) was used to measure total protein content. Milliunits of β-Galactosidase enzyme expressed per mg of protein was used as indicator of transfection efficiency. Different N-acyl LMWC/DNA complexes, LMWC/DNA complexes and naked DNA were studied for their transfection.

Based on results of this experiment, N-acyl derivatives were synthesized using oleic, linoleic and linolenic acid and evaluated for their transfection efficiency. Plasmids encoding for IL-4 (pUMVC-mIL4) and IL-10 (pUMVC-mIL10) were used and transfection experiments were performed as described earlier. FuGENE HD and LMWC were used as positive controls. At 24, 48, and 72 h post-transfection, cell supernatants were collected. Mouse IL-4 ELISA MAX

Deluxe and Mouse IL-10 ELISA MAX Deluxe (Biolegend, CA) were used to determine the concentrations of IL-4 and IL-10, respectively, as per the manufacturer's protocol. One day prior to running the ELISA, multiple 96-well plates were coated with 100 µl/well of capture antibodies for IL-4 and IL-10, separately. After 24 h, plates were washed and blocked with 200 µl assay diluent. The cell supernatants were added at 100 µl per well and incubated for 2 h with continuous shaking. The plates were then washed with wash buffer (0.05% Tween 20 in PBS, pH 7.4) and 100 µl of detection antibody was added to each well followed by incubation for 1 h. Finally, 100 µl of diluted Avidin-horseradish peroxidase solution was added to each well and incubated for 30 min. Plates were subsequently washed and 100 µl of freshly mixed 3,3',5,5'-tetramethylbenzidine (TMB) substrate solution was added to each well, followed by incubation in the dark for 20 min. The reaction was stopped by adding 100 µl of 2N sulfuric acid and the resultant yellow color intensity was measured at 450 nm. Concentrations of IL-4 and IL-10 were determined using the calibration curves prepared by measuring the absorbance of known concentrations of IL-4 and IL-10, respectively. Four replicates were used and data was presented as mean ± SD.

2.4.13. In vivo delivery of pDNA using N-acyl LMWC nanomicelles in MLD-STZ induced diabetic mice

The ability of N-acyl LMWC to deliver the plasmids encoding for IL-4 and IL-10 was studied in vivo using multiple, low dose streptozotocin (MLD-STZ) induced diabetic mouse model. The ability of a bicistronic plasmid encoding for IL-4 and IL-10 to protect the pancreatic islets from MLD-STZ-induced insulitis was compared with individual plasmids encoding IL-4, IL-10 and a physical mixture (1:1 v/v) of these plasmid solutions.

2.4.13.1. Grouping structure and in vivo experimentation

The BALB/c mice were divided into 18 groups of six animals each. The animals in the control group were treated with saline, while streptozotocin treated animals were used as a negative control. Passive control groups consisted of animals treated with either naked plasmids (IL-4 or IL-10) or a physical mixture of equal volumes of plasmids (IL-4+IL-10) or bicistronic plasmid encoding for both IL-4 and IL-10, directly administered into the anterior tibialis muscle without any polymeric delivery system. Animals in the positive control groups were treated with either IL-4, or IL-10 or a mixture of IL-4 and IL-10, or a bicistronic plasmid encoding for both IL-4 and IL-10 using FuGENE HD as a delivery vector. The treatment groups were divided into 8 different groups and the details about the grouping structure is depicted in table 2.

The formulations were injected as a single dose, corresponding to 50 µg of pDNA per animal, into the anterior tibialis muscle of mice. Except for the animals in the saline control group, all other groups received intraperitoneal injections of streptozotocin (40 mg/kg of body weight) for 5 consecutive days. The blood samples, collected at weekly time points, were centrifuged at 4°C in a cooling centrifuge, and the serum was separated. The serum was stored at -20°C until further analysis. ELISA was used to determine the levels of IL-4, IL-10, TNF-α and Interferon-γ (IFN-γ) in the serum samples. The expression of the proteins IL-4 and IL-10 was compared throughout the study. At the end of the six week period, the animals were euthanized by injecting pentobarbital (150 mg/kg body weight) intravenously through tail vein. The pancreas and anterior tibialis muscle were dissected and studied for histopathological changes to assess the ability of formulation to protect pancreatic beta cells and the biocompatibility of the formulations, respectively.

Table 2: The grouping structure for in vivo studies

Group Number	Treatment
1	Saline (Control)
2	Streptozotocin Control (Negative control)
3	Naked IL-10 Plasmid (Passive Control)
4	Naked IL-4 Plasmid (Passive Control)
5	Mixture of naked IL-4 and IL-10 Plasmids (Passive Control)
6	Bicistronic IL-4 and IL-10 Plasmid (Passive Control)
7	FuGENE HD + IL-4 Plasmid (Positive Control)
8	FuGENE HD + IL-10 Plasmid (Positive Control)
9	FuGENE HD + Mixture of IL-4 and IL-10 Plasmid (Positive Control)
10	FuGENE HD + Bicistronic IL-4/ IL-10 Plasmid (Positive Control)
11	N-oleoyl LMWC + IL-4 Plasmid
12	N-oleoyl LMWC + IL-10 Plasmid
13	N-oleoyl LMWC + Mixture of IL-4 and IL-10 Plasmids
14	N-oleoyl LMWC + Bicistronic IL-4/IL-10 Plasmid
15	N-linoleoyl LMWC + IL-4 Plasmid
16	N-linoleoyl LMWC + IL-10 Plasmid
17	N-linoleoyl LMWC + Mixture of IL-4 and IL-10 Plasmids
18	N-linoleoyl LMWC + Bicistronic IL-4/IL-10 Plasmid

2.4.13.2. Blood glucose level determination

After the first STZ injection, the blood glucose levels of the animals were monitored on a daily basis for the first week, and the animals were considered diabetic if the random blood

glucose level for the animal was 200 mg/dl or more for two consecutive days. After first week, blood sampling was performed after on a weekly basis using tail vein puncture. A glucometer (Bayer Contour Glucometer, Mishawaka, IN, USA) was used to measure the blood glucose levels of mice.

2.4.13.3. ELISA for determination of IL-4, IL-10, IFN-γ and TNF-α in serum

BioLegend's ELISA Max Deluxe Set sandwich Enzyme Linked Immunosorbent Assays were used to determine the concentration of IL-4, IL-10, IFN-γ and TNF-α cytokines in the blood samples of mice. The procedures were followed as per manufacturer's protocol. In short, prior running the ELISA, mouse specific capture antibodies for IL-4, IL-10, IFN-γ and TNF-α were coated on the plates by incubating at for 16 h at 4°C. The plates were washed thoroughly with wash buffer (PBS + 0.05% Tween-20, pH 7.4) and residual buffer was removed by tapping the plate. The plates were then incubated with assay diluent at room temperature (RT) for 1 h to block the non-specific binding. Plates were washed again, and suitable dilutions of standard stock solution of IL-4, IL-10, IFN-γ and TNF-α as well as the samples were added to the plates, followed by incubation at RT for 2 h. After incubation, plates were washed followed by addition of biotinylated anti-mouse detection antibodies for IL-4, IL-10, IFN-γ and TNF-α, respectively, to produce an 'antibody-antigen-antibody sandwich'. After 4 h of incubation, an enzyme, avidin-horseradish peroxidase (avidin-HRP) was added to the plates, and the plates were incubated a RT under shaking conditions followed by addition of TMB substrate. The plates were incubated in dark for 20 min until the blue color was developed, followed by addition of stop solution (150 µl of 2 N H_2SO_4). The reaction color changed from blue to yellow after addition of the stop solution. The intensity of yellow color developed was measured at 450 nm with a microplate reader. The standard curves plotted using the dilutions of standard stock solutions prepared in the

ranges of 2-125 pg/ml, 31.3-2000 pg/ml, 15.6-1000 pg/ml and 7.8-500 pg/ml were used to estimate the concentration of IL-4, IL-10, IFN-γ and TNF-α, respectively, in mice serum.

2.4.13.4. In vivo biocompatibility of the delivery system

At 1, 4, and 6 week after the administration of formulations, the animals were euthanized by injecting pentobarbital (150 mg/kg body weight) intravenously through tail vein. The injection site of the formulations (anterior tibialis muscle) was dissected, fixed in 10% neutral buffered formalin solution, sectioned, stained with hematoxylin-eosin (H&E) stain and studied for histopathological changes to assess the biocompatibility of the formulations. The presence of inflammatory cells, mononuclear infiltration, fibrosis, and necrosis if any, was noted.

2.4.13.5. Histopathological changes in pancreas

At 1 week, 4 week and 6 week time after the administration of formulations, the mice were euthanized, the pancreas were removed and fixed in 10% neutrally buffered formalin solution, sectioned and stained with hematoxylin-eosin stain. The the progression of insulitis in the pancreatic cells of treated animals was asseseed and copared with control (untreated) pancreas to determine the therapeutic efficacy of expressed IL-4 and IL-10 to supress the autoimmune insulitis.

2.5. Statistical Analysis

Minitab® 16 (Minitab Inc., PA) software was used to design the experiments for the optimization studies. For cytotoxicity and transfection efficiency studies, four replicates were used and single factor ANOVA was performed using SAS® 9.2 (SAS Institute, NC). For all in vivo studies, six replicates were used and single factor ANOVA was performed using SAS 9.2. A p value of less than 0.05 was considered to be significant.

3. RESULTS

3.1. Depolymerization of Chitosan

Chitosan was successfully depolymerized and the formation of LMWC was indicated by a reduction in the viscosity of the chitosan solution. LMWC was soluble in water at pH 7.4.

3.2. Fractionation and Molecular Weight Determination

The molecular weights of the fractions were determined by GPC and are shown in Table 3. The chitosan fraction with average molecular weight of 6504 was the major fraction (~64%) and was used for further studies. Low polydispersity index (1.16) of the major fraction as well as the lower yields of other chitosan fractions (ranging from 1 to 11%) indicated that the depolymerization followed by fractionation by SEC led to the generation of soluble, low molecular weight chitosan fractions having narrow molecular weight distribution.

3.3. Synthesis of N-acyl LMWCs

N-acyl LMWCs were synthesized by EDC/NHS mediated grafting of fatty acids (myristic, palmitic, stearic, arachidic, oleic, linoleic and linolenic acids) on LMWC (average molecular weight ~6500 Da). Synthesized products were characterized for their structure using IR spectroscopy and elemental analysis.

3.4. Structural Characterization N-acyl LMWCs

The IR spectra of LMWC and N-acyl LMWC were analyzed using KnowItAll® Informatics System (Bio-Rad, CA) in order to confirm the reaction between fatty acids and LMWC (Figure 8). The increase in the intensity of asymmetric stretching band at the 2936 to 2916 cm^{-1} and symmetric stretching band at 2863 to 2843 cm^{-1} indicated that the alkyl chains of the fatty acids had been successfully attached to the chitosan backbone. An increase in the

intensity of C=O stretching band at 1680 to 1630 cm^{-1}, amide II and amide III combination bands at 1570 to 1515 cm^{-1} and 1305 to 1200 cm^{-1}, respectively, and C-N stretching bands at wavenumber 1140 to 1080 cm^{-1} indicated the formation of amide bonds.

The degree of substitution was determined using the following equation of Baxter et al (Baxter et al., 1992)

$$\% \text{ N-Substitution } (\% \text{ DS}) = (A_{1655}/A_{3450}) \times 115$$

The calculated % DS values (indicating the % free amine groups being substituted) are shown in table 4. The results were confirmed using elemental analysis for percentages of C, H and N in the polymers.

Table 3: Molecular weight distribution of depolymerized chitosan fractions

Fraction	Average Molecular Weight	Weight Average Molecular Weight (M_W)	Number Average Molecular Weight (M_N)	Polydispersity Index (PDI, M_W/M_N)	% Yield
1	39245	39912	32449	1.23	2
2	36102	35741	28593	1.25	3
3	32709	33265	25787	1.29	3
4	25113	24862	18967	1.31	3
5	21673	22041	17040	1.29	10
6	9322	9229	8240	1.12	11
7	6504	6615	5702	1.16	64
8	3725	3688	3073	1.20	3
9	12643	12858	8868	1.45	1

Table 4: Determination of the degree of substitution by IR spectroscopy and elemental analysis

Polymer	Degree of substitution (%)	% C in Polymer		% N in Polymer		% H in Polymer	
	From IR data	Based on IR data	Based on elemental analysis)	Based on IR data	Based on elemental analysis)	Based on IR data	Based on elemental analysis)
LMWC	16	44.80	45.48	8.28	8.55	7.37	7.17
N-Myristoyl LMWC	31	53.45	54.52	6.25	5.95	8.62	8.29
N-Palmitoyl LMWC	39	56.17	53.87	5.65	5.57	9.06	9.30
N-Stearoyl LMWC	37	56.81	54.59	5.55	5.51	9.18	8.90
N-Arachidoyl LMWC	33	56.83	56.15	5.57	5.84	9.21	9.63
N-Oleoyl LMWC	36	56.73	54.91	5.61	5.88	8.93	8.65
N-Linoleoyl LMWC	35	56.64	56.52	5.68	5.63	8.68	8.88
N-Linolenoyl LMWC	39	57.68	57.57	5.49	5.28	8.54	8.55

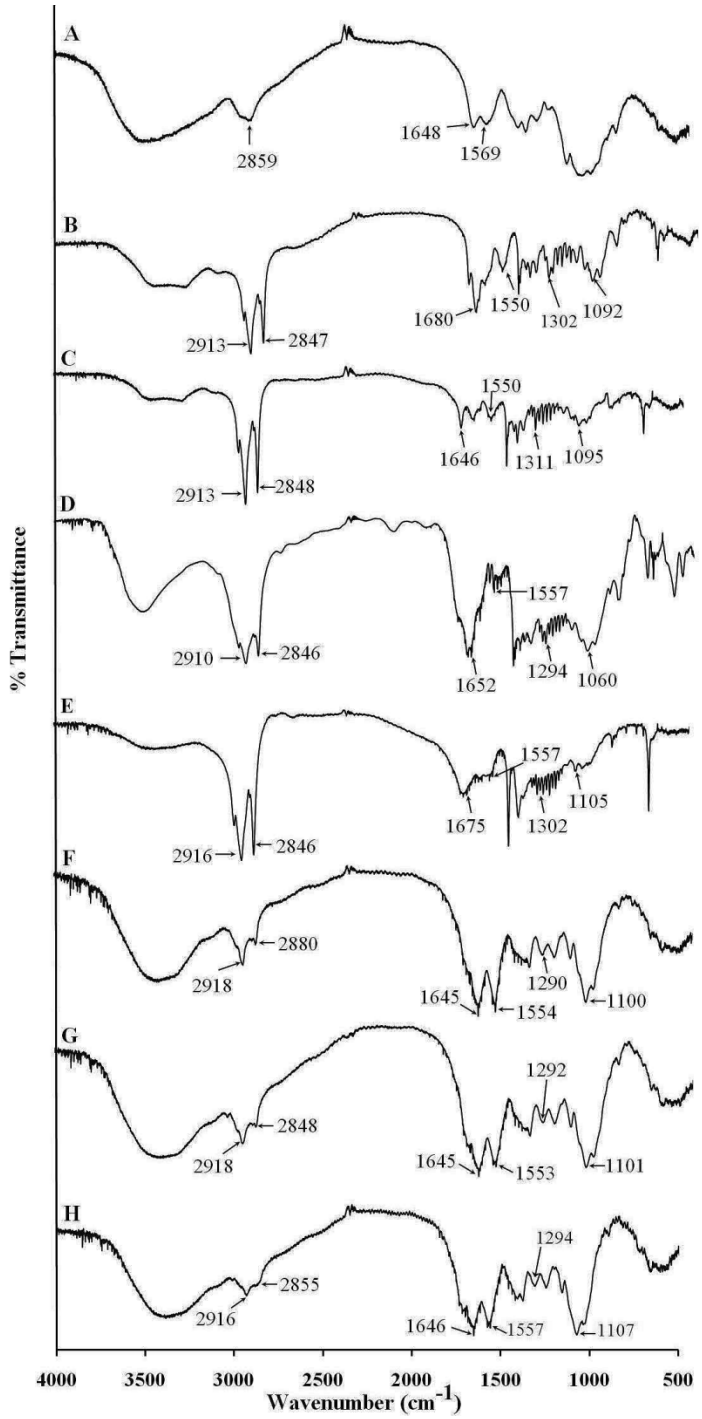

Figure 8: Infrared spectra of LMWC and N-acyl LMWC
(A) LMWC, (B) Myristic acid derivative, (C) Palmitic acid derivative, (D) Stearic acid derivative, (E) Arachidic acid derivative, (F) Oleic acid derivative, (G) Linoleic acid derivative and (H) Linolenic acid derivative of LMWC

3.5. Determination of Critical Micellar Concentration (CMC) of N-acyl LMWC

The CMC values N-acyl LMWCs are shown in table 5. Generally, the unsaturated fatty acyl grafted LMWC exhibited lower CMC values, which could be attributed to increased hydrophobicity of the N-acyl grafts due to presence of unsaturation.

Table 5: Degree of substitution and CMC values for N-acyl LMWCs

Polymer	Degree of substitution (%)	CMC (mg/ml)
N-Myristoyl LMWC	31	< 0.0313
N-Palmitoyl LMWC	39	< 0.0625
N-Stearoyl LMWC	37	< 0.0625
N-Arachidoyl LMWC	33	< 0.0313
N-Oleoyl LMWC	36	< 0.0156
N-Linoleoyl LMWC	35	< 0.0313
N-Linolenoyl LMWC	39	< 0.0156

3.6. Topology, Hydrodynamic Size and Zeta Potential Characterization for N-acyl LMWC: Effect of Formulation Parameters

3.6.1. Effect of pH, sonication duration and filtration on hydrodynamic size and zeta potential of N-acyl LMWC

The effects of pH, sonication duration and filtration through 0.8 μ membrane on the physicochemical properties of N-acyl LMWCs are shown in figures 9-16. It was observed that sonication duration and filtration affected the hydrodynamic size of the N-acyl LMWC nanomicelles while pH had little effect. Increasing the sonication duration up to 5 min and filtering the N-acyl LMWC nanomicelles through a 0.8 μ membrane led to formation of nanomicelles smaller than 100 nm with narrow size distribution. On the other hand, the zeta

potential was not affected by sonication duration and filtration. However, as pH increased, the zeta potential of the nanomicelles decreased for all polymers.

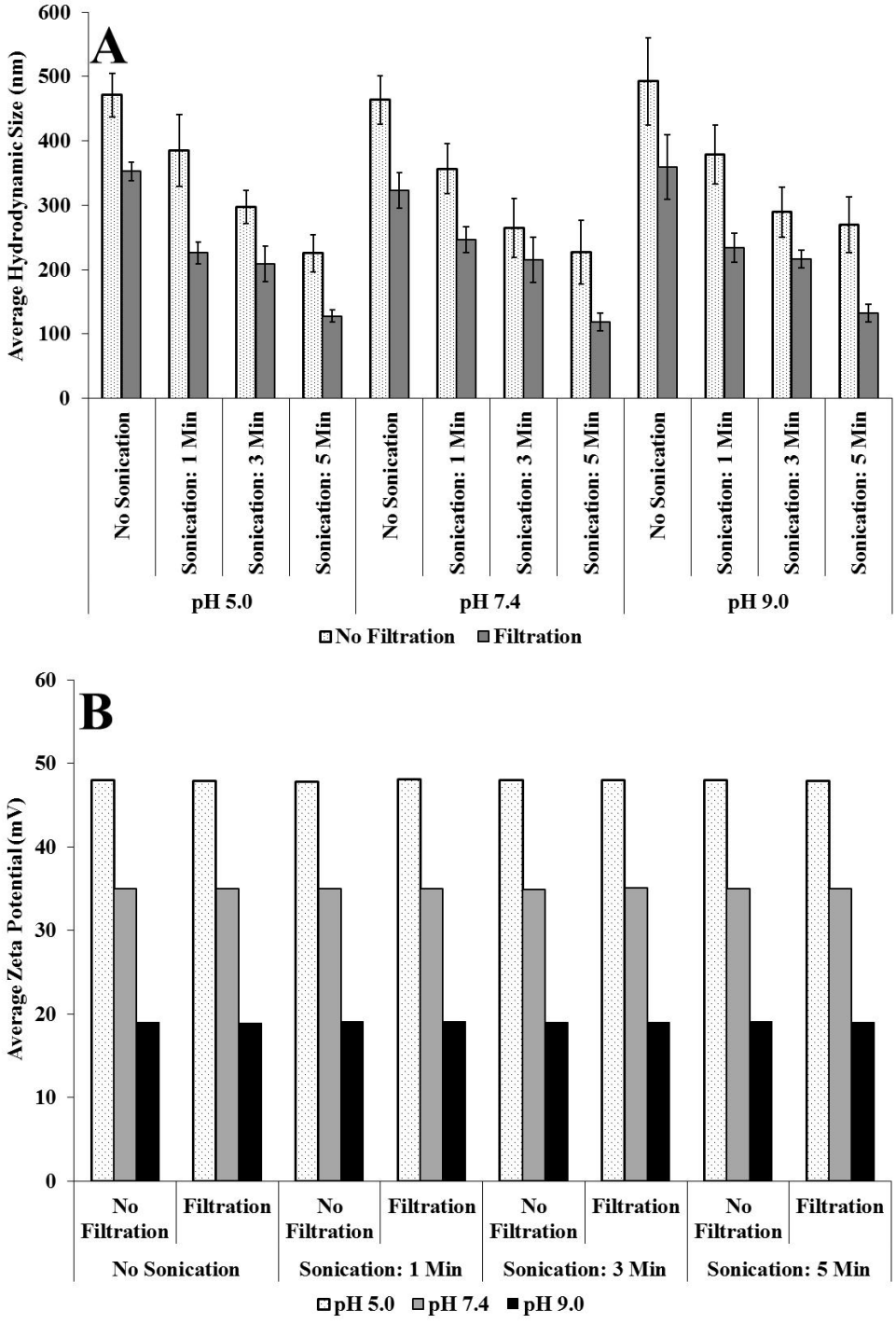

Figure 9: Effect of pH, sonication and filtration on the average hydrodynamic size (A) and zeta potential (B) of N-Myristoyl LMWC nanomicelles

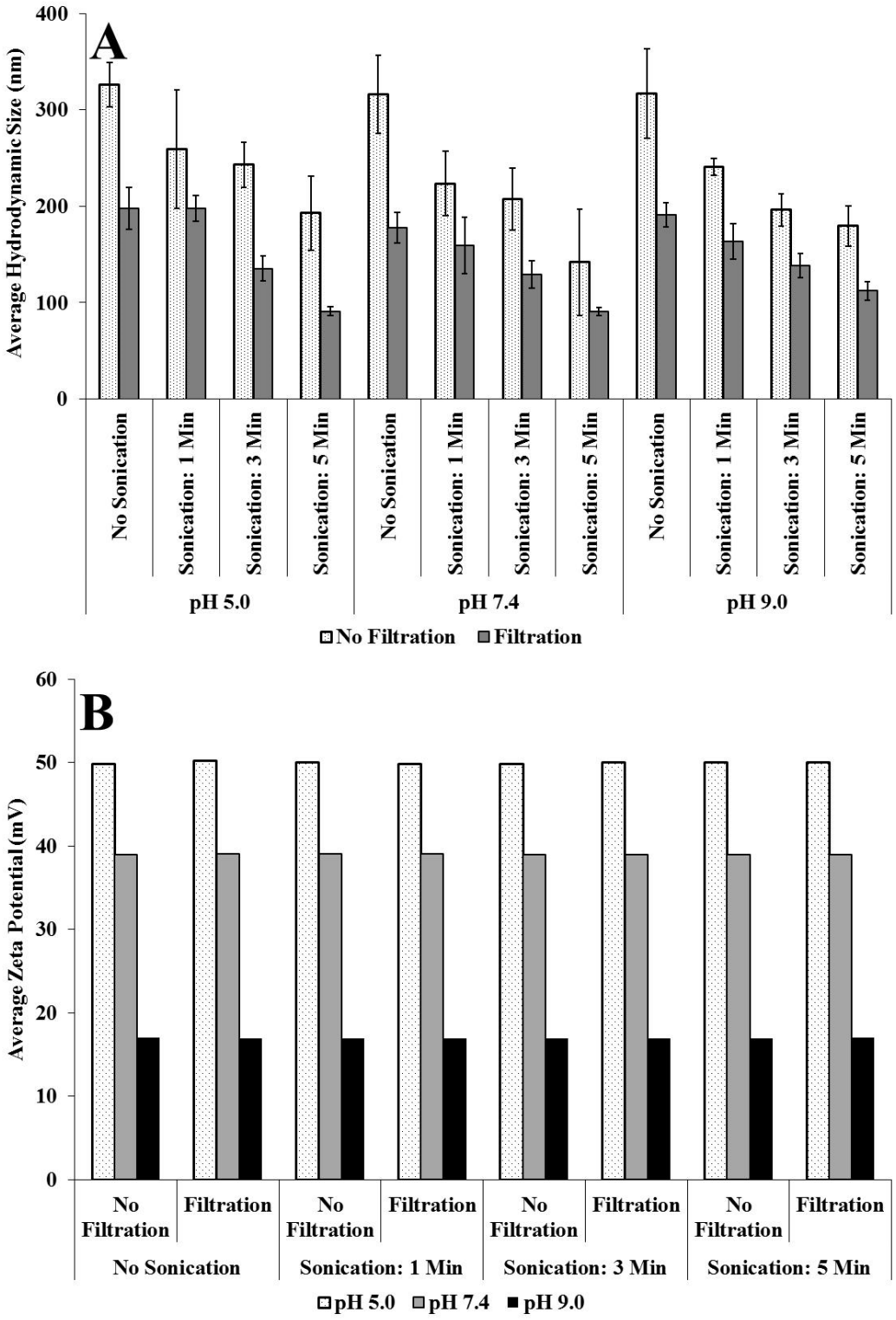

Figure 10: Effect of pH, sonication and filtration on the average hydrodynamic size (A) and zeta potential (B) of N-Palmitoyl LMWC nanomicelles

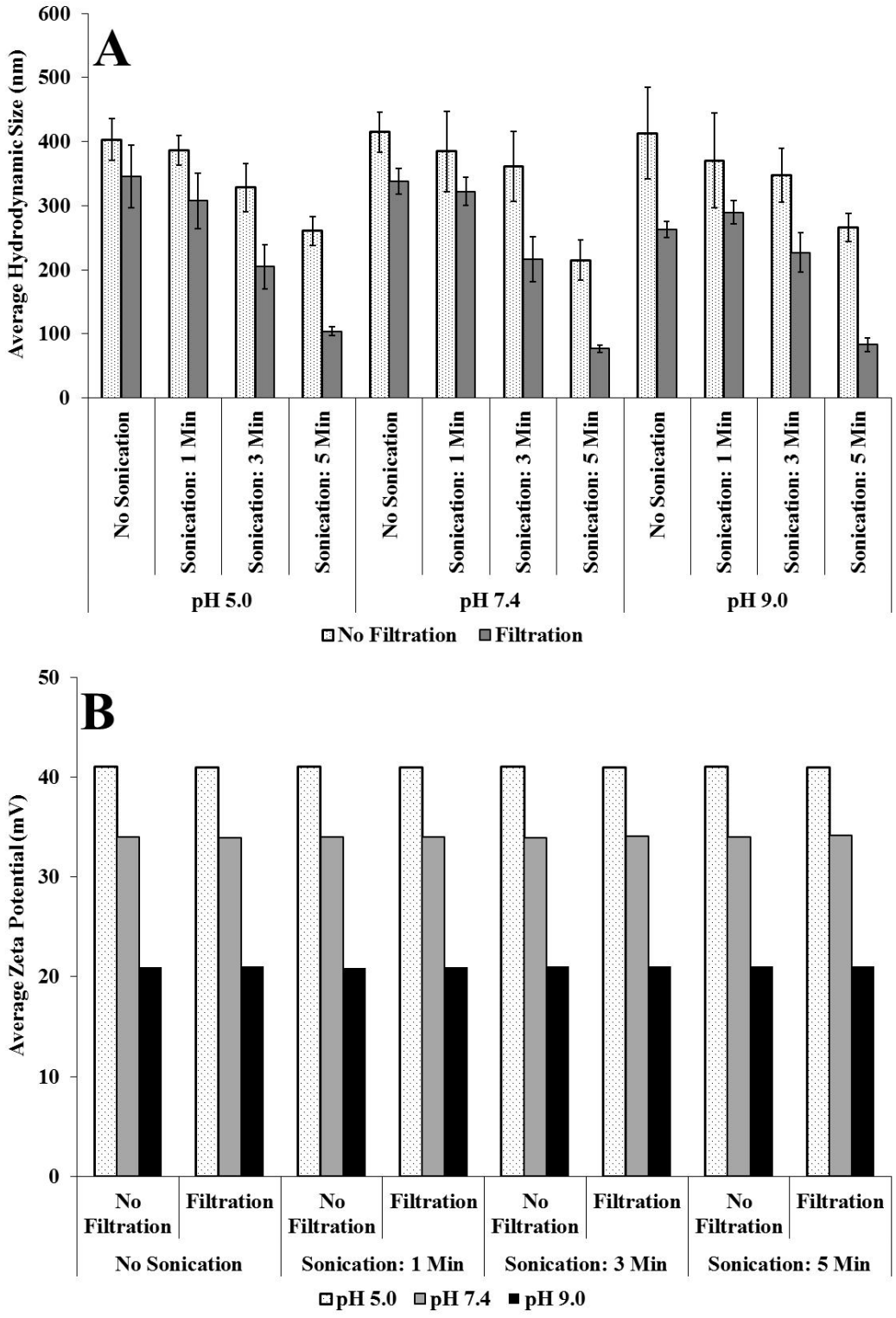

Figure 11: Effect of pH, sonication and filtration on the average hydrodynamic size (A) and zeta potential (B) of N-Stearoyl LMWC nanomicelles

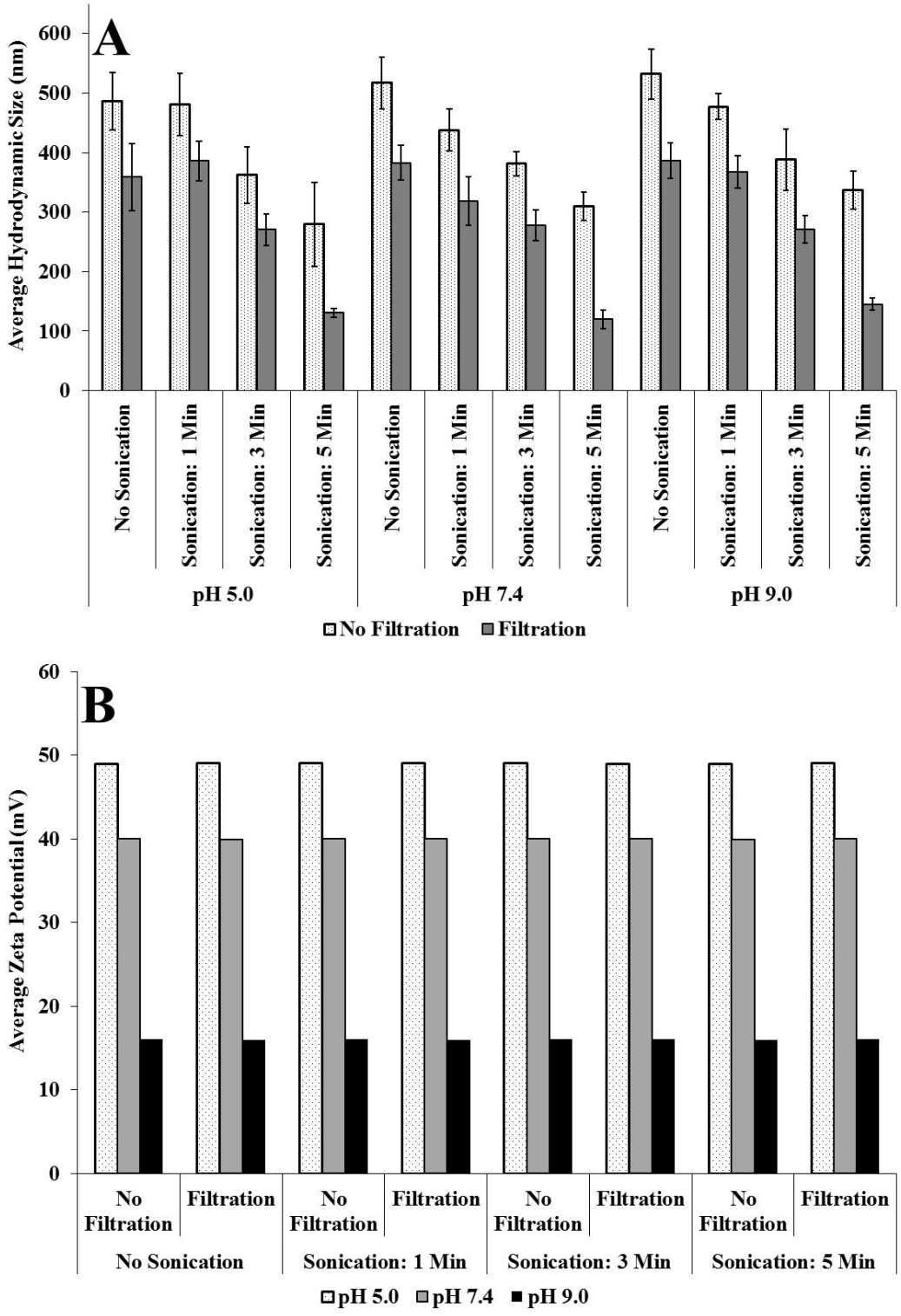

Figure 12: Effect of pH, sonication and filtration on the average hydrodynamic size (A) and zeta potential (B) of N-Arachidoyl LMWC nanomicelles

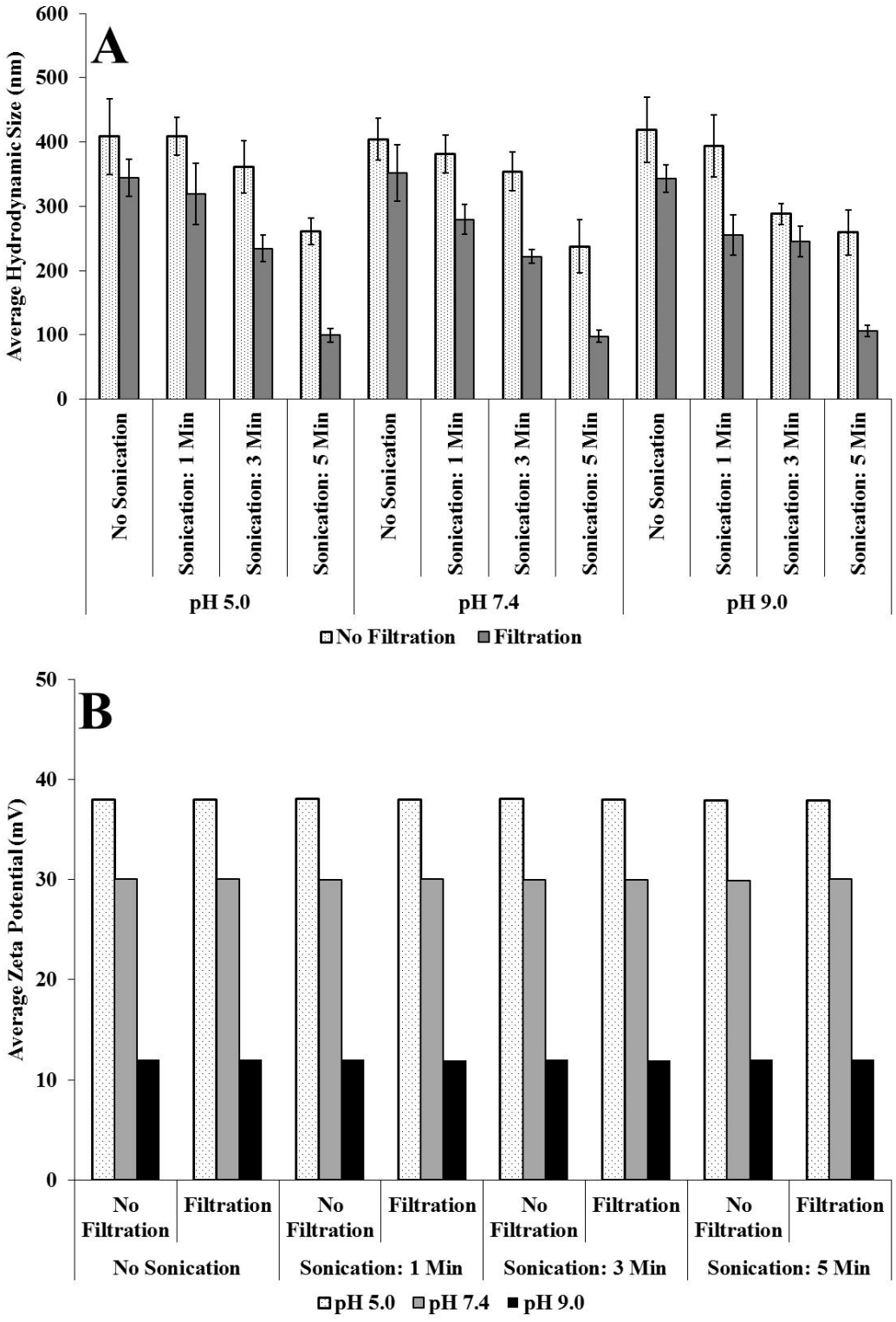

Figure 13: Effect of pH, sonication and filtration on the average hydrodynamic size (A) and zeta potential (B) of N-Oleoyl LMWC nanomicelles

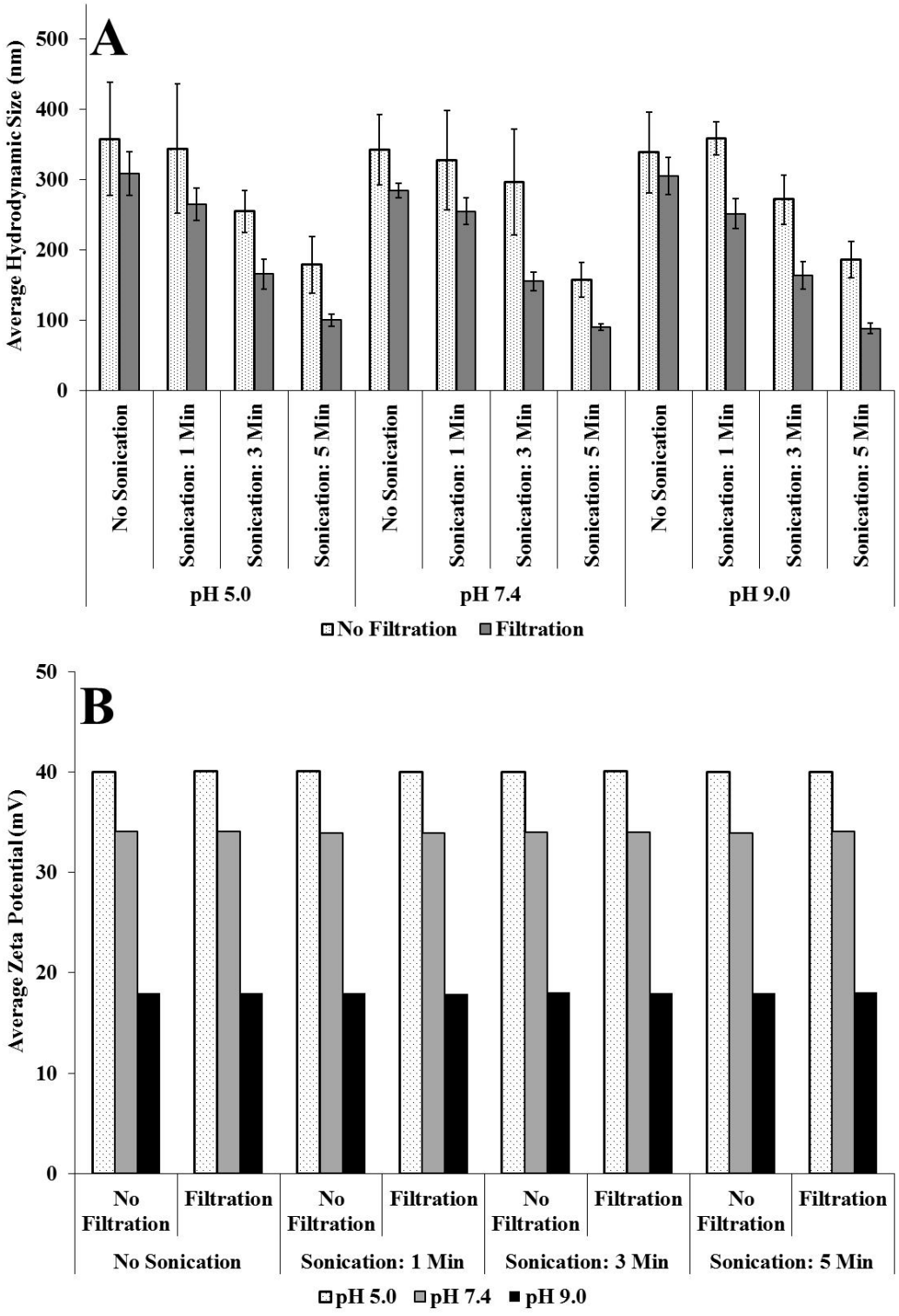

Figure 14: Effect of pH, sonication and filtration on the average hydrodynamic size (A) and zeta potential (B) of N-Linoleoyl LMWC nanomicelles

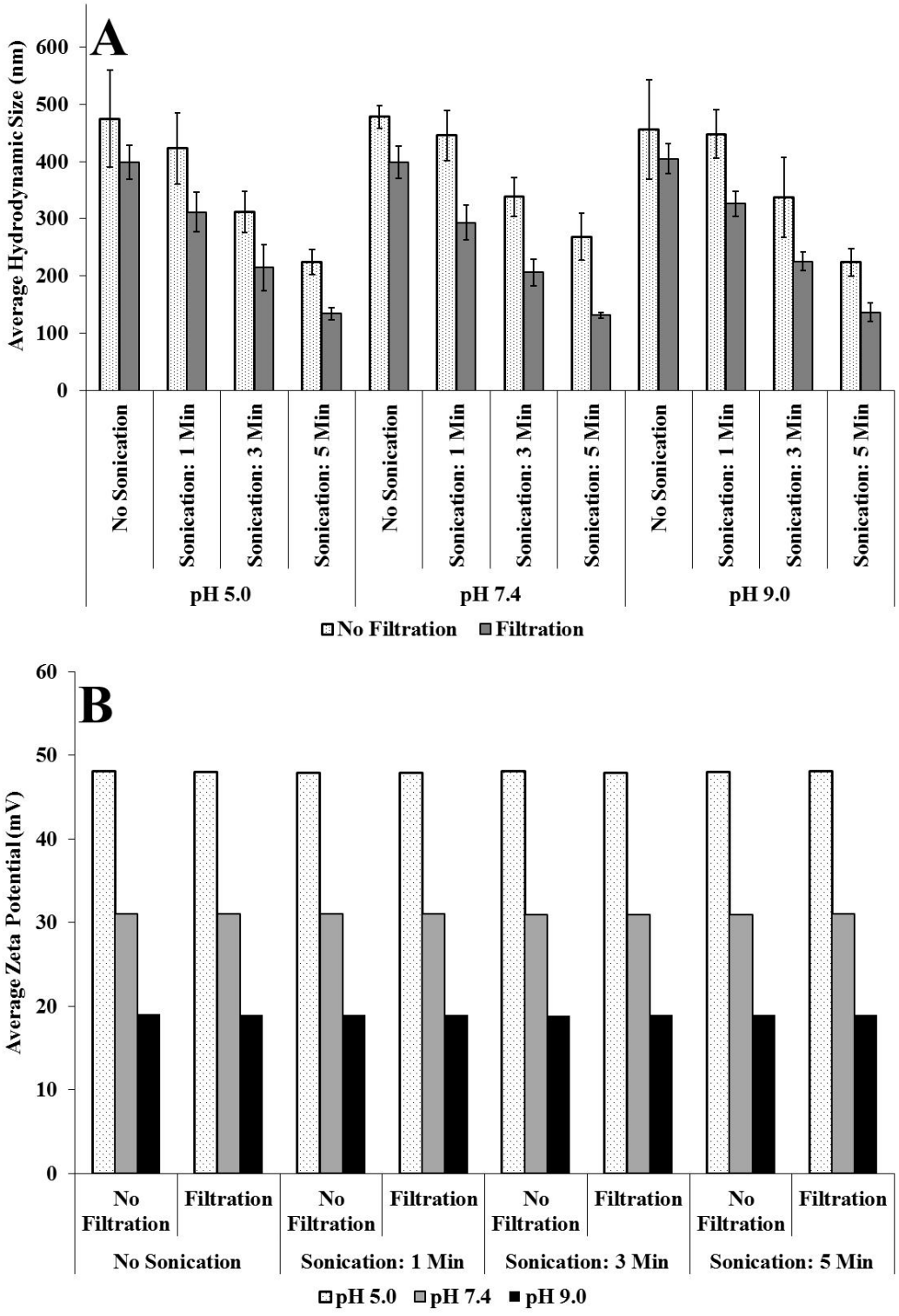

Figure 15: Effect of pH, sonication and filtration on the average hydrodynamic size (A) and zeta potential (B) of N-Linolenoyl LMWC nanomicelles

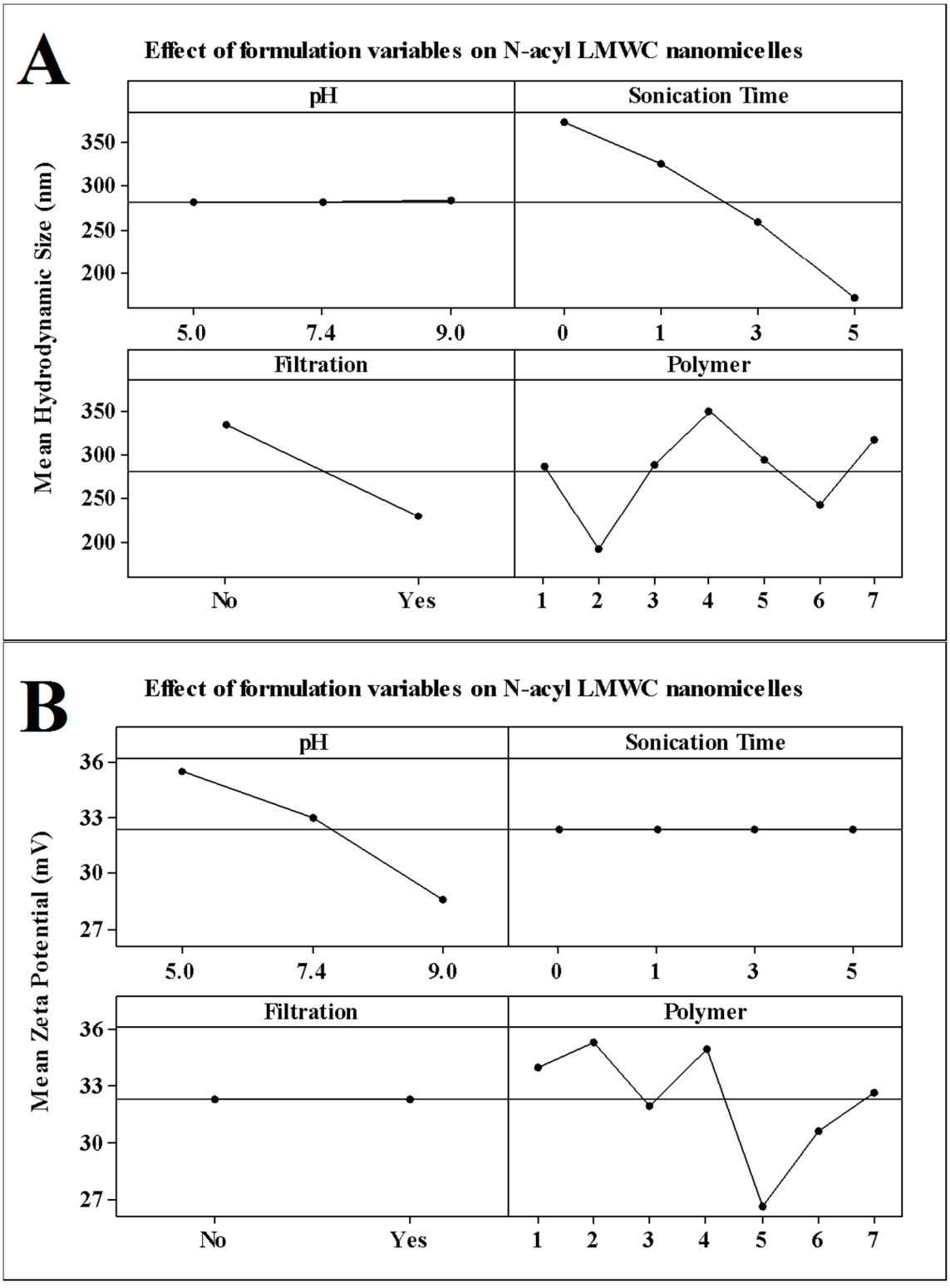

Figure 16: Effect of pH, sonication and filtration on the average hydrodynamic size (A) and zeta potential (B) of N-acyl LMWC nanomicelles

3.6.2. Effect of DNA addition on surface topology of N-acyl LMWC nanomicelles

Figure 17 (A-G) shows the AFM images for N-acyl LMWC nanomicelles before (I) and after (II) addition of plasmid DNA. AFM studies revealed that, upon addition of plasmid DNA, there was no apparent change in the surface topology of the nanomicelles, indicating that the N-acyl LMWC were able to form stable and compact complexes with the DNA.

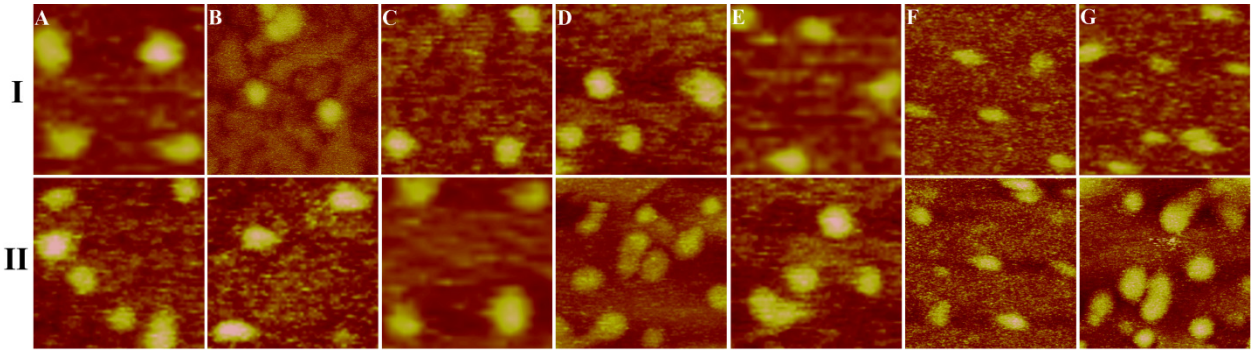

Figure 17: Atomic force microscopy images of N-acyl LMWC nanomicelles (A) Myristic acid derivative, (B) Palmitic acid derivative, (C) Stearic acid derivative, (D) Arachidic acid derivative, (E) Oleic acid derivative, (F) Linoleic acid derivative and (G) Linolenic acid derivative of LMWC before (I) and after (II) addition of DNA. Each panel in the image represents a scan area of 1 µm x 1 µm

3.6.3. Effect of DNA addition on hydrodynamic size and zeta potential of N-acyl LMWC

The DNA addition had impact on the hydrodynamic size and zeta potential of the nanomicelles as seen in figure 4. Overall, hydrodynamic size slightly increased while the zeta potential decreased significantly ($p<0.05$) upon addition of DNA. The insignificant increase in the micellar size indicated that the pDNA was effectively compacted by the cationic nanomicelles. Upon storage for 7 days, the N-acyl LMWC/DNA polyplexes exhibited a tendency to aggregate and increase in size. However, it was noticed that this aggregation could be reversed by simple vortex mixing.

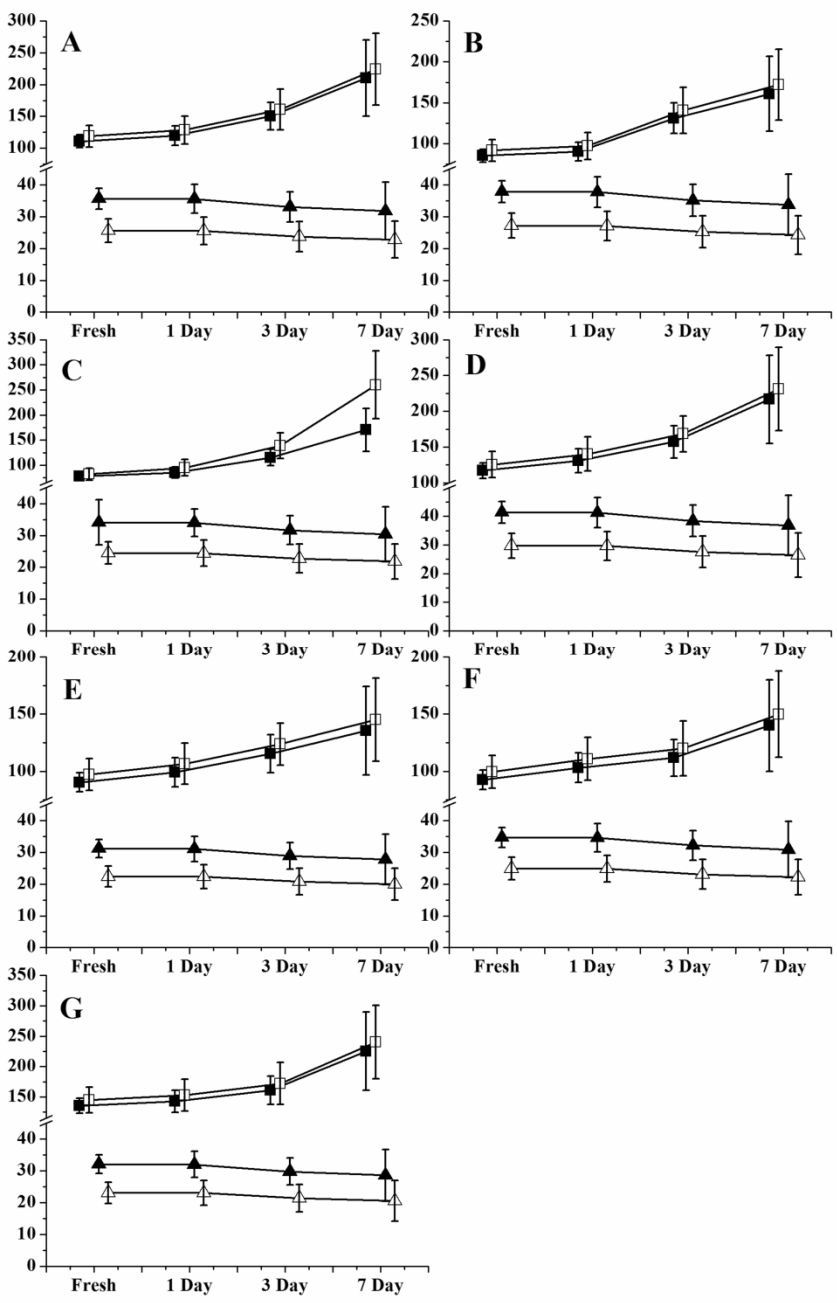

Figure 18: Hydrodynamic size (nm) before (■) and after (□) addition of DNA and zeta potential (mV) before (▲) and after (Δ) addition of DNA
for (A) Myristic acid derivative, (B) Palmitic acid derivative, (C) Stearic acid derivative, (D) Arachidic acid derivative, (E) Oleic acid derivative, (F) Linoleic acid derivative and (G) Linolenic acid derivative of LMWC. Vertical bars indicate standard deviation (N=4)

3.7. Buffering Ability Results

The results of buffering ability determination by titrimetric analysis are shown in figure 19. It was observed that, though the N-acyl LMWC had lower buffering ability than the parent LMWC; they could still resist the drop in pH caused by the addition of 0.1 N HCl.

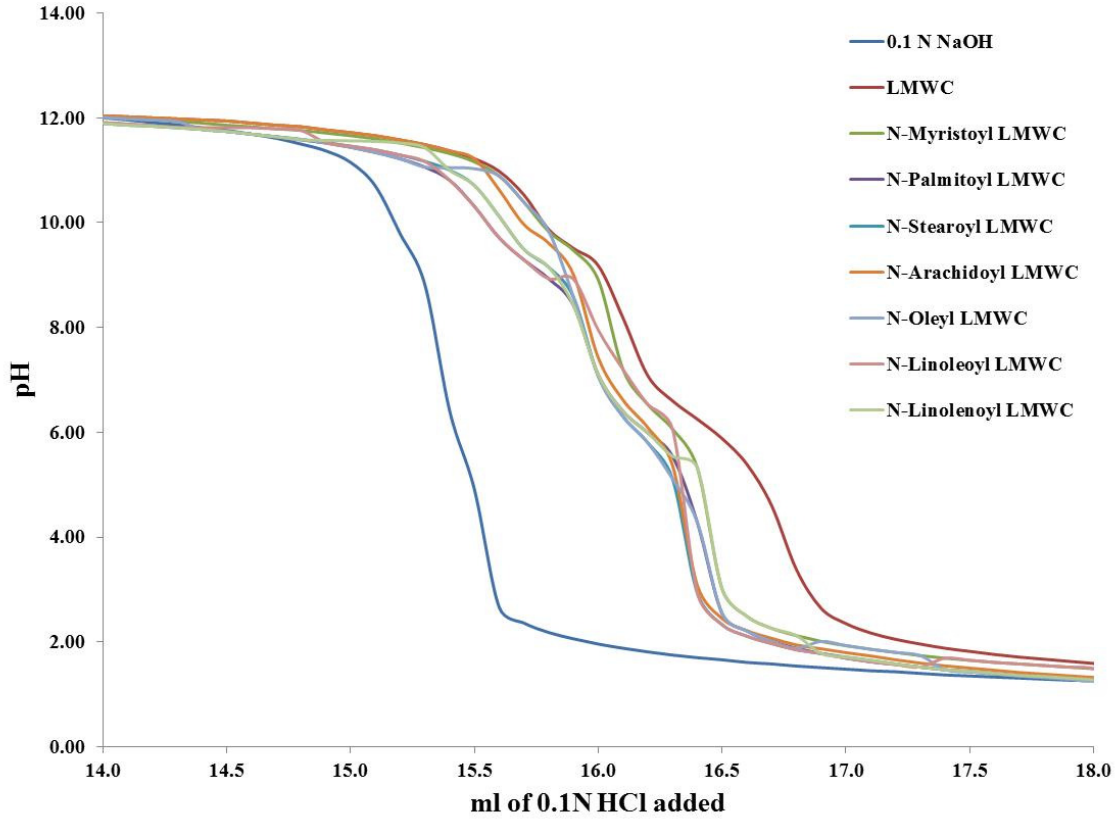

Figure 19: Buffering ability of N-acyl LMWC nanomicelles

3.8. Optimization of N:P Ratio

The N:P ratio was optimized in HEK293 cells using a plasmid encoding β-galctosidase and the results are shown in figure 20. Since N:P ratio of 20:1 led to expression of maximum amount of β-galactosidase per mg of protein for N-palmitoyl LMWC and N-stearoyl LMWC, this N:p ratio was chosen for further experiments.

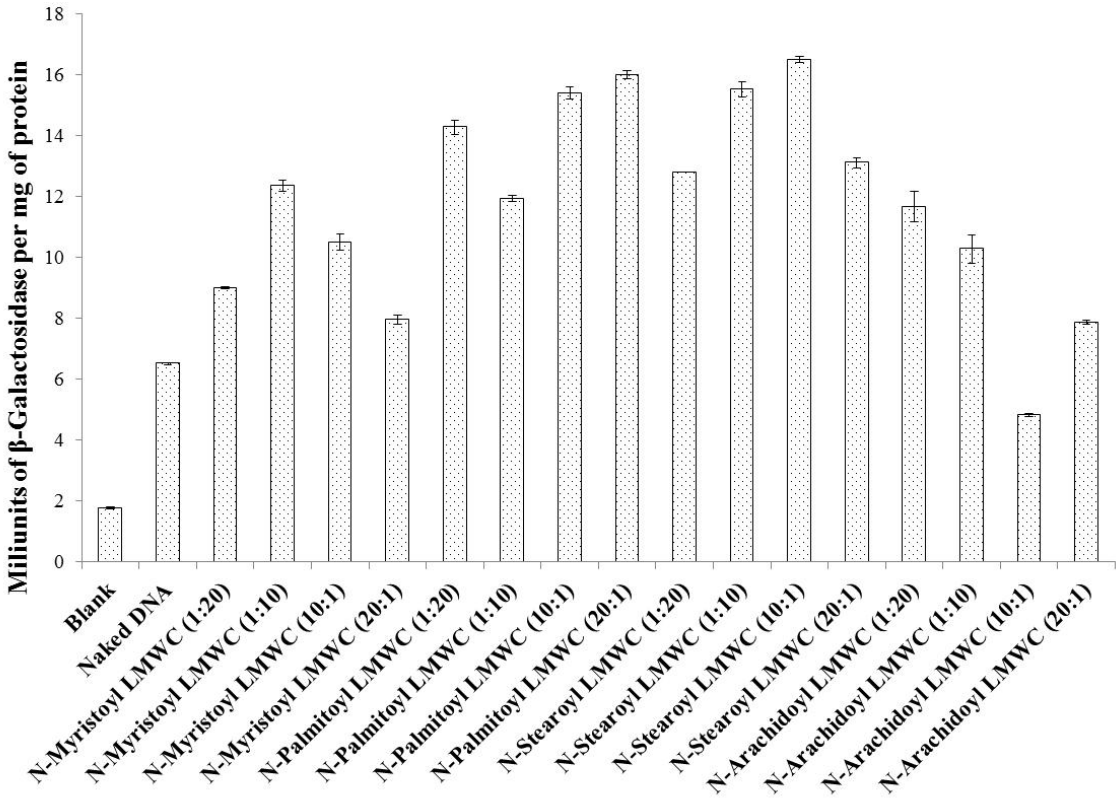

Figure 20: Optimization of N:P ratios for transfection experiments.
Vertical bars represent standard deviation (N=4)

3.9. Stability Evaluation of the Formulations

3.9.1. Storage stability of N-acyl LMWC/pDNA polyplexes

The migration of the polyplexes between N-acyl LMWC and pDNA was completely retarded during agarose gel electrophoresis at 30 min post-formation (Figure 21). Similarly, complete retardation of the polyplexes at 7 days post-formation (Figure 22 [L-S]) indicated that the polyplexes were stable up to 7 days upon storage at 4°C.

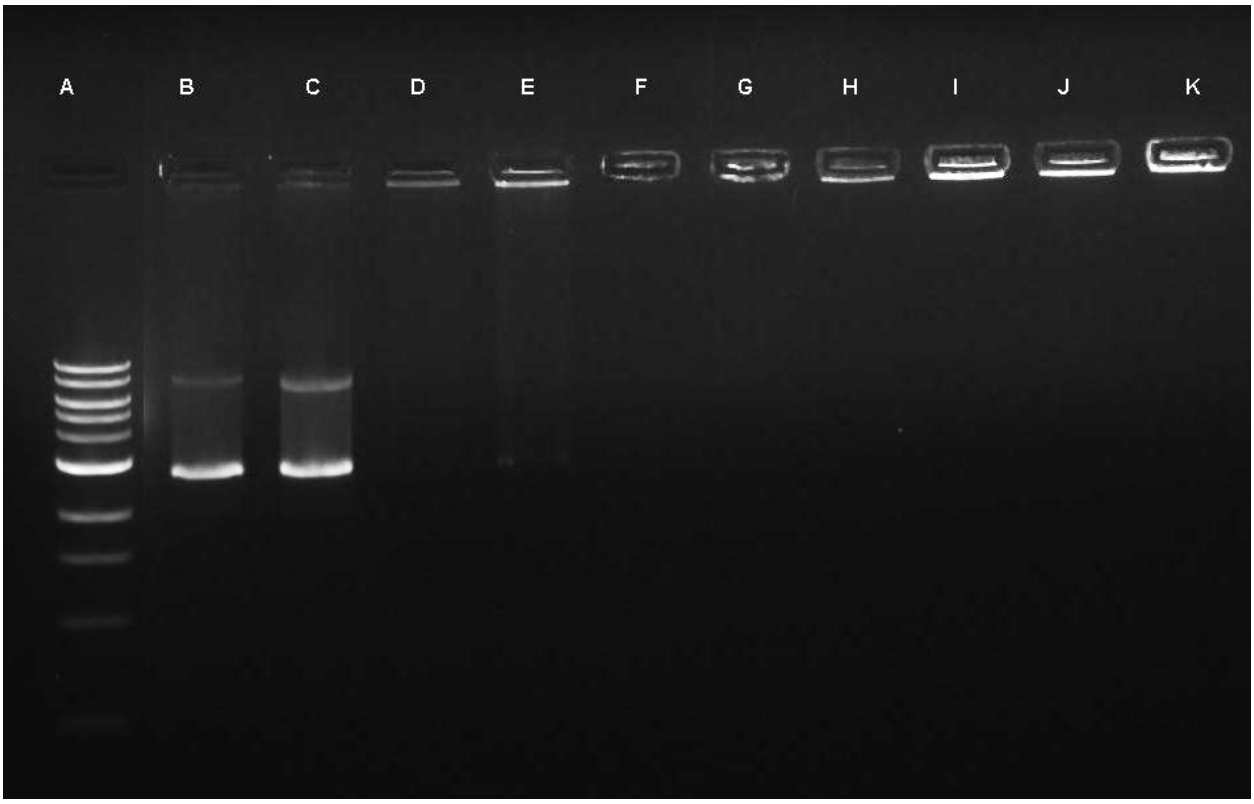

Figure 21: DNA binding ability of N-acyl LMWC
DNA ladder (A), Plasmid (gWIZ™ Blank) at 0.1µg/ml (B) and 1µg/ml (C) and polyplexes of gWIZ™ Blank with (D) LMWC, (E) Myristic acid derivative, (F) Palmitic acid derivative, (G) Stearic acid derivative, (H) Arachidic acid derivative, (I) Oleic acid derivative, (J) Linoleic acid derivative and (K) Linolenic acid derivative of LMWC

3.9.2. Stability of DNA released from N-acyl LMWC/pDNA polyplexes and DNase protection assay

The ability of the N-acyl LMWC polyplexes to protect the DNA from degradation by DNase I was evident from the DNase I protection studies. It could be observed that the DNA, which was not complexed with chitosan or N-acyl LMWC, was completely degraded after incubation with DNase I. The DNA complexed with either chitosan or N-acyl LMWC was protected from such degradation as seen in during the agarose gel electrophoresis of the released DNA.

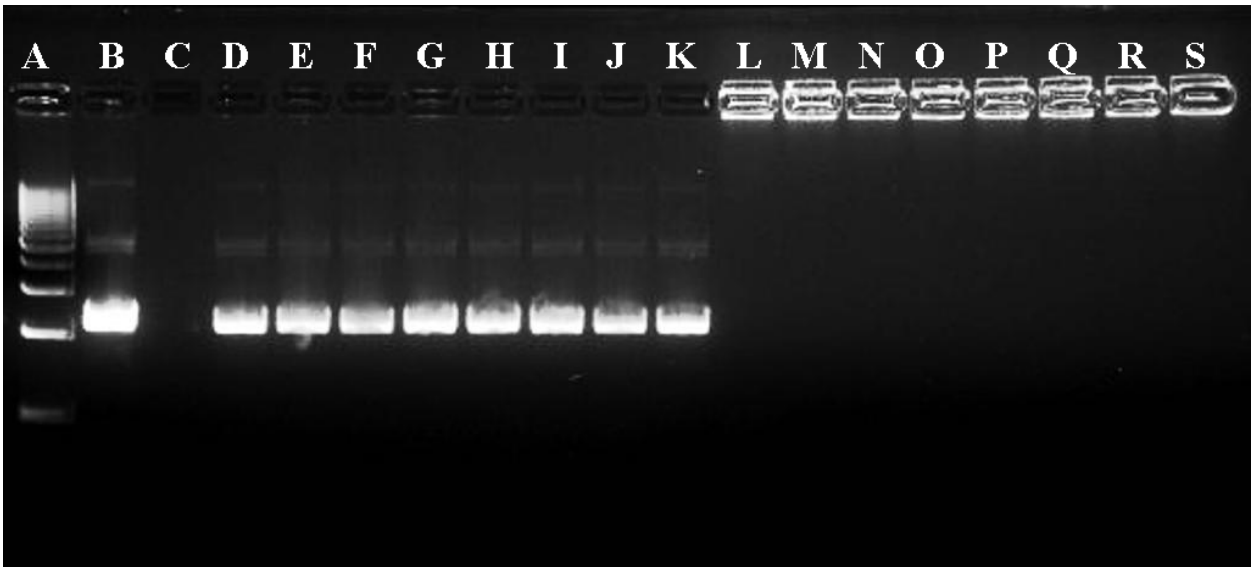

Figure 22: DNase protection assay and storage stability
DNA ladder (A), Freshly prepared plasmid solution (B), Plasmid solution incubated with DNase I (C), DNA released from polyplexes of LMWC (D), Myristic acid derivative (E), Palmitic acid derivative (F), Stearic acid derivative (G), Arachidic acid derivative (H), Oleic acid derivative (I), Linoleic acid derivative (J) and Linolenic acid derivative (K) of LMWC after incubation with DNase I. Storage stability of polyplexes at 7 days for polyplexes of LMWC (L), Myristic acid derivative (M), Palmitic acid derivative (N), Stearic acid derivative (O), Arachidic acid derivative (P), Oleic acid derivative (Q), Linoleic acid derivative (R), and Linolenic acid derivative (S) of LMWC

3.10. Determination of In Vitro Cytotoxicity of N-acyl LMWC Nanomicelles

The in vitro cytotoxicity of N-acyl LMWC was tested in HEK293 cells and the results are presented in figure 23. It was observed that neither LMWC nor any of its fatty acyl derivatives exhibited significant ($p<0.05$) toxicity in the tested concentration range of 1-2.5 mg/ml relative to the untreated cells.

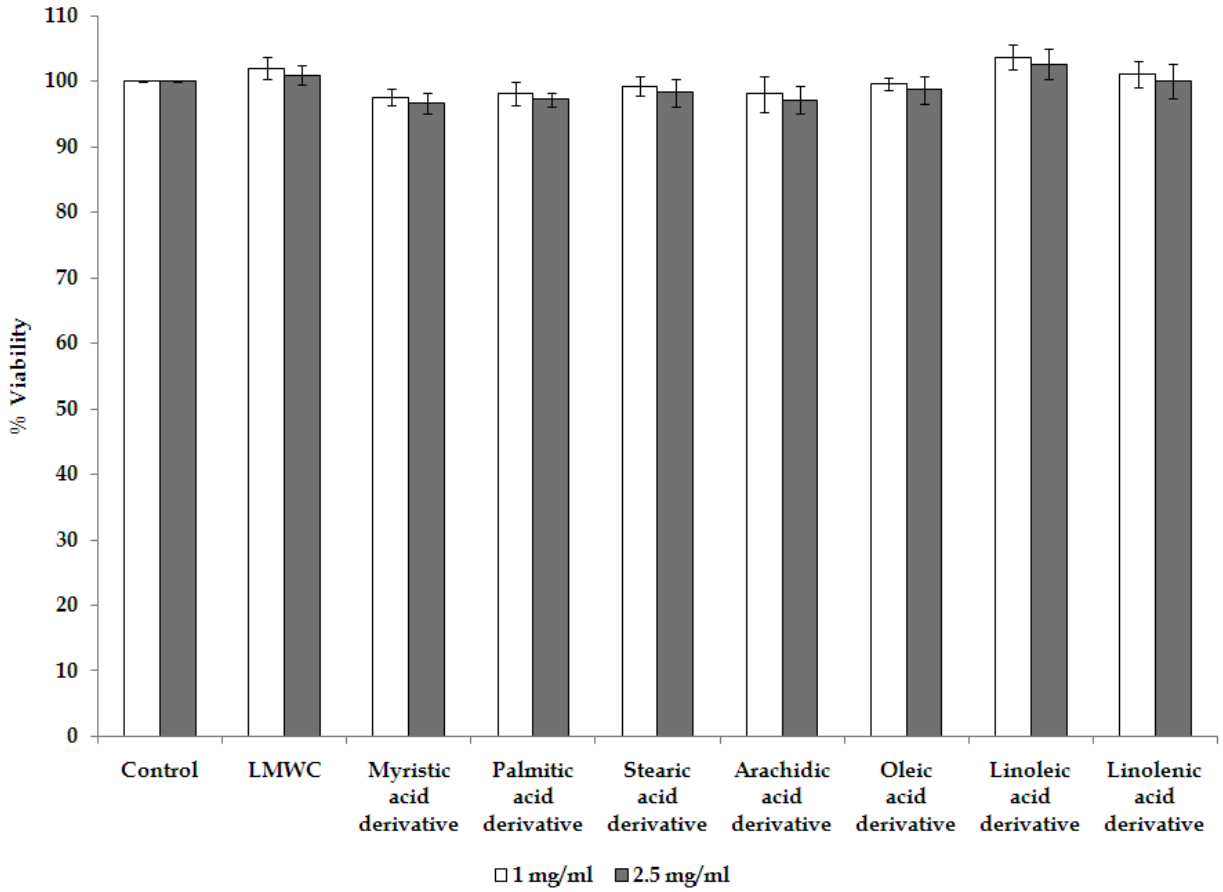

Figure 23: Evaluation of cytotoxicity of LMWC and N-acyl LMWC using MTT assay. Vertical bars indicate standard deviation (N=4)

3.11. Visualization of Transfection Ability of the N-acyl LMWC Nanomicelles Using Confocal Microscopy

Transfection efficiency of the N-acyl LMWC polyplexes was visualized using a confocal laser scanning microscope. An N:P ratio of 20:1 was used. This data is shown in figure 24 (A-J). The N-acyl LMWCs synthesized using oleic and linoleic acids exhibited higher transfection compared to LMWC and comparable transfection to FuGENE HD (illustrated by the green fluorescence in the cytosol). The transfections exhibited by other N-acyl LMWCs were lower when compared to FuGENE HD, as well as oleic and linoleic acid derivatives.

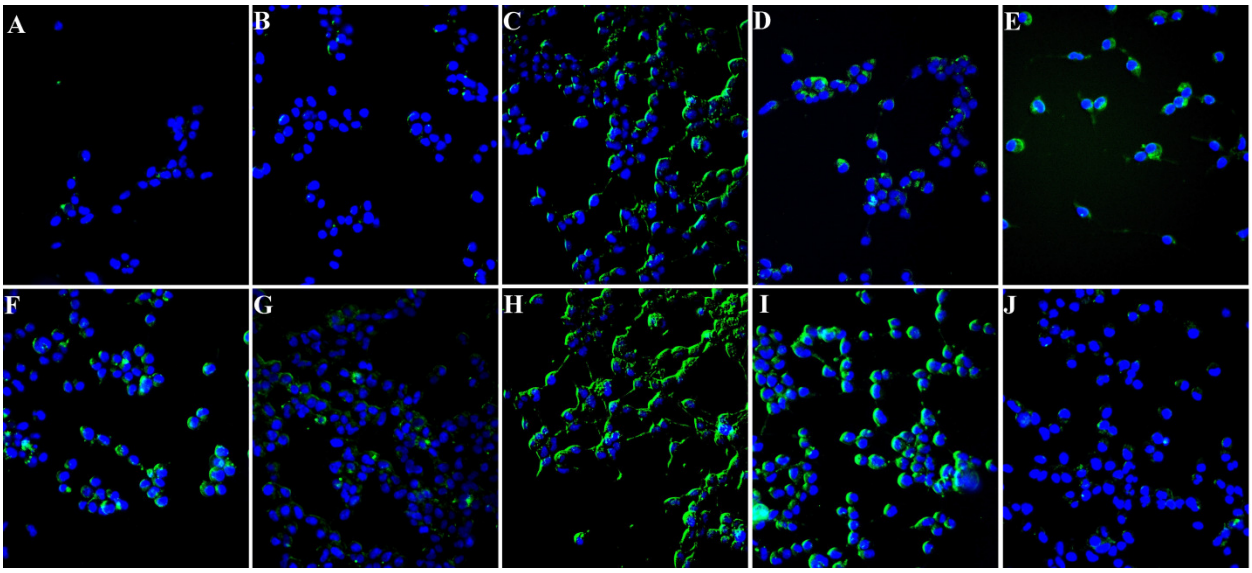

Figure 24: Expression of GFP at 72 h post-transfection
for naked DNA (A), LMWC (B), FuGENE HD (C), Myristic acid derivative (D), Palmitic acid derivative (E), Stearic acid derivative (F), Arachidic acid derivative (G), Oleic acid derivative (H), Linoleic acid derivative (I) and Linolenic acid derivative (J) of LMWC. The nuclei are stained with DAPI (blue). Magnification 40X

3.12. In Vitro Transfection Efficiency of N-acyl LMWC/pDNA Polyplexes

The transfection ability of the N-acyl LMWC polyplexes quantified using HEK293 cells is presented in figure 25. The ratio of milliunits of β-galactosidase per milligram of protein in the cell lysate was used as an indicator of transfection efficiency. It was observed that the N-acyl LMWC/pDNA polyplexes exhibited significantly ($p<0.05$) higher transfection efficiency as compared to respective controls (Figure 25). The arachidic acid derivative of LMWC was significantly ($p<0.05$) more efficient as compared to naked DNA but was comparable with LMWC at all the time points. Myristic acid derivative of LMWC exhibited significantly ($p<0.05$) superior expression of β-galactosidase as compared to both LMWC and naked DNA at 48 and 72 h post-transfection. However, among the N-acyl LMWCs synthesized from saturated fatty acids, stearic acid derivative of LMWC showed overall better transfection at 72 h, and exhibited 2- and 8-folds increase in transfection as compared to LMWC and naked DNA, respectively.

When quantified for expression of therapeutic cytokines IL-4 and IL-10, the unsaturated fatty acyl derivatives performed exceedingly well as compared to naked DNA or LMWC. Though the stearic and linolenic acid derivatives were significantly ($p<0.05$) better than LMWC and naked DNA, they showed less than 50% expression of cytokines as compared to FuGENE HD as shown in figure 26. In contrast, the oleic and linoleic acid derivatives of LMWC were found to be as efficient ($p\geq0.05$) as FuGENE HD and at 72 h, exhibited about 8-fold and 35-fold greater protein expression as compared to LMWC and naked DNA, respectively.

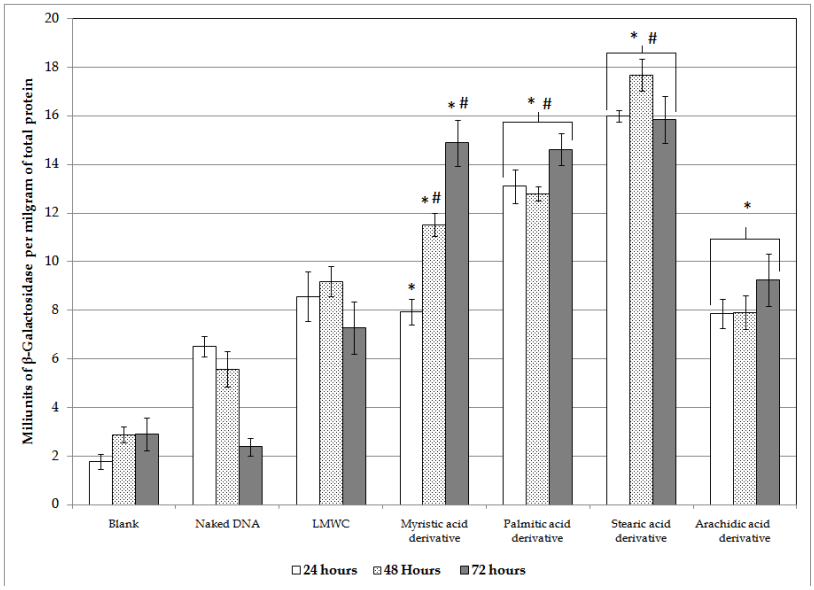

Figure 25: Expression of milliunits of β-galactosidase per milligram of protein for LMWC and N-acyl LMWCs at 24, 48 and 72 h post-transfection at N:P ratio of 20:1. Vertical bars indicate standard deviation (N=4). *=significant compared to naked DNA ($p<0.05$), #= significant compared to LMWC ($p<0.05$)

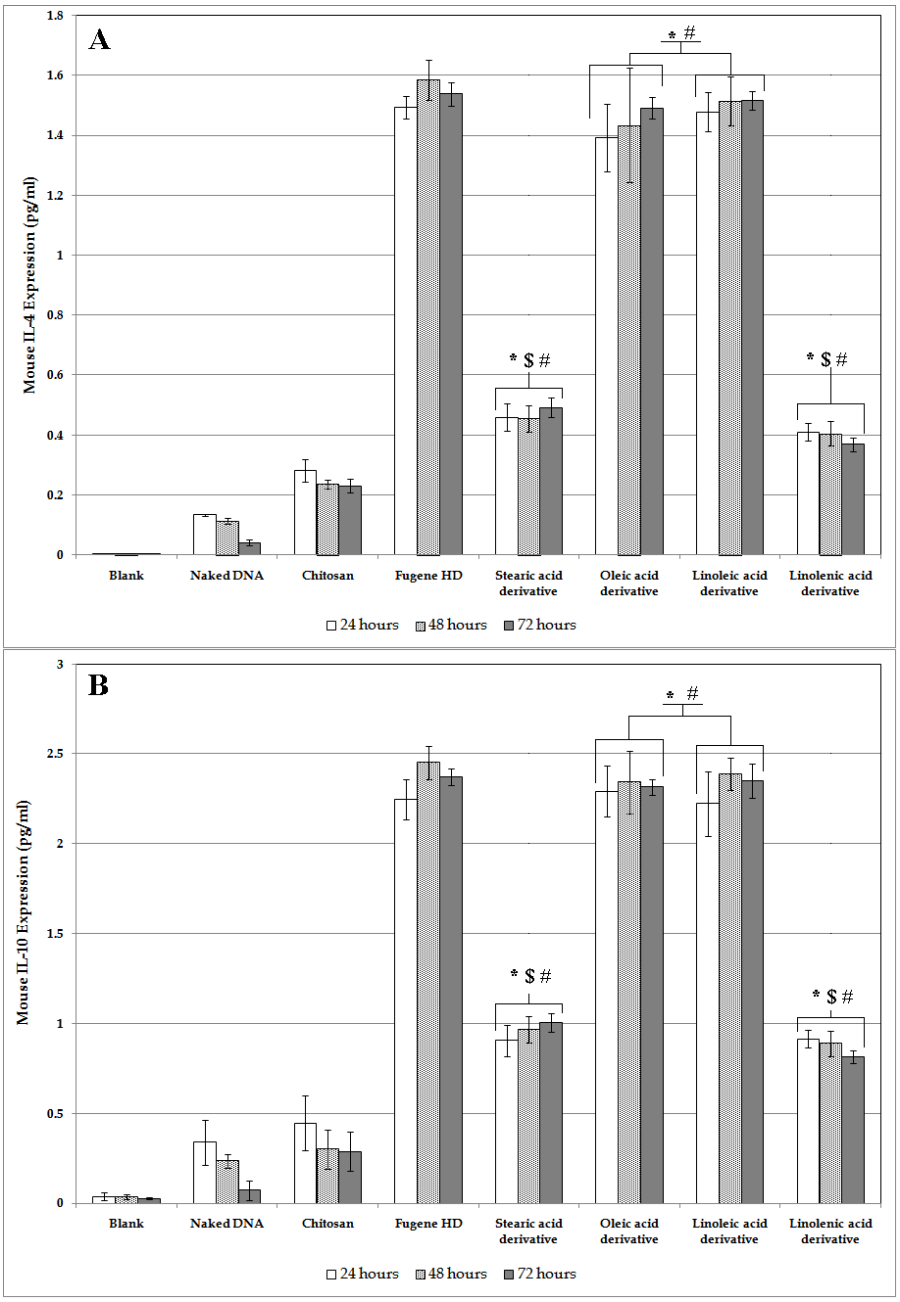

Figure 26: Expression of Interleukin-4 (A) and Interleukin-10 (B) for LMWC, FuGENE HD and N-acyl LMWCs at 24, 48 and 72 h post-transfection at N:P ratio of 20:1. Vertical bars indicate standard deviation (N=4). *=significant compared to naked DNA ($p<0.05$), #= significant compared to LMWC ($p<0.05$), $=significant compared to FuGENE HD ($p<0.05$)

3.13. In Vivo Transfection Efficiency of N-acyl LMWC/pDNA Polyplexes

3.13.1. Blood glucose level determination

The blood glucose levels in mice treated with the polymeric delivery systems as well as the control groups are presented in figure 27 (A-D). It was observed that the blood glucose levels of mice in passive control groups (figure 27-A) (naked plasmid DNA encoding for IL-4, IL-10, mixture of IL-4 and IL-10, and bicistronic plasmid encoding for both IL-4 and IL-10, injected intramuscularly) were significantly higher compared to saline control and were comparable with STZ treatment group from week 1 to 6. This indicates that there is no appreciable advantage of direct injection of naked plasmids in vivo. The animals in the positive control groups where FuGENE HD was used as a delivery vector showed higher blood glucose levels compared to saline control, but were significantly lower than STZ treatment group, indicating the need of a delivery system to deliver the plasmid DNA in vivo (figure 27-B). Among these four positive control groups the blood glucose levels in the animals treated with bicistronic plasmid were lower compared to that of IL-4, IL-10 or mixture of IL-4 and IL-10.

The blood glucose levels of the mice in the treatment groups 11-14, where N-oleoyl LMWC was used as a delivery vector is presented in figure 27-C. It was observed that the blood glucose levels were significantly lower ($p<0.05$) than the streptozotocin control. Even though the mice treated with bicistronic plasmid (group 14) performed better compared to the rest treatment groups, the blood glucose levels were higher than the saline control at all the time points.

The animals treated with plasmid DNA in a N-linoleoyl LMWC micellar system, showed significantly ($p<0.05$) low blood glucose levels as compared to STZ control. When the treatment groups 15-18 were compared among themselves, it was noted again that the group containing N-linoleoyl LMWC delivery system containing bicistronic plasmid performed considerably better.

The blood glucose levels were comparable to saline control and were significantly lower ($p<0.05$) than the groups treated with single gene expression plasmids or physical mixture of IL-4 and IL-10 plasmids (figure 27-D).

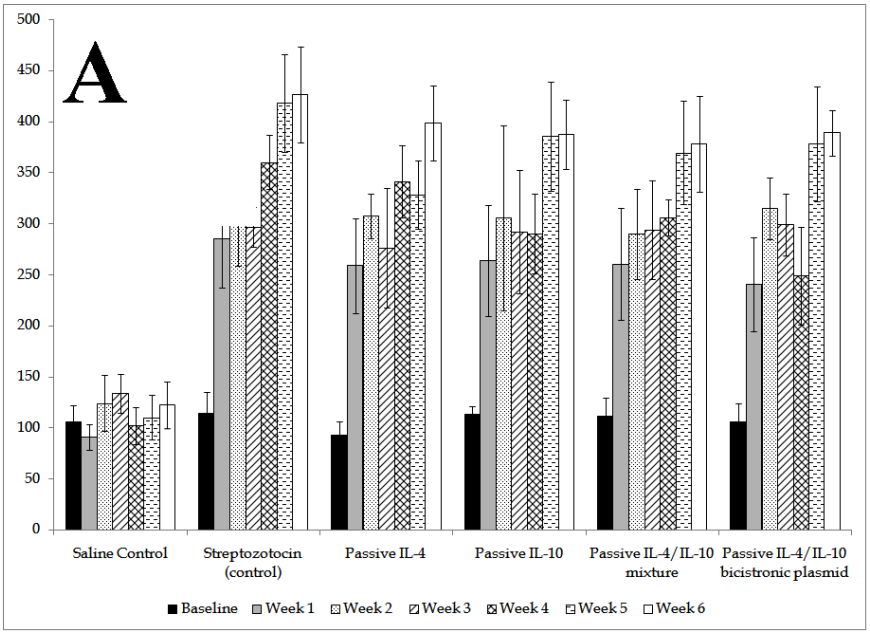

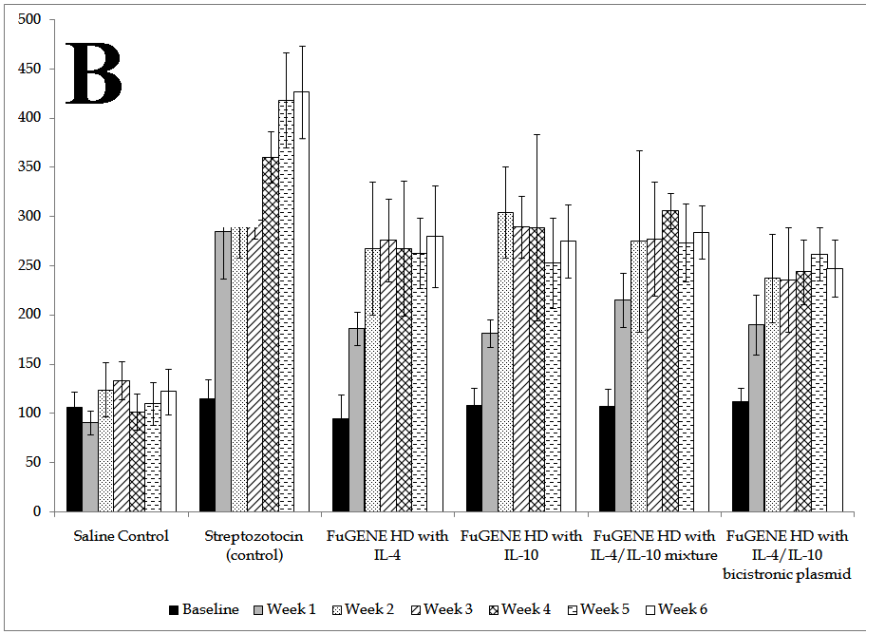

Figure 27 (A-B): Mean blood glucose levels.
Mean blood glucose levels in mg/dl on Y axis. Vertical bars indicate standard deviation (N=6)

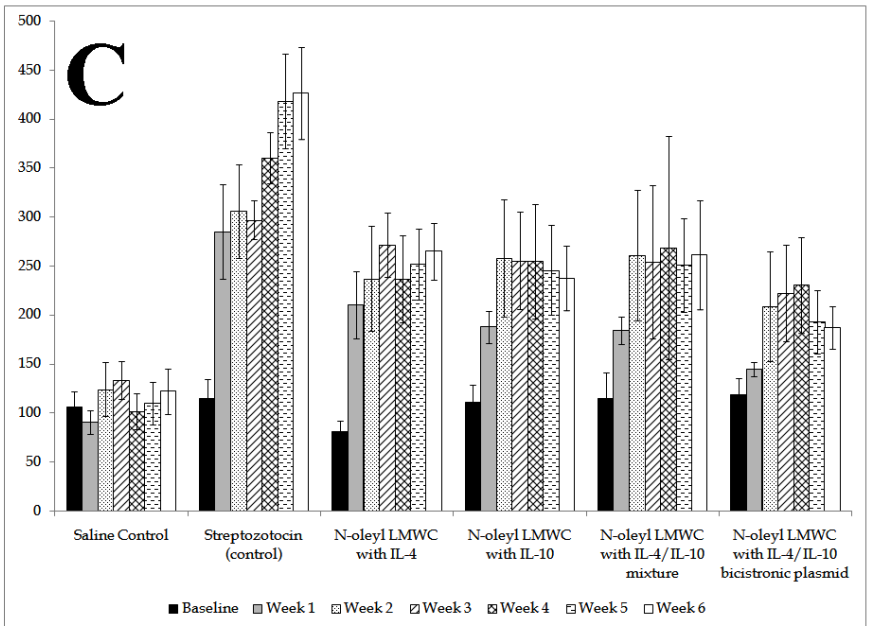

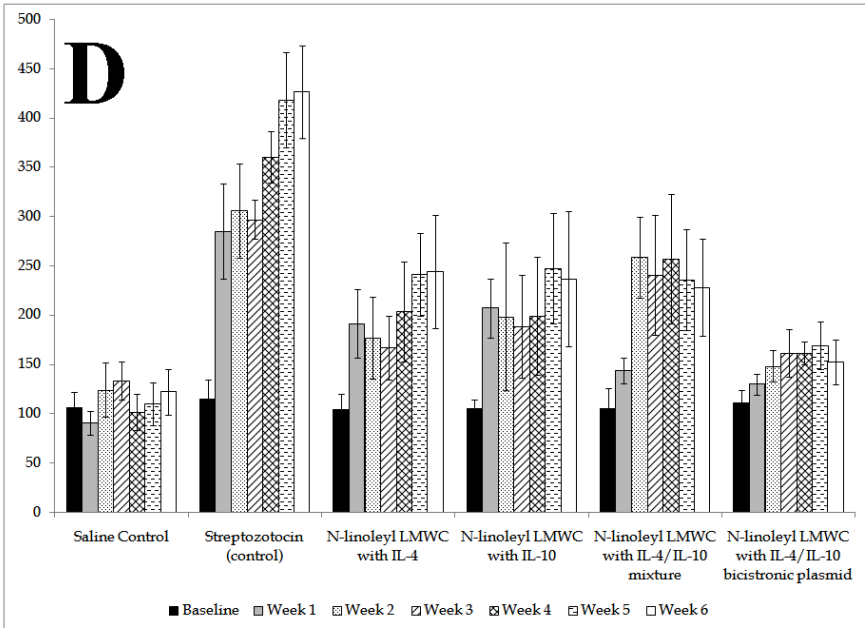

Figure 27 (C-D): Mean blood glucose levels.
Mean blood glucose levels in mg/dl on Y axis. Vertical bars indicate standard deviation (N=6)

3.13.2. Comparison of IL-4 expression

The results of IL-4 expression determined by ELISA are presented in figure 28 (A-D). Figure 28-A depicts the IL-4 level of animals treated with naked plasmids (passive controls, groups 3, 5 and 6). It was observed that the expression of IL-4 was significantly higher in the passive control

groups treated with naked IL-4 plasmid (group 3), mixture of IL-4 and IL-10 (group 5), and bicistronic plasmid (group 6) initially at weeks 1 and 2. But, the levels of IL-4 dropped significantly after week 3 and were comparable to that of saline control as well as STZ control at the end of six week period. This indicated the transient expression resulted due to the injection of naked plasmids.

The expression levels of IL-4 in the FuGENE HD treated groups is shown in figure 28-B. The delivery system containing FuGENE HD performed significantly better at all the time points compared to saline and STZ control. IL-4 expression was significantly higher ($p<0.05$) in the group treated with bicistronic plasmid delivered with FuGENE HD, as compared to other positive controls, saline treated as well as STZ treated groups.

The expression results for IL-4 using N-oleoyl LMWC and N-linoleoyl LMWC are presented in figure 28-C and 28-D, respectively. When N-oleoyl LMWC was used as a gene carrier, it was observed that the IL-4 cytokine expression increased significantly from baseline (11.4 ± 1.6 pg/ml) to 52.7 ± 5.3 pg/ml for IL-4 plasmid, 56.9 ± 4.7 pg/ml for physical mixture (IL-4+IL-10), and 90.5 ± 6.6 pg/ml for bicistronic plasmid at week 1. Similar trend was observed in case of treatment groups containing N-linoleoyl LMWC polymeric delivery system. The expression of IL-4 was 9.9 ± 1.7 pg/ml at baseline, and was highest at one week. The IL-4 levels were found to be 64.4 ± 7.1, 64.89 ± 6.8, and 98.9 ± 9.9 pg/ml for treatment groups 18, 17 and 18, respectively. The IL-4 levels then continuously decreased over the period of six weeks, for all treatment groups but were still significantly higher than saline and STZ control groups. In all cases, the IL-4 expression was significantly higher in the group treated with bicistronic plasmid compared to that of single expression plasmids or physical mixture group.

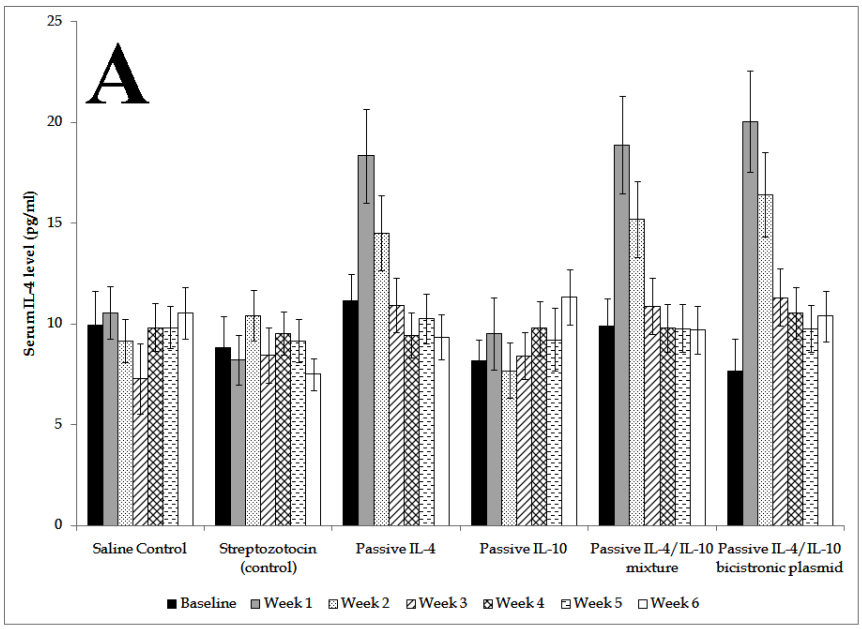

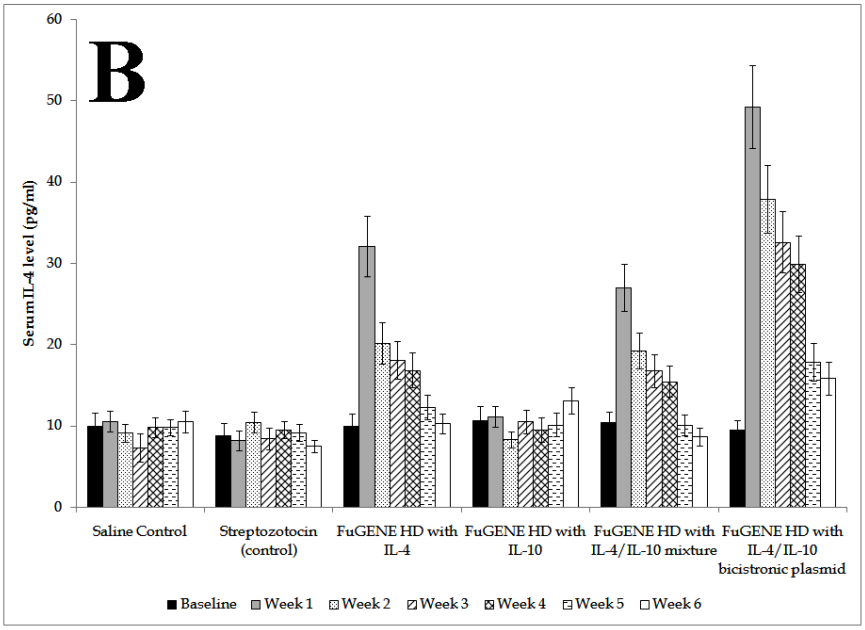

Figure 28 (A-B): Mean serum IL-4 levels (pg/dl).
Vertical bars indicate standard deviation (N=6)

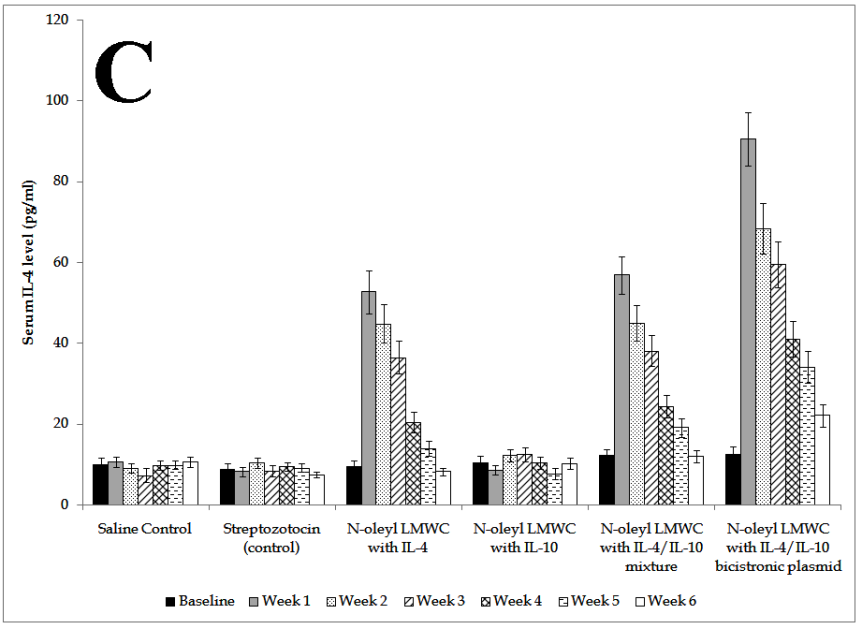

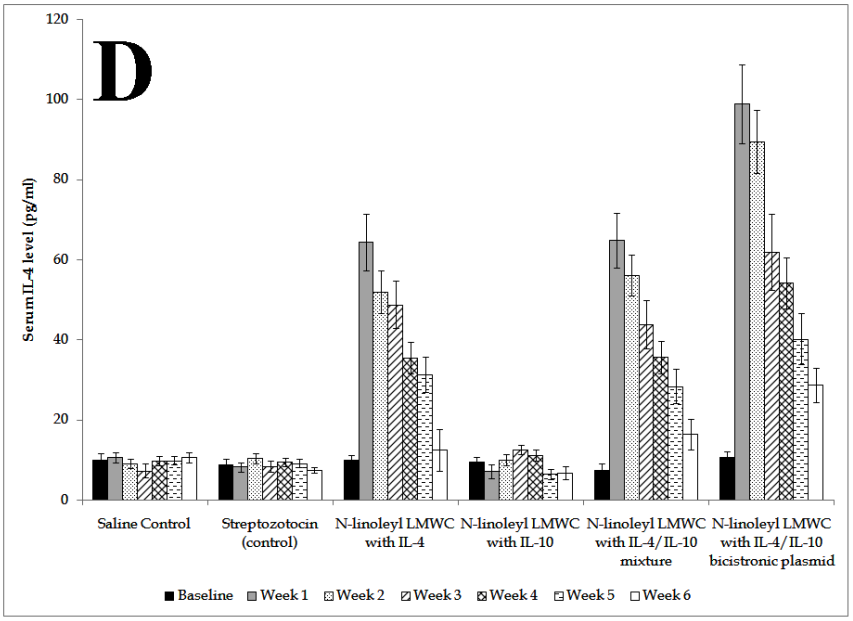

Figure 28 (C-D): Mean serum IL-4 levels (pg/dl).
Vertical bars indicate standard deviation (N=6)

3.13.3. Comparison of IL-10 expression

IL-10 cytokine expression results are shown in figure 29 (A-D). The expression pattern for IL-10 was similar to IL-4. Even though the expression of IL-10 was significantly higher ($p<0.05$) initially for two weeks in the passive control groups treated with naked IL-10 plasmid (group 3),

mixture of IL-4 and IL-10 (group 5), and bicistronic plasmid (group 6), the levels fall significantly after three weeks period. The IL-10 levels were comparable to that of saline and STZ control at week 6, indicating a temporary expression due to the injection of naked plasmids.

Mice treated with IL-10 plasmid in FuGENE HD delivery system, showed significantly higher ($p<0.05$) IL-10 levels till six weeks compared to that of saline and STZ controls (figure 29-B). Significantly ($p<0.05$) higher IL-10 expression was observed in the group treated with bicistronic plasmid delivered with FuGENE HD, as compared to other positive controls, saline treated as well as STZ treated groups.

IL-10 expression results for the polymeric micellar delivery system containing N-oleoyl LMWC and N-linoleoyl LMWC are presented in figure 29-C and 29-D, respectively. The baseline IL-10 expression observed was 41.2 ± 6.3 pg/ml. IL-10 expression increased significantly in the N-oleoyl LMWC treated group and observed to be 329.0 ± 34.1 pg/ml for pUMVC3-mIL-10, 358.9 ±29.0 pg/ml for physical mixture (IL-4+IL-10), and 628 ± 43.4 pg/ml for bicistronic plasmids at week 1.

Similarly, in case of treatment group containing N-linoleoyl LMWC, the expression of IL-10 was 427.3 ± 47.7, 379.3 ± 39.6 and 665.8 ± 66.3 pg/ml at week 1 for groups treated with pUMVC3-mIL-10, mixture of IL-4 and IL-10, and bicistronic plasmid, respectively. The expression reduced gradually till the end of six week period, but was significantly higher in all treatment groups compared to saline and STZ control. The expression of IL-10 was significantly higher in animals treated with bicistronic plasmid compared to all other groups in the experiment.

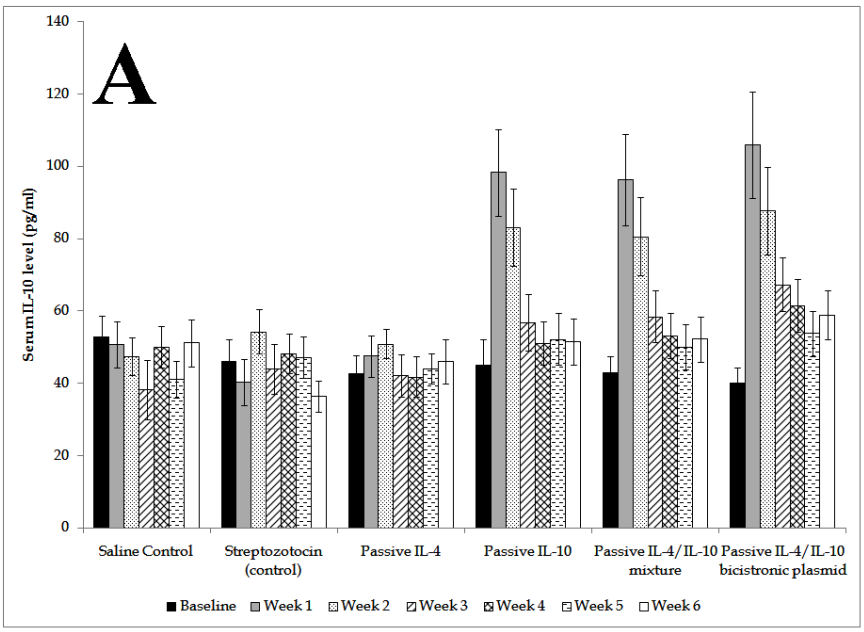

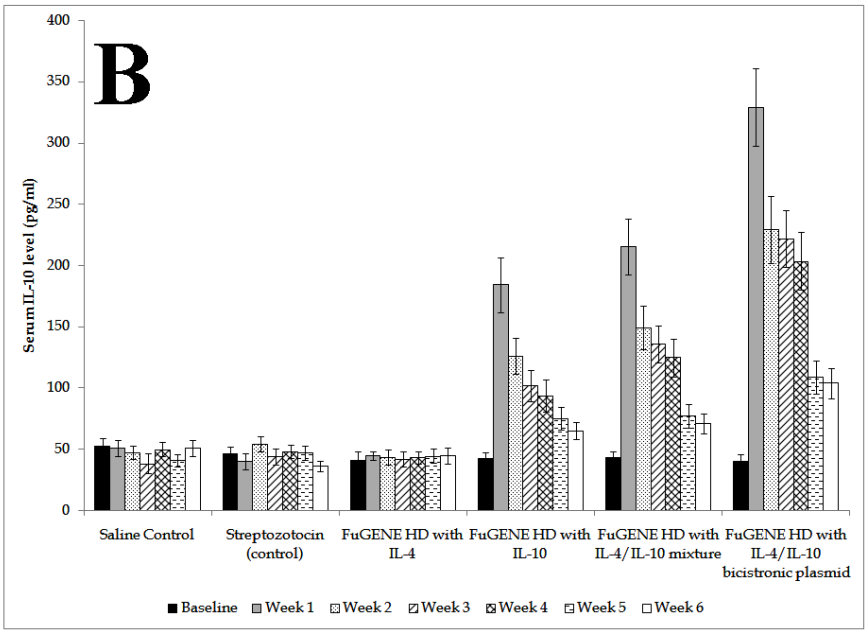

Figure 29 (A-B): Mean serum IL-10 levels (pg/dl).
Vertical bars indicate standard deviation (N=6)

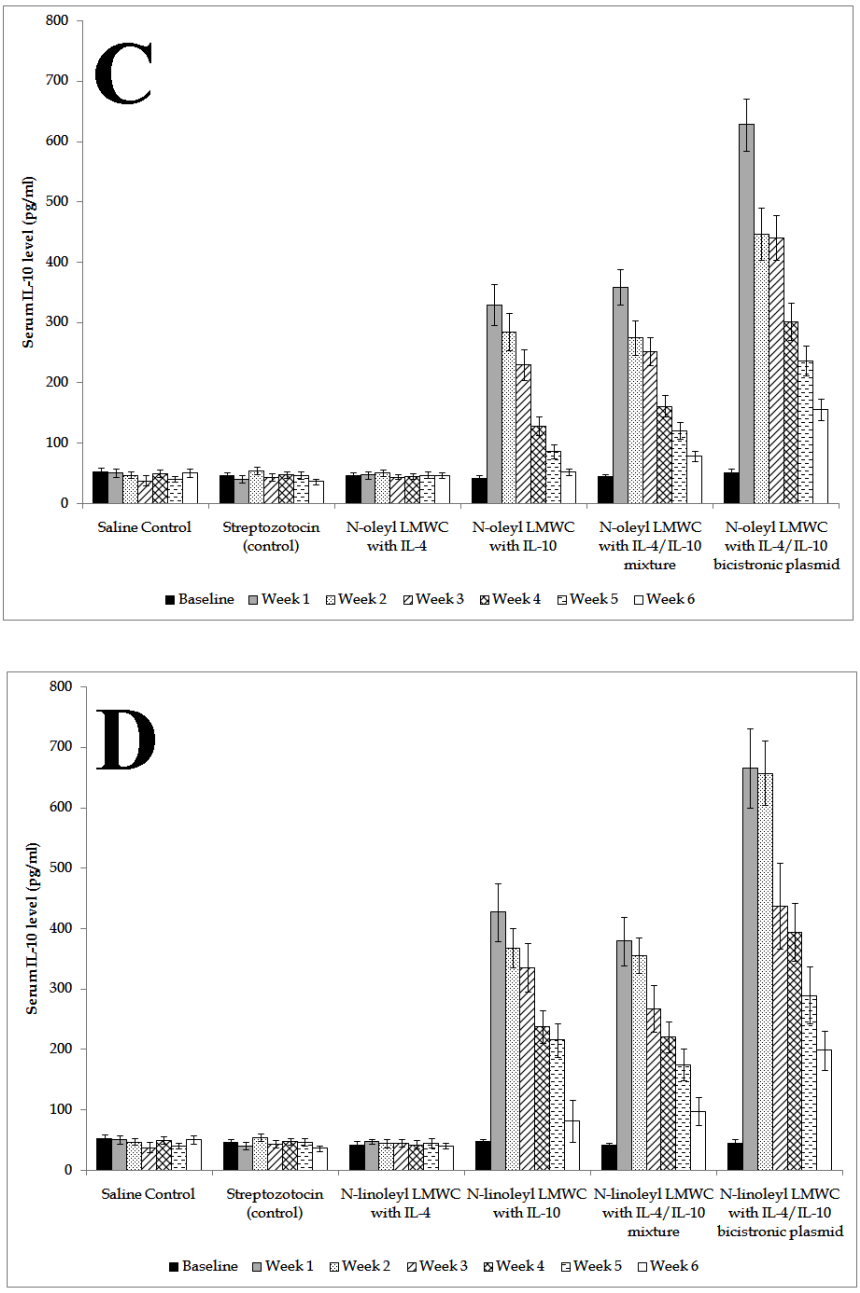

Figure 29 (C-D): Mean serum IL-10 levels (pg/dl).
Vertical bars indicate standard deviation (N=6)

3.13.4. Determination of INF-γ and TNF-α in mouse serum

The serum levels of type 1 cytokines; INF-γ and TNF-α were also evaluated to determine the progression of autoimmune diabetes induced by multiple low doses of streptozotocin (STZ) (figures 30 and 31). Considerable elevation in the plasma level of INF-γ and TNF-α were

observed in passive control groups compared to saline control. The serum levels of both the cytokines remained elevated till the end of six week period in streptozotocin control group and well as all passive control groups.

INF-γ and TNF-α levels were significantly lower in FuGENE HD treated mice at all the time points compared to STZ control. But, it was observed that, though the levels of both cytokines reduced gradually, they were significantly higher ($p<0.05$) in all groups (7, 8, 9, and 10) compared to saline control.

The INF-γ level reduced considerably in case of mixture (IL-4+IL-10, group 13), and bicistronic (group 14) plasmid treated mice. Similar trend was observed in case of the mice treated with the delivery system containing N-linoleoyl LMWC. Except for initial one week period, this polymeric system performed significantly better when used for bicistronic plasmid delivery.

At the end of six weeks, the serum INF-γ levels in the mice treated with bicistronic plasmids were comparable to saline control, and were significantly lower ($p<0.05$) as compared to the animals in STZ, IL-10, IL-4, and IL-10+IL-4 mixture treatment groups.

In case of animals treated with naked unformulated plasmids (groups 3-6), the levels of TNF-α were significantly higher ($p<0.05$) compared to baseline as well as saline control and remained higher till the end of six weeks. Similarly, in case of FuGENE HD delivery vector, it was noted that there is a significant rise in the TNF-α serum concentration even in case of bicistronic plasmid delivery group. The TNF-α concentration was higher in both N-acyl LMWC treatment groups at week 1, and then reduced sufficiently. Though the TNF-α levels were significantly lower ($p<0.05$) in bicistronic plasmid/N-oleoyl LMWC and bicistronic plasmid/N-linoleoyl

LMWC treatment groups as compared to all other treatment groups, they remained significantly higher as compared to saline control throughout the study period.

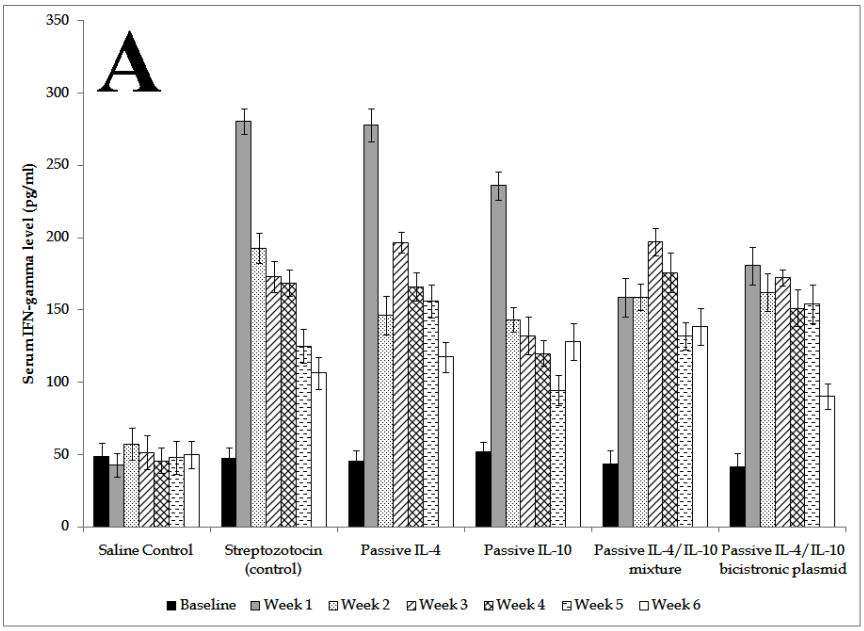

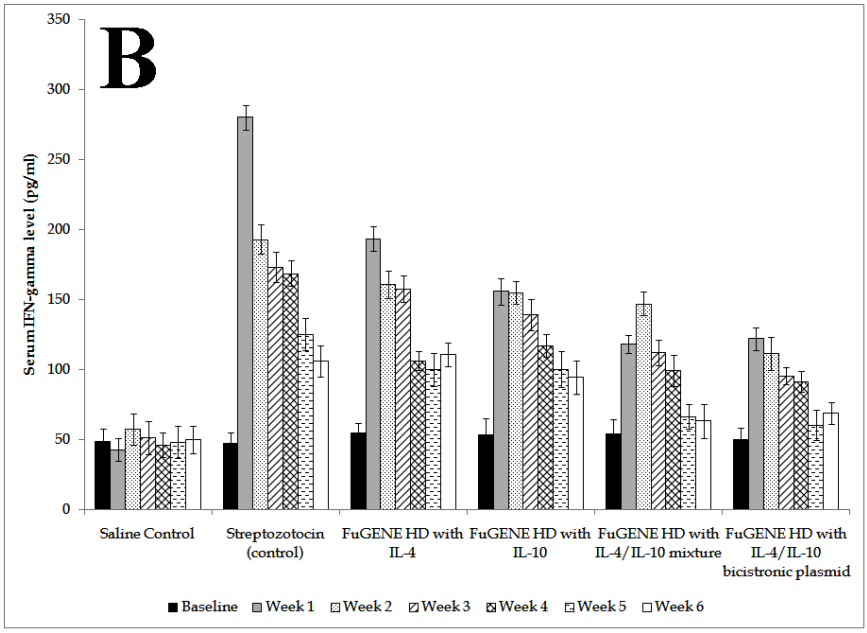

Figure 30 (A-B): Mean serum IFN-γ levels (pg/dl).
Vertical bars indicate standard deviation (N=6)

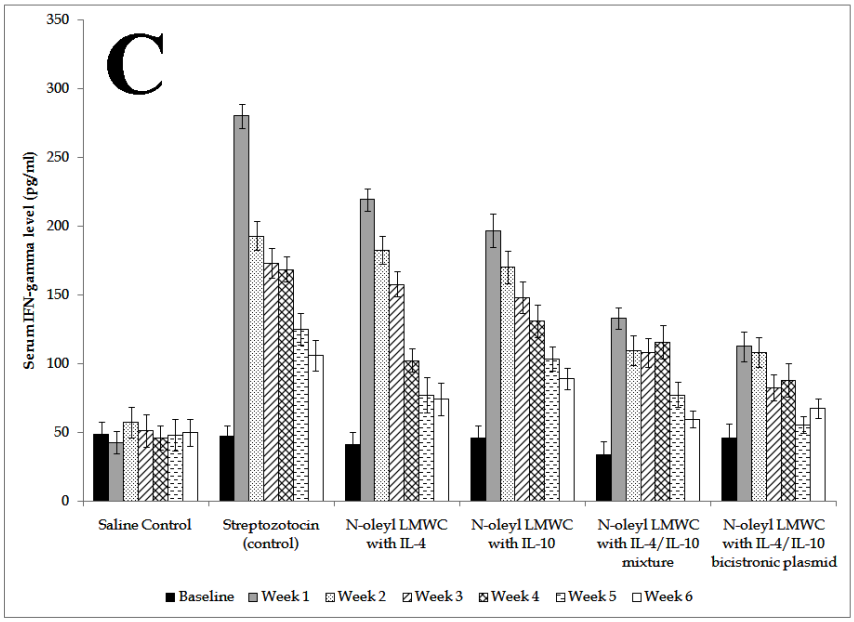

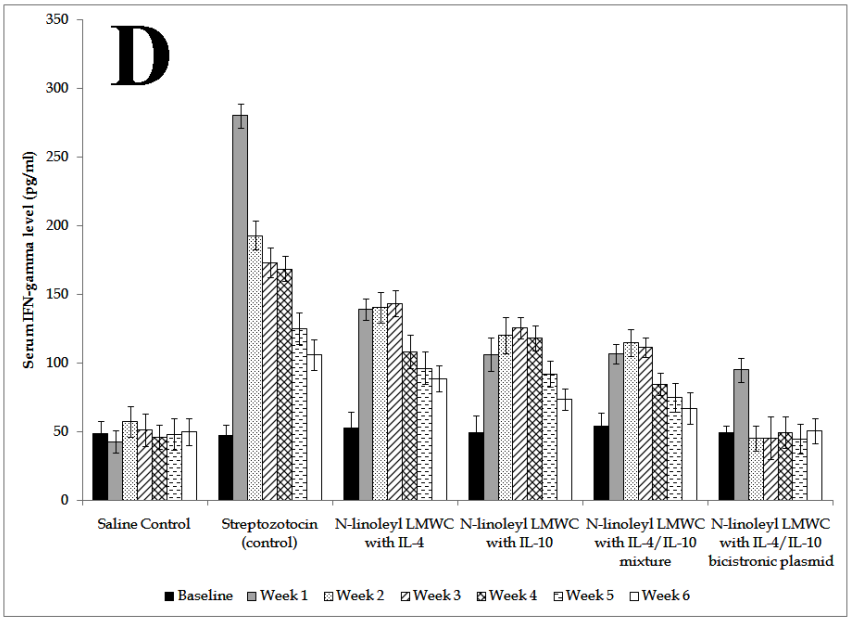

Figure 30 (C-D): Mean serum IFN-γ levels (pg/dl).
Vertical bars indicate standard deviation (N=6)

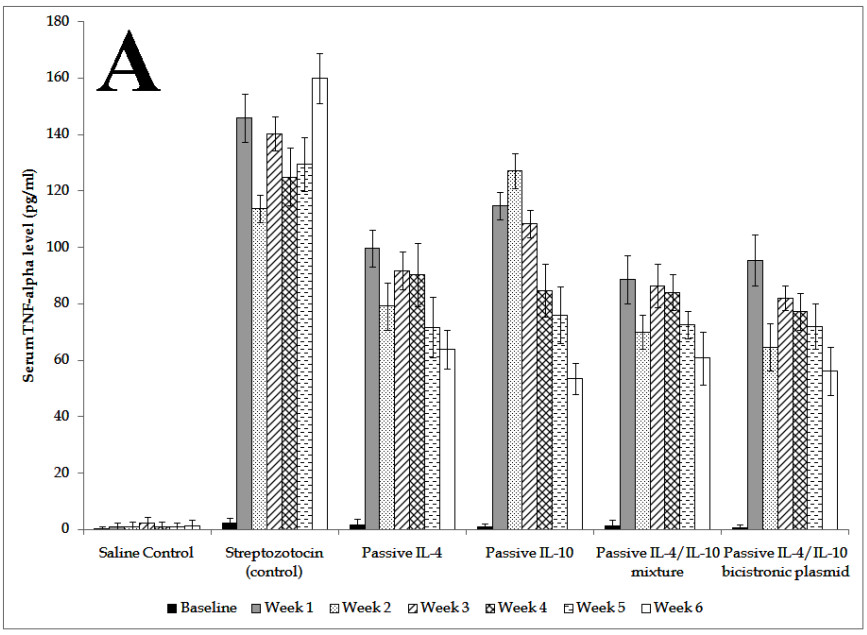

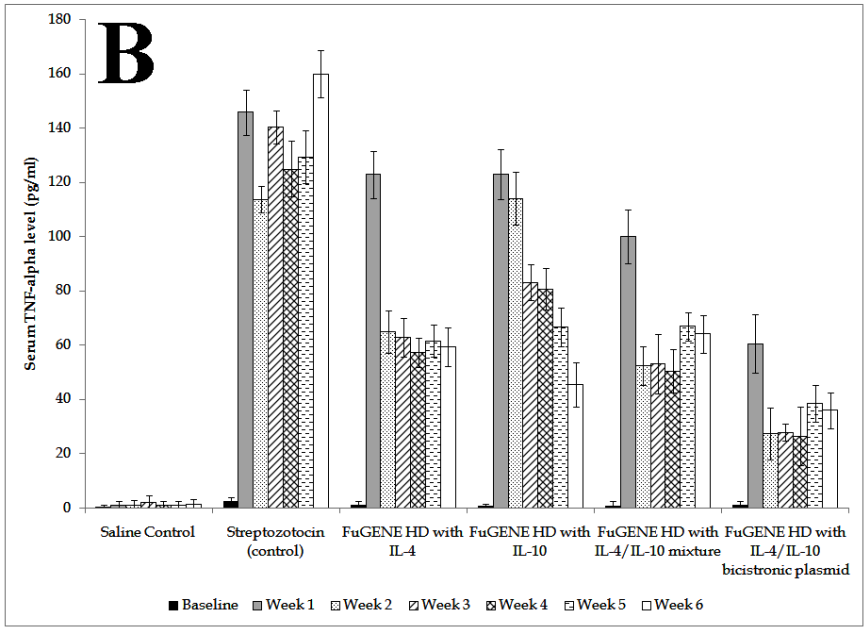

Figure 31 (A-B): Mean serum TNF-α levels (pg/dl).
Vertical bars indicate standard deviation (N=6)

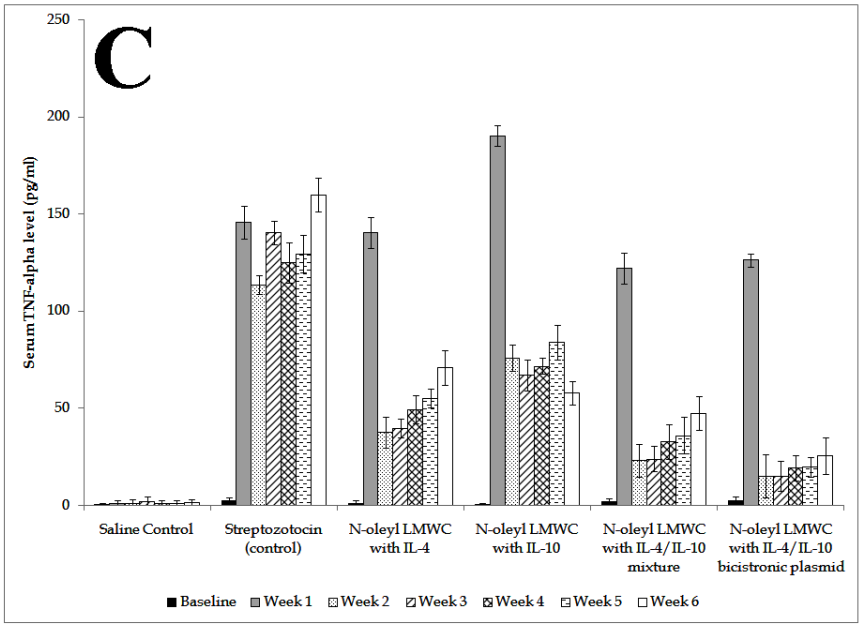

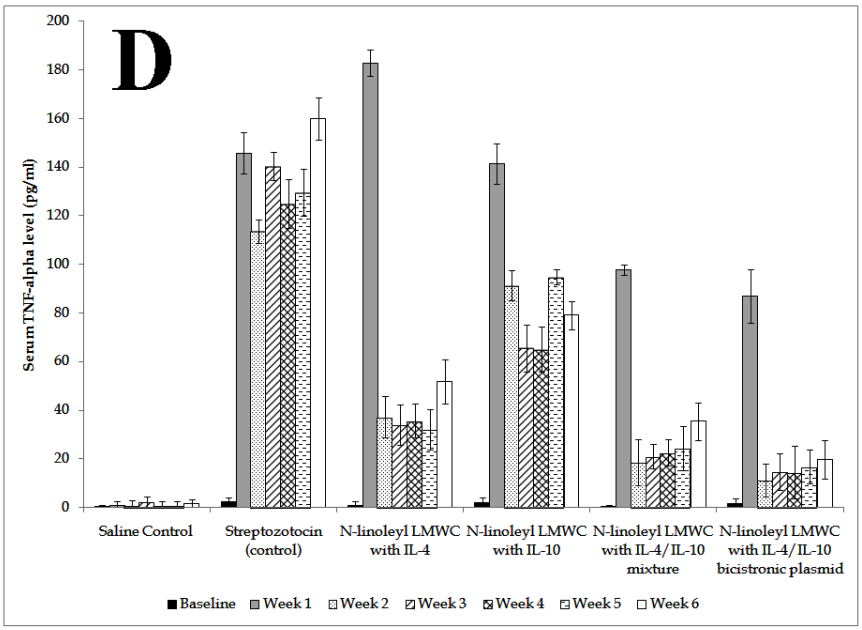

Figure 31 (C-D): Mean serum TNF-α levels (pg/dl).
Vertical bars indicate standard deviation (N=6)

3.13.5. Histopathological changes in pancreas

The level of destruction of pancreatic β cells due to immune infiltration and progression of insulitis if any was observed and compared here, and is presented in figure 32. Figure 32-A represents histology of normal untreated pancreas. STZ injection, showed severe destruction of

pancreatic islets, with high degree of infiltration of lymphocytes and macrophages. The islets were surrounded by the mononuclear cells as shown in figure 32-B. The histology of pancreas treated with polymer treatment groups are represented in figures 32 C-D. Pancreatic histology of mice treated with unformulated plasmids showed some beta cell infiltration but was lower as compared to STZ treatment group. The histology of pancreas of the mice in the treatment group showed the presence of very few mononuclear cells, indicating the protecting effect exerted by the expressed IL-4 and IL-10.

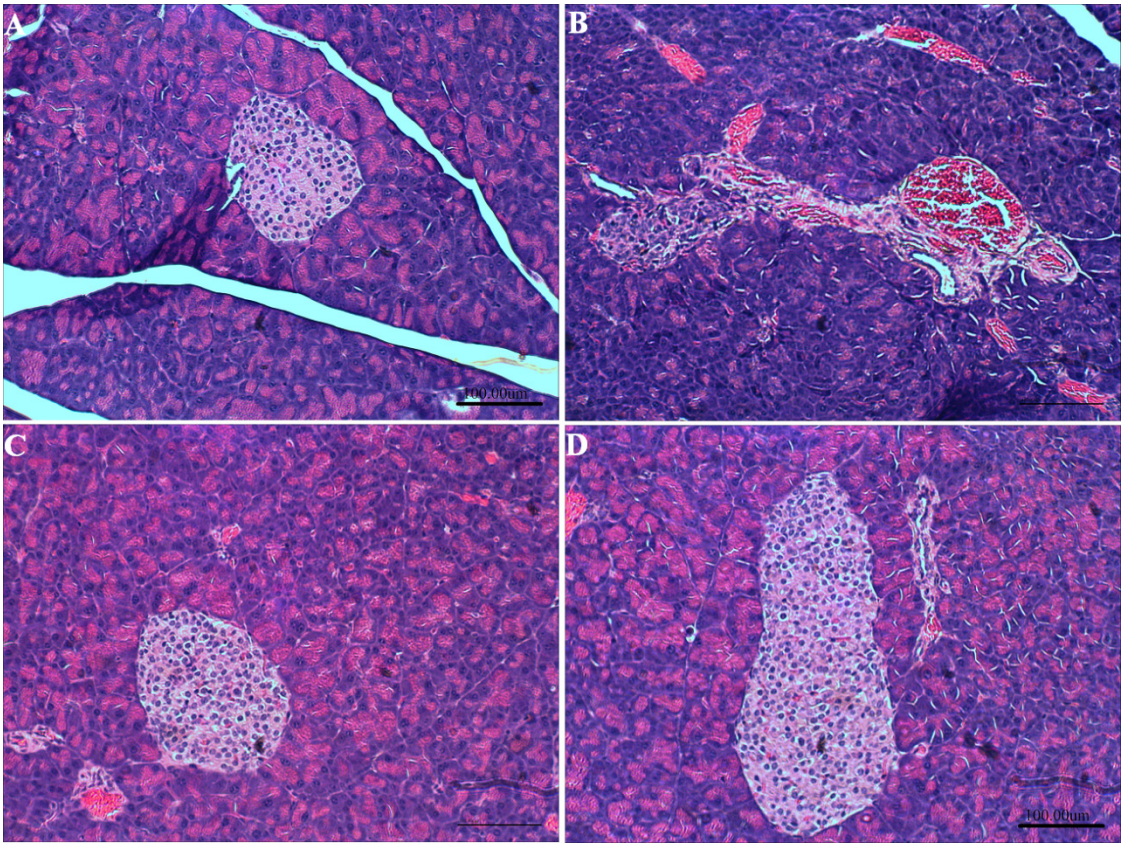

Figure 32: Pancreatic islets of animals at six weeks post-treatment from (A) control group, (B) STZ treated group, (C) N-oleoyl LMWC treated group and (D) N-linoleoyl LMWC treated group. The scale bar represents 100 µm

3.13.6. Biocompatibility of the delivery system

The histological changes in the anterior tibialis muscle were studied to evaluate the in vivo biocompatibility of the polymeric nanomicelles containing pDNA and presented in

figure 33. It was observed that one week after injection of the delivery system into the muscle, large number of macrophages and lymphocytes were observed at the site of injection. But, after 2-3 weeks of treatment, the inflammation subsided considerably indicated by the presence of less number of inflammatory cells. The muscle histology was comparable to that of control at the end of six weeks showing the biocompatible nature of the delivery system. However, even after six weeks post-administration, the injection site muscles of the animals treated with FuGENE HD exhibited signs of inflammation (Figure 33-B).

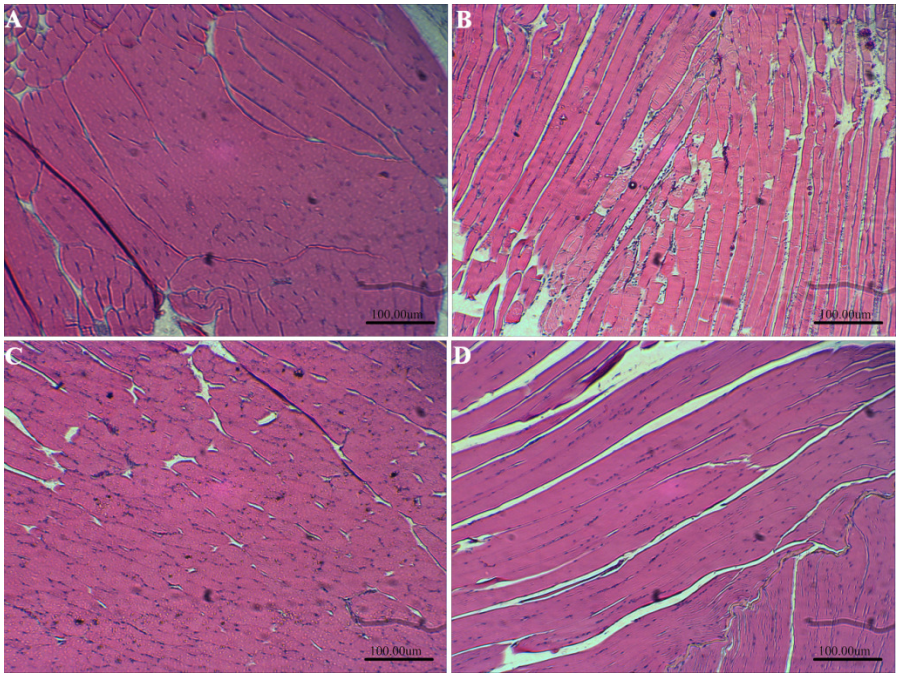

Figure 33: Anterior tibialis muscle at the injection site of animals from (A) control group, (B) FuGENE HD treated group, (C) N-oleoyl LMWC treated group and (D) N-linoleoyl LMWC treated group at six weeks post administration. The scale bar represents 100 µm

4. DISCUSSION

A large number of cationic polymers which effectively condense the DNA and mask their negative charge have been investigated for gene therapy (30–34). Though the viral vectors were initially used as gene carriers, the benefits of non-viral polymeric delivery systems are now being fully appreciated. The obvious advantages of non-viral vectors, including superior safety profile, ease of modification, amenability to attachment of targeting ligands and absence of the possibility of insertional mutagenesis add to their attractiveness. Chitosan, a cationic polymer, has been explored as a safe and versatile gene delivery carrier. However, low and pH dependent solubility as well as low transfection efficiency have been reported to be the major hurdles in its widespread use as a non-viral vector of choice. To circumvent these two problems, we took a dual approach of preparing soluble, low-molecular weight chitosan and further derivatizing it with a series of fatty acids of increasing alkyl chain length. Once the graft chain length was determined, the effect of increasing unsaturation in this optimized chain length was studied. This novel approach enabled us to synthesize N-acyl LMWCs optimized for gene delivery applications. The effect of increasing chain lengths of the substituents on the transfection efficiency of the polyplexes was also assessed. The fatty acyl modification of the LMWC leads to the conversion of a fraction of free primary amine moieties (pKa 10-11) on chitosan into amide groups (pKa ~17 for conjugate acid) (Smith and March, 2001) by reducing the charge density on the polymer. Such grafting of saturated alkyl chain also introduces hydrophobic regions in the polymer, leading to the formation of micellar structures and possibly aiding transport through lipid bilayers. The micellar structures, due to their hydrophobic core and hydrophilic shell, might lead to surface presentation of the plasmids, which is reported to have

specific advantage**s, s**uch as fast and complete release (Basarkar et al., 2007; Basarkar and Singh, 2009).

For the preparation of the LMWC, we employed the oxidative depolymerization technique, using $NaNO_2$. The rigid crystalline domains in the structure of high molecular weight chitosan accompanied by the intra- and intermolecular hydrogen bonding has been implicated in low solubility of chitosan at physiological pH (Nishimura et al., 1991). The extent of oxidative depolymerization of chitosan by $NaNO_2$ can be easily controlled by changing the initial chitosan concentration, $NaNO_2$ concentration and duration of the reaction (Mao et al., 2004). The control of the reaction accompanied by the resolution of the products using a preparative scale size-exclusion column led to generation of soluble chitosan fractions having well-defined, narrow molecular weight distributions. The major fraction (~64%) of soluble chitosan, having average molecular weight of ~6.5 kDa and polydispersity index (PDI) of 1.17 was used to prepare the fatty acid derivatives. The series of the N-acyl LMWCs was characterized for their structure and degree of substitution using IR spectroscopy. Various reported procedures to determine the degree of acetylation of chitin and chitosan by IR spectroscopy have been reviewed (Kasaai, 2008). The ratio of intensity of C=O (amide I) stretching band at 1655 cm^{-1} to stretching band of hydroxyl groups at 3450 cm^{-1} can be applied to determine the degree of N-substitution for crystalline and well-dried samples. The results obtained from IR-analysis reinforced the results of elemental analysis of the polymers. There was agreement between the theoretical percentages of nitrogen, hydrogen and carbon derived from IR data, and the actual percentages of those elements as observed from elemental analysis (Table 4).

The critical micellar concentration of an amphiphillic molecule like N-acyl LMWC is an important property affecting it colloidal behavior. In aqueous environment, it was observed that

the CMC values of N-acyl LMWC were between 0.015 to 0.0625 mg/ml. Such low CMC values ensured that, under working conditions of pDNA/N-acyl LMWC polyplex formation, the N-acyl LMWC existed in a micellar state.

Hydrodynamic size and zeta potential are known to be the critical parameters affecting the performance of a gene delivery system (Pang et al., 2002). According to Behr, the non-viral gene vector experiences changes in pH *en route* to its delivery site (cytosol) (Behr, 1997). Therefore, we studied the effects of various formulation parameters including pH, sonication duration and filtration on the size and hydrodynamic radius of the N-acyl LMWC micelles. Sonication duration as well as the filtration had an impact on the size of the micelles. By carefully controlling duration of sonication, followed by the filtration through the 0.8 µ membrane, we could achieve a reduction in the size of the micelles. The sonication as well as filtration led to disruption of the spontaneously formed larger micelles, which again self-assembled to form smaller micellar structures. High recovery of the N-acyl LMWC (>90%) after filtration indicated that the process of filtration led to the reorganization of the micellar structures rather than removal of larger micelles. The IR spectra of the recovered material indicated that the sonication had no adverse impact on the structure of N-acyl LMWC. It is interesting to note that, though filtration and sonication had a major role affecting the hydrodynamic size, they had no impact on the zeta potential of the nano-micelles. pH was the only factor found to have a role in determining the zeta potential of the micelles. As the pH conditions become more basic, the zeta potential on the micelles was lesser in magnitude. This can be explained by the suppression in the ionization of the amine moieties on chitosan in basic conditions. Overall, under optimized formulation conditions, it is possible to obtain nano-sized micelles from the fatty acyl derivatives

of depolymerized chitosan, which can form stable complexes with DNA and can efficiently transfect HEK293 cells.

Buffering ability is the ability of a molecule to resist the change in the pH. According to proton sponge theory, the buffering ability of a non-viral vector plays a crucial role in endosomal escape of the polyplexes (Behr, 1997). During the formation of N-acyl LMWC, ~ 40% of the free amino groups were converted into amide moieties. Though this conversion was intended to reduce the cationic charge density on chitosan and to facilitate the release of DNA from LMWC after endosomal escape, it also reduced the buffering ability of the graft polymer. It was observed that though N-acyl LMWCs could resist the change in pH due to addition of 0.1 N HCl to a lesser extent, they still retained considerable buffering ability (Figure 19)

Hydrodynamic size and zeta potential are known to be the critical parameters affecting the performance of a gene delivery system (Pang et al., 2002). The interaction of a polymer with DNA can affect the size and zeta potential of the resultant polymeric delivery system. Dynamic light scattering was employed to assess the effects of interaction between DNA and N-acyl LMWC on these parameters. Upon addition of DNA, the decrease in the zeta potential of N-acyl LMWC nanomicelles was expected due to negative charges present on DNA. However, the polyplexes had an overall positive charge, which can be explained on the basis of the high N:P ratio used and can be an important factor in DNA compaction in the polyplexes and could theoretically aid the internalization of the polyplexes by cells. It was also observed that the polyplexes were stable upon storage for 7 days as observed from the dynamic light scattering and agarose gel electrophoresis experiments, and the pDNA released from the stored samples was comparable with the pDNA from fresh solutions. Moreover, ability to protect the DNA from enzymatic degradation can have major impact on the transfection efficiency of such delivery

systems. The agarose gel electrophoresis experiments indicated that N-acyl LMWC could protect the DNA from enzymatic degradation by DNase I.

The polymeric non-viral vectors are reported to have some inherent cytotoxicity owing to their cationic nature, which results in interaction with cellular and blood components (Halama et al., 2009). Numerous reports have emphasized on the relatively non-toxic nature of chitosan (Duceppe and Tabrizian, 2010; Rudzinski and Aminabhavi, 2010). The toxicological evaluation of depolymerized chitosan as well as the N-acyl LMWC indicated that the increasing doses of chitosan as well as its derivatives displayed no significant ($p<0.05$) toxicity in HEK293 cells. Such lack of toxicity is indeed an attractive feature of a non-viral vector, when most of the cationic polymers and lipids are known to display dose dependent toxicity (Wiethoff and Middaugh, 2003). In vitro transfection studies indicated that N-acyl LMWC polyplexes performed significantly ($p<0.05$) better transfection than depolymerized chitosan. Moreover, the effect could be linked to the chain lengths of the fatty acyl grafts on N-acyl LMWC. Overall, C16:0 (palmitic acid) and C18:0 (stearic acid) derivatives were found to be the most efficient for gene delivery. This may be due to enhanced transport of C16-C18 fatty acids through lipid bilayers (Bhatia and Singh, 1998, 1999; Rastogi and Singh, 2004). With reference to these observations, it was interesting to study the effect of unsaturation in the fatty acyl grafts in C16-C18 range on depolymerized chitosan on CMC, hydrodynamic size (which was an indicator of micellar packing), zeta potential, toxicity and transfection efficiency of the derivative polymers. The excellent cytotoxicity profiles and improved transfection efficiencies of the N-acyl LMWCs along with their comparable transfection profile with marketed FuGENE HD makes them suitable candidates for investigating the in vivo gene therapy applications.

Type 1A diabetes is generally explained by T_H1/T_H2 balance model which concludes that autoimmunity is caused due to dominance of T_H1 cytokines. T_H1 cells with their cytokine effectors such as IFN-γ, IL-2 and TNF-α elicit cell-mediated responses; whereas T_H2 cells through their cytokines such as IL-4 and IL-10 elicit humoral responses. Restoration of balance between T_H1 and T_H2 cytokines by upregulation of TH2 cytokine expression may lead to prevention of autoimmune diabetes. Delivery of cytokines, however, is not feasible due to high cost and very short plasma half-life. Delivery of genes encoding T_H2 cytokines has the potential to eliminate these shortcomings by facilitating in situ expression of cytokines. It may also circumvent the problems associated with immune reaction against foreign cytokines (Chernajovsky et al., 2004; Li et al., 2008; Basarkar and Singh, 2009).

IL-4 is a prototypical T_H2 cytokine and has been widely used for gene therapy of experimental models of autoimmune disorders such as experimental allergic encephalomyelitis and collagen-induced arthritis (Kageyama et al., 2004). Gene encoding IL-4 has been delivered using both viral and non-viral vectors. Expressed IL-4 inhibits the production of proinflammatory cytokines thereby suppressing autoimmunity and the delivery of gene encoding IL-4 had been only partially successful in preventing the spontaneously developing IDDM in NOD mice. Similarly, IL-10 gene has been delivered in a number of studies using both viral and non-viral vectors and has been found to prevent or slow down the progression of autoimmune diabetes. IL-10 gene delivered using adeno-associated viral vector resulted in protection of pancreatic islets along with suppression of T cell activation (Goudy et al., 2001; Carter et al., 2005). Intramuscular injection of naked plasmid DNA encoding IL-10 also led to prevention of STZ-induced diabetes (Zhang et al., 2003). Therefore, plasmids encoding IL-4 and IL-10 were used as model therapeutic plasmids in this study. In vitro transfection studies indicated that N-

acyl LMWC polyplexes performed significantly ($p<0.05$) better transfection than LMWC. Moreover, the effect could be linked to the chain lengths of the fatty acyl grafts on N-acyl LMWC. Overall, C18 derivatives were found to be the most efficient polymers for gene delivery. This may be due to enhanced transport of C18 fatty acids through lipid bilayers. Multiple studies have already demonstrated that unsaturated fatty acids can lead to channel formations in lipid bilayers and aid the transport of various macromolecules across the barrier membranes (Bhatia and Singh, 1998, 1999; Rastogi and Singh, 2004). Current study confirms that such phenomenon could be applicable for gene delivery and should be studied further. The oleic acid (1 double bond) and linoleic acid (2 double bonds) grafting on LMWC improved the transfection efficiency significantly ($p<0.05$) as compared to their saturated analogues. But further increase in the unsaturation led to a decrease in the transfection efficiency. There are conflicting reports about the effects of unsaturation in alkyl groups of non-viral vectors on their transfection efficiencies. The detrimental effect of more than one double bond in the alkyl chain on the transfection has been reported (Koynova et al., 2009). However; another study has reported that the increasing unsaturation in alkyl chain in a series of cationic lipids led to an increase in their transfection efficiency (Heyes et al., 2005). In our case, a decrease in the transfection beyond two double bonds in an alkyl chain can be explained on the basis of the size of the nanomicelles/pDNA polyplexes. It is observed that, in spite of similar % DS and CMC values, the hydrodynamic size of N-Linolenoyl LMWC/pDNA polyplexes (144.9 ± 20.9 nm) differs significantly ($p<0.05$) from N-linoleoyl LMWC/pDNA polyplexes (99.5 ± 14.4 nm). Such an increase in the hydrodynamic size of the polyplex could be a factor affecting the cellular uptake and subsequent transfection by N-Linolenoyl LMWC.

The delivery system was investigated for its transfection efficiency in vitro and compared with a marketed transfection reagent, FuGENE HD. In vitro studies performed to determine/quantify the expression of therapeutic cytokines IL-4 and IL-10, using N-oleoyl and N-linoleoyl LMWC showed that there is approximately a 8 and 35 fold increase in expression as compared to LMWC and naked DNA, respectively (Mandke and Singh, 2012b). The delivery systems were as efficient as FuGENE HD ($p \geq 0.05$) in vitro. The reason for this high transfection might be due to the buffering ability, small size or due to fast endosomal escape of the nanomicelles. After conversion of ~ 35% of free primary amine groups into amide moieties, the polymers retain sufficient buffering ability and this might lead to their eventual endosomal escape due to the 'proton sponge' effect as described by Behr and coworkers (Boussif et al., 1996; Behr, 1997), resulting in superior transfection.

The ability of these hydrophobically modified low molecular weight chitosans was evaluated for therapeutic plasmids delivery in vivo. It has been reported that the use of multiple, low-dose STZ approach partially damage pancreatic islets, and trigger an inflammatory response which leads to further destruction of β-cells and results in insulin deficiency leading to hyperglycemia. This phenomenon usually closely resembles the pathogenesis and morphologic changes that occur due to type 1 diabetes mellitus (T1DM) (Wu and Huan, 2008). Though MLD- STZ induced diabetic mouse model has been less studied as compared to other models of Type 1A diabetes such as NOD mouse and bio-breeding rats, it offers multiple advantages including a quicker and more reliable onset of diabetes and ability to produce diabetes irrespective of genetic background of the mice (Schmidt et al., 2003). The advantages of intravenous administration of a chimeric plasmid to prevent insulitis in NOD mice have been demonstrated (Lee et al., 2003), but no study has evaluated the effects of administration of a

bicistronic plasmid in multiple, low-dose STZ induced diabetic mouse model via the intramuscular route. It has already been demonstrated that the use of skeletal muscle for gene therapy results in sustained and systemic expression of therapeutic proteins (Blau and Springer, 1995; Lu et al., 2003; Basarkar and Singh, 2009). A single intramuscular (i.m.) injection of β-galactosidase (AAV-lacZ) gene or human erythropoietin (AAV-Epo) using viral vector into adult BALB/c mice resulted in long-term protein expression.

4.1. Comparison Among the Polymer Groups

In our studies, we have compared the expression of plasmids encoding for IL-4, IL-10 and a bicistronic plasmid encoding for both IL-4 and IL-10 using hydrophobically modified LMWC. We have also determined the effect of successful IL-4 and IL-10 gene delivery on multiple, low-dose STZ induced insulitis. The blood glucose levels as well as serum cytokine levels of animals treated with IL-4, IL-10 and bicistronic plasmid polyplexes were compared with those of untreated and naked plasmid treated animals. There is a gradual increase in blood glucose levels in animals treated with IL-4 plasmid with either of the delivery systems. Though low blood glucose levels were observed in animals treated with the delivery system containing N-linoleoyl LMWC compared to passive, STZ, FuGENE HD and N-oleoyl LMWC groups, N-linoleoyl LMWC was superior to rest of the treatments. When the serum IL-4 levels were analyzed, it was noted that both the N-oleoyl LMWC and N-linoleoyl LMWC showed marked ($p<0.05$) increase in IL-4 expression compared to passive or FuGENE HD controls. Such improved transfection by N-acyl LMWCs can be explained on the basis of their low cytotoxicity and stable nature of their polyplexes with pDNA. Serum IL-4 levels reduced eventually at the end of six weeks, but remained elevated in N-linoleoyl LMWC group. Although there is a drop in IL-4 expression observed over the period of time, the levels remained significantly higher

($p<0.05$) than physiological levels (compared to saline control). Similar findings have been reported by Basarkar and Singh, explaining that the reduction in expression may be a result of deactivation of promoter or due to the turnover of muscle fibers (Basarkar and Singh, 2009).

Similar results were observed in case of mice treated with IL-10 plasmid. Animals treated with hydrophobically modified chitosan showed considerably low blood glucose levels compared to STZ and passive treatment groups. Higher IL-10 concentration was observed as a result of higher expression of IL-10 plasmid formulated in N-oleoyl LMWC and N-linoleoyl LMWC delivery systems. The expression reduced over the period of six weeks, but was high enough to reduce the destruction of pancreatic islets and resultant progression of insulitis. This high expression resulted in marked decrease in IFN-γ and TNF-α levels, which eventually lengthened the progression of disease. In all cases, N-linoleoyl LMWC was found to be superior compared to naked plasmids, FuGENE HD as well as N-oleoyl LMWC treatments.

Since it has been reported that the combined administration of IL-4 and IL-10 plasmid is effective in preventing the autoimmune insulitis, a physical mixture of IL-4 and IL-10 was prepared at a weight ratio of 1:1 and incorporated into the micellar delivery system. The effect of co-administration of both the plasmids was evaluated and compared. Though the blood glucose levels were significantly ($p<0.05$) low in case of N-oleoyl LMWC, N-linoleoyl LMWC and FuGENE HD treated groups compared to STZ, it is difficult to obtain the exact correlation between the effect and the plasmid expression. At the same time it could be noted that the N-linoleoyl LMWC treatment group showed lower glucose levels.

IL-4 and IL-10 cytokines were highly expressed in animals treated with IL-4+IL-10 mix in N-oleoyl LMWC and N-linoleoyl LMWC, indicated the polymeric delivery systems (N-oleoyl and N-linoleoyl LMWC) worked with better efficacy as compared to passive and FuGENE HD

treatments. The marked reduction in the IFN-γ and TNF-α serum levels also supports the fact that the co-administration of both plasmids in N-oleoyl LMWC and N-linoleoyl LMWC worked efficiently as compared unformulated or FuGENE HD controls. It was noted that, though the levels of INF-γ were higher in the animals treated with plasmids in N-oleoyl LMWC delivery system initially and reduced gradually at the end of six week period. An initial transient increase in IFN-γ has been previously observed (Basarkar and Singh, 2009), and is mainly attributed to the acute inflammation caused due to needle injury or due to the presence of the delivery system.

Maximum expression of IL-4, and IL-10 was observed in case of mice treated with bicistronic plasmid formulated in N-linoleoyl LMWC delivery system. The expression gradually reduced but the concentrations were sufficient enough to prevent the autoimmune diabetes progression. The amount of IL-4 and IL-10 copies in the bicistronic plasmids are higher than the single expression plasmids in the mixture groups but lower than single expression plasmids in the individual plasmid groups. Lee and coworkers have reported that such difference in the number of plasmid copies as well as the plasmid size do not have any significant effect on the transfection and subsequent expression of therapeutic proteins (Lee et al., 2003). From these results it could be said that the delivery vector (N-linoleoyl LMWC) enhanced the transfection efficiency of the plasmid incorporated irrespective of the size and number of plasmid copies administered. This can be explained on the basis of the excellent binding and effective condensation of pDNA by hydrophobically modified LMWCs. Such polymer/pDNA interaction led to formation of nanomicelles-based polyplexes which are easily taken up by the cells and resulted in sustained transgene expression after a single i.m. injection.

Though FuGENE HD exhibited high transfection efficiency in vitro, its in vivo biocompatibility is questionable. It is reported to be moderately cytotoxic in a dose dependant

manner in vivo (Lee et al., 2002b). We found that the acute inflammatory responses were more pronounced at the injection site of FuGENE HD. Such toxicity might have led to destruction of the injected skeletal myocytes resulting in reduced expression of the delivered genetic cargo as compared to nontoxic N-acyl LMWCs.

4.2. Comparison Among the Plasmid Groups

When the treatment groups were compared on the basis of plasmid efficiency, mice treated with bicistronic plasmid, showed significantly lower ($p<0.05$) plasma glucose levels. Moreover, the animals treated with bicistronic plasmid/N-linoleoyl LMWC group exhibited low blood glucose levels which were comparable to saline control at all the time points. Mice injected with bicistronic plasmid in the N-oleoyl LMWC and FuGENE HD showed marked reduction in blood glucose, but was significantly higher than saline control as well as N-linoleoyl LMWC treatment groups. Unformulated plasmid treated animals did not show any change in the glucose level and the levels remained elevated till the end of six weeks.

Even though the expression levels of individual expression plasmids, or physical mixture of IL-4 and IL-10, are good with N-linoleoyl LMWC as a delivery vector, bicistronic plasmid treated animals exhibited greater expression of the cytokines. Animals treated with naked unformulated plasmids showed transient expression of IL-10 and IL-4 cytokines. The serum levels of both the cytokines dropped rapidly after two weeks indicated that frequent administration is required to maintain the therapeutic protein levels. Similar results have been reported by Basarkar and Singh (Basarkar and Singh, 2009).

Proinflammatory cytokines such as TNF-α, and IFN-γ, produced primarily by T_H1 cells play an important role in the pathogenesis of Type 1A diabetes by causing activation and migration of more inflammatory cells into the pancreas (Devendra and Eisenbarth, 2003). The

levels of inflammatory markers IFN-γ and TNF-α were observed to determine the inhibitory effect of IL-4 and IL-10 cytokines expressed. The levels of IFN-γ and TNF-α were significantly ($p<0.05$) high initially (week 1) but lowered over six week period, indicating inhibitory effect of IL-4 or IL-10 on IFN-γ production and reduction in the progression of insulitis in case of N-oleoyl LMWC, N-linoleoyl LMWC and FuGENE HD treated animals. The inhibitory effect was sustained for animals treated with N-oleoyl LMWC and N-linoleoyl LMWC throughout the study duration. The initial acute immune response might be due to needle injury or due to the presence of polymeric formulation. Animals in passive control group (naked IL-4 plasmid injection) showed reduction in IFN-γ levels at week 2 but later on increased in IFN-γ concentration showed that there was a transient expression of IL-4 resulted in temporary inhibitory effect on IFN-γ. The levels remain higher and were comparable to that of STZ control till six weeks.

Histopathology of pancreas showed severe infiltration by the inflammatory cells in STZ group. Even though the pancreas of animals treated with unformulated plasmids showed reduction in infiltration initially at week 1, it was not sustained, and severe inflammation was observed after four weeks of treatment. Thus, the expression of IL-4 and IL-10 cytokines was temporary and did not persist long and sufficient enough to protect the pancreas from progression of insulitis. On the other hand, the pancreas preserved their morphology, and no inflammation was seen in case of animals treated with N-oleoyl and N-linoleoyl LMWC polyplexes, probably due to the higher and sustained expression of IL-4 and IL-10.

Since cationic polymers are known to cause immune response, the muscle histology of anterior tibialis muscle was studied after injection of the formulations. Except for transient inflammation observed at week 1, there was no infiltration/inflammatory response seen in case of

either of the formulations. In contrast, the injection site muscles of the animals treated with FuGENE HD exhibited marked signs of inflammation at four and six weeks post-administration. At the end of six weeks, the histology of muscles of polymer treated animals was comparable to untreated control indicates that the delivery systems were biocompatible and safe to deliver through i.m. route.

5. SUMMARY, CONCLUSIONS, AND FUTURE DIRECTIONS

5.1. Summary and Conclusions

Gene therapy represents an exciting research area in recent drug delivery, since it is possible to treat/prevent many genetic disorders by simply inserting the correct copy of the defective gene into target cells. It offers multiple opportunities of curing diseases rather than just treating the symptoms of diseases or disorders. Safe and efficient delivery of gene and its subsequent stable expression in vivo are still major obstacles which need to be addressed before gaining clinical acceptance. Delivery of genetic cargo into target tissue in a safe and efficient manner has been a challenge for many years, and various viral and non-viral vectors are employed to facilitate such delivery. Though viral vectors are extremely efficient in targeting a specific cell type, their potential immunological and biocompatibility issues can greatly reduce their acceptance in clinical settings. Non-viral gene delivery vectors possess number of advantages over viral counterparts including, control over DNA release, stability, ease of modification by various functional groups to specifically target certain type of cells, and non-immunogenicity. Therefore, development of a safe, efficient, and biodegradable vector would overcome the obstacles towards greater success of gene therapy.

The goal of this study was to formulate a safe, nano-scale gene delivery vehicle, which can effectively transport the loaded DNA into the target cell without causing harmful side effects. We were particular in selecting cationic delivery vehicle with a good safety profile. Chitosan, a natural polymer, is cationic in nature, biocompatible and biodegradable, and has excellent safety record. However, its transfection efficiency is low, mainly due to its insoluble nature and inability to release the genetic cargo effectively inside the target cell. In our research, we have taken a novel approach to improve the transfection efficiency of chitosan. Chitosan was

depolymerized, and a series of fatty acid grafted low-molecular-weight chitosan (N-acyl LMWCs) were synthesized, purified and characterized for their physicochemical properties using analytical techniques such as infrared spectroscopy, elemental analysis and dynamic light scattering. The depolymerization process, and fatty acid grafting helped to improve the solubility of chitosan at physiological pH while retaining its essential cationic characteristics, and also helped reduce the overall charge density on chitosan, thereby facilitating the dissociation of the polymer from DNA in the cytosol. Moreover, grafting fatty acyl chain introduced hydrophobic regions in the polymer, leading to the formation of nanomicellar structures with better transfection efficiencies due to improved permeability characteristics.

The effects of acyl chain length and unsaturation on physicochemical characteristics and transfection efficiency of novel nanomicelles of N-acyl substituted low molecular weight chitosan (N-acyl LMWC) were studied. Initially, N-acyl LMWCs were synthesized by grafting LMWC with myristic (14:0), palmitic (16:0), stearic (18:0), and arachidic (20:0) acids. After transfection optimization, 18 carbon chain length grafts were selected, and N-acyl LMWCs were prepared with increasing unsaturation by grafting with oleic (18:1), linoleic (18:2), and linolenic (18:3) acids. N-acyl LMWCs were characterized for their structure using infrared spectroscopy and elemental analysis. The effect of DNA addition on size and zeta potential of N-acyl LMWCs was determined by dynamic light scattering. The N-acyl LMWCs formed cationic nanomicelles with average hydrodynamic size between 73 to 132 nm and DNA addition to nanomicelles led to minimal increase in the size. N-acyl LMWC/pDNA polyplex stability was confirmed using gel electrophoresis. N-acyl LMWC/pDNA polyplexes showed excellent stability on storage and could protect DNA from enzymatic degradation. The in vitro biocompatibility of the formulations was tested in Human Embryonic Kidney (HEK293) cells at concentrations ranging

from 1-2.5 mg/ml of polymers using an MTT assay. The formulations were well tolerated by the cells, and no change in percent cell viability was observed in case of cells treated with formulations prepared with N-acyl LMWCs.

Transfection efficiency of the derivative polymers was visualized in HEK293 cells using a plasmid encoding green fluorescent protein by confocal fluorescence microscopy, and was quantified using therapeutic plasmids encoding for interleukin-4 and interleukin-10. The in vitro transfection efficiencies of N-acyl LMWCs with 18:1 and 18:2 grafts (oleic and linoleic acid derivatives) were comparable with FuGENE HD (marketed non-viral vector) but were ~8-fold and 35-fold greater as compared to LMWC and naked DNA, respectively. To further evaluate the in vivo transfection efficiency of N-acyl LMWC to deliver pVIVO2-mIL4-mIL10 plasmid encoding interleukin-4 (IL-4) and interleukin-10 (IL-10) a multiple, low-dose streptozotocin induced diabetic mouse model was used. The ability of N-oleoyl and N-linoleoyl derivatives of LMWC to successfully deliver the therapeutic genes encoding for IL-4, IL-10, their physical mixtures (IL-4 + IL-10), and a bicistronic plasmid encoding for both IL-4 and IL-10 was studied in detail. The formulations containing pDNA/N-acyl LMWC polyplexes were injected intramuscularly at a single dose into the anterior tibialis muscle of mice, and the serum IL-4 and IL-10 levels were measured for 6 weeks by enzyme-linked immunosorbent assay (ELISA) and compared to that of control. Since INF-γ and TNF-α are among the cytokines that lead to enhanced β cell destruction, their levels were also measured throughout the study period as an indication of progression of insulitis. Further, the in vivo biocompatibility of the delivery system was determined by histological analysis of the muscle at various time points after injecting a single dose of delivery system.

The N-acyl LMWC (oleic and linoleic) led to significantly higher ($p<0.05$) expression of IL-4 and IL-10 and reduced the levels of blood glucose, TNF-α and IFN-γ, especially in animals treated with pVIVO2-mIL4-mIL10 bicistronic plasmid. The pancreas of pDNA/N-acyl LMWC polyplex treated animals exhibited protection from insulitis and the delivery systems were found to be biocompatible. No signs of chronic inflammation at the injection site were observed in histological studies. The expression of IL-4 and IL-10 was significantly ($p<0.05$) greater with the bicistronic plasmid which demonstrated the feasibility of bicistronic plasmid/N-acyl LMWC nanomicelles-based polyplexes as an efficient and biocompatible system for the prevention of autoimmune diabetes.

In conclusion, a series of N-acyl LMWC was synthesized in order to find the optimum chain length and degree of unsaturation in the N-acyl grafts and were evaluated for gene delivery application. This work demonstrates the development of a nanomicellar gene delivery system based on N-acyl LMWCs, which are efficient and biocompatible gene delivery vectors. Moreover, the administration of bicistronic pVIVO2-mIL4-mIL10 plasmid polyplexes can protect the pancreatic islets from insulitis, possibly due to the synergistic effect of IL-4 and IL-10 encoding plasmids.

5.2. Future Directions

Development of N-acyl LMWCs has opened an avenue for a variety of chitosan-based non-viral delivery systems. In this work, we have studied the grafting of fatty acyl groups ranging from 14 to 20 carbons in length and 0 to 3 double bonds in structure. Moreover, we used LMWC of ~ 6500 Da MW. The availability of chitosan in a variety of molecular weights, some of which can be rendered soluble, and the availability of fatty acids and other hydrophobic moieties with diverse structures and unsaturation can lead to some interesting possibilities. Even

the use of chitosan with higher MW in conjugation with a highly hydrophilic moiety can lead to formation of micelles with chitosan at the core. Such micelles would prevent the surface presentation of genetic cargo and can have potential in gene delivery. Attachment of targeting ligands can theoretically give target specificity to these micelles. However, the effect of dynamic nature of micelles (concentration-dependent formation/dissociation) will be interesting to study in these systems, especially if these micelles are not cross-linked in shell. Genetic cargo of the nanomicellar systems can be varied and these systems can be used to deliver DNA vaccines and siRNAs for preventive/therapeutic purposes. Micelles are previously used for delivery of various small molecules and hydrophobic drugs. N-acyl LMWCs can also be tested for such applications.

The use of a bicistronic plasmid encoding for IL-4 and IL-10 to prevent autoimmune insulitis in MLD-STZ induced diabetic mice is another important feature of this work. The bicistronic plasmid was significantly superior to the individual plasmids and their physical mixture. This demonstrated superiority of IL-4/IL-10 bicistronic plasmid can be exploited for treatment of various other autoimmune disorders. Grave's disease and Addison's disease involve lymphocytic infiltrations in thyroid and adrenal glands, respectively, and resemble the immunological pathogenesis of Type 1A diabetes (Devendra and Eisenbarth, 2003) and therefore, it would be interesting to see the efficacy of expression of IL-4 and IL-10 in these disease models.

6. LITERATURE CITED

Acharya, G., Shin, C.S., Vedantham, K., McDermott, M., Rish, T., Hansen, K., Fu, Y., and Park, K. (2010). A study of drug release from homogeneous PLGA microstructures. J Control Release *146*, 201–206.

Akinc, A., and Langer, R. (2002). Measuring the pH environment of DNA delivered using nonviral vectors: Implications for lysosomal trafficking. Biotechnol Bioeng *78*, 503–508.

Basarkar, A., Devineni, D., Palaniappan, R., and Singh, J. (2007). Preparation, characterization, cytotoxicity and transfection efficiency of poly(DL-lactide-co-glycolide) and poly(DL-lactic acid) cationic nanoparticles for controlled delivery of plasmid DNA. Int J Pharm *343*, 247–254.

Basarkar, A., and Singh, J. (2007). Nanoparticulate systems for polynucleotide delivery. Int J Nanomedicine *2*, 353–360.

Basarkar, A., and Singh, J. (2009). Poly (lactide-co-glycolide)-polymethacrylate nanoparticles for intramuscular delivery of plasmid encoding interleukin-10 to prevent autoimmune diabetes in mice. Pharm Res *26*, 72–81.

Baxter, A., Dillon, M., Anthony Taylor, K.D., and Roberts, G.A.F. (1992). Improved method for I.R. determination of the degree of N-acetylation of chitosan. Int J Biol Macromol *14*, 166–169.

Behr, J.-P. (1997). The proton sponge: a trick to enter cells the viruses did not exploit. Chimia *51*, 34–36.

Bhatia, K.S., and Singh, J. (1998). Synergistic effect of iontophoresis and a series of fatty acids on LHRH permeability through porcine skin. J Pharm Sci *87*, 462–469.

Bhatia, K.S., and Singh, J. (1999). Effect of linolenic acid/ethanol or limonene/ethanol and iontophoresis on the in vitro percutaneous absorption of LHRH and ultrastructure of human epidermis. Int J Pharm *180*, 235–250.

Bhattarai, N., Ramay, H.R., Chou, S.-H., and Zhang, M. (2006). Chitosan and lactic acid-grafted chitosan nanoparticles as carriers for prolonged drug delivery. Int J Nanomedicine *1*, 181–187.

Blau, H.M., and Springer, M.L. (1995). Muscle-mediated gene therapy. N Engl J Med *333*, 1554–1556.

Bontha, S., Kabanov, A.V., and Bronich, T.K. (2006). Polymer micelles with cross-linked ionic cores for delivery of anticancer drugs. J Control Release *114*, 163–174.

Borchard, G. (2001). Chitosans for gene delivery. Adv Drug Deliv Rev *52*, 145–150.

Borish, L.C., and Steinke, J.W. (2003). 2. Cytokines and chemokines. J Allergy Clin Immunol *111*, S460–S475.

Boussif, O., Zanta, M.A., and Behr, J.P. (1996). Optimized galenics improve in vitro gene transfer with cationic molecules up to 1000-fold. Gene Ther *3*, 1074–1080.

Bowman, W.J., Ofner, C.M., and Schott, H. (2005). Colloidal Dispersions. In Remington: The Science and Practice of Pharmacy, University of the Sciences in Philadelphia, ed. (Lippincott Williams & Wilkins), pp. 293–308.

Brendel, M., Hering, B., Schluz, A., and Bretzel, R. (1999). International Islet Transplant Registry Report (Giessen, Germany: Justus-Liebis University of Giessen).

Carter, J.D., Ellett, J.D., Chen, M., Smith, K.M., Fialkow, L.B., McDuffie, M.J., Tung, K.S., Nadler, J.L., and Yang, Z. (2005). Viral IL-10-mediated immune regulation in pancreatic islet transplantation. Mol Ther *12*, 360–368.

Chailertvanitkul, V.A., and Pouton, C.W. (2010). Adenovirus: a blueprint for non-viral gene delivery. Curr Opin Biotechnol *21*, 627–632.

Chao, Y.-C., Chang, S.-F., Lu, S.-C., Hwang, T.-C., Hsieh, W.-H., and Liaw, J. (2007). Ethanol enhanced in vivo gene delivery with non-ionic polymeric micelles inhalation. J Control Release *118*, 105–117.

Chernajovsky, Y., Gould, D.J., and Podhajcer, O.L. (2004). Gene therapy for autoimmune diseases: quo vadis? Nat Rev Immunol *4*, 800–811.

Choi, S.W., Lee, S.H., Mok, H., and Park, T.G. (2010). Multifunctional siRNA delivery system: polyelectrolyte complex micelles of six-arm PEG conjugate of siRNA and cell penetrating peptide with crosslinked fusogenic peptide. Biotechnol Prog *26*, 57–63.

Colonna, C., Conti, B., Perugini, P., Pavanetto, F., Modena, T., Dorati, R., and Genta, I. (2007). Chitosan glutamate nanoparticles for protein delivery: development and effect on prolidase stability. J Microencapsul *24*, 553–564.

Cox, N.J., Wapelhorst, B., Morrison, V.A., Johnson, L., Pinchuk, L., Spielman, R.S., Todd, J.A., and Concannon, P. (2001). Seven Regions of the Genome Show Evidence of Linkage to Type 1 Diabetes in a Consensus Analysis of 767 Multiplex Families. Am J Hum Genet *69*, 820–830.

Craig, M.E., Hattersley, A., and Donaghue, K.C. (2009). Definition, epidemiology and classification of diabetes in children and adolescents. Pediatr Diabetes *10 Suppl 12*, 3–12.

Croy, S.R., and Kwon, G.S. (2006). Polymeric micelles for drug delivery. Curr Pharm Des *12*, 4669–4684.

Dambies, L., Vincent, T., Domard, A., and Guibal, E. (2001). Preparation of chitosan gel beads by ionotropic molybdate gelation. Biomacromolecules *2*, 1198–1205.

Dass, C.R., and Choong, P.F.M. (2008). Chitosan-mediated orally delivered nucleic acids: a gutful of gene therapy. J Drug Target *16*, 257–261.

Daya, S., and Berns, K.I. (2008). Gene Therapy Using Adeno-Associated Virus Vectors. Clin Microbiol Rev *21*, 583–593.

Deng, J.-Z., Sun, Y.-X., Wang, H.-Y., Li, C., Huang, F.-W., Cheng, S.-X., Zhuo, R.-X., and Zhang, X.-Z. (2011). Poly(β-amino amine) cross-linked PEIs as highly efficient gene vectors. Acta Biomater.

Devendra, D., and Eisenbarth, G.S. (2003). 17. Immunologic endocrine disorders. J Allergy Clin Immunol *111*, S624–S636.

Diabetes Prevention Trial--Type 1 Diabetes Study Group (2002). Effects of insulin in relatives of patients with type 1 diabetes mellitus. N Engl J Med *346*, 1685–1691.

Ding, Y., and Xia, X.-H. (2006). Facile synthesis of hollow carbon nanospheres from hollow chitosan nanospheres. J Nanosci Nanotechnol *6*, 1101–1106.

Du, Y.-Z., Cai, L.-L., Li, J., Zhao, M.-D., Chen, F.-Y., Yuan, H., and Hu, F.-Q. (2011). Receptor-mediated gene delivery by folic acid-modified stearic acid-grafted chitosan micelles. Int J Nanomedicine *6*, 1559–1568.

Du, Y.-Z., Lu, P., Zhou, J.-P., Yuan, H., and Hu, F.-Q. (2010). Stearic acid grafted chitosan oligosaccharide micelle as a promising vector for gene delivery system: factors affecting the complexation. Int J Pharm *391*, 260–266.

Duceppe, N., and Tabrizian, M. (2010). Advances in using chitosan-based nanoparticles for in vitro and in vivo drug and gene delivery. Expert Opin Drug Deliv *7*, 1191–1207.

During, M.J. (1997). Adeno-associated virus as a gene delivery system. Adv Drug Deliv Rev *27*, 83–94.

Francis Suh, J.-K., and Matthew, H.W.. (2000). Application of chitosan-based polysaccharide biomaterials in cartilage tissue engineering: a review. Biomaterials *21*, 2589–2598.

Friedmann, T. (1992). A brief history of gene therapy. Nat Genet *2*, 93–98.

Ganguly, S., and Dash, A.K. (2004). A novel in situ gel for sustained drug delivery and targeting. Int J Pharm *276*, 83–92.

Gao, X., Kim, K.-S., and Liu, D. (2007). Nonviral gene delivery: what we know and what is next. Aaps J *9*, E92–104.

Gehl, J. (2008). Electroporation for drug and gene delivery in the clinic: doctors go electric. Methods Mol Biol *423*, 351–359.

Genta, I., Conti, B., Perugini, P., Pavanetto, F., Spadaro, A., and Puglisi, G. (1997). Bioadhesive microspheres for ophthalmic administration of acyclovir. J Pharm Pharmacol *49*, 737–742.

Gilhotra, R.M., and Mishra, D.N. (2008). Alginate-chitosan film for ocular drug delivery: effect of surface cross-linking on film properties and characterization. Pharmazie *63*, 576–579.

Gilmore, J.L., Yi, X., Quan, L., and Kabanov, A.V. (2008). Novel nanomaterials for clinical neuroscience. J Neuroimmune Pharmacol *3*, 83–94.

Goudy, K., Song, S., Wasserfall, C., Zhang, Y.C., Kapturczak, M., Muir, A., Powers, M., Scott-Jorgensen, M., Campbell-Thompson, M., Crawford, J.M., et al. (2001). Adeno-associated virus vector-mediated IL-10 gene delivery prevents type 1 diabetes in NOD mice. Proc Natl Acad Sci U S A *98*, 13913–13918.

Grenha, A., Seijo, B., Serra, C., and Remuñan-López, C. (2007). Chitosan nanoparticle-loaded mannitol microspheres: structure and surface characterization. Biomacromolecules *8*, 2072–2079.

Guo, X., and Huang, L. (2011). Recent Advances in Nonviral Vectors for Gene Delivery. Acc Chem Res.

Halama, A., Kuliński, M., Librowski, T., and Lochyński, S. (2009). Polymer-based non-viral gene delivery as a concept for the treatment of cancer. Pharmacol Rep *61*, 993–999.

Hashemi, M., Parhiz, B.H., Hatefi, A., and Ramezani, M. (2011). Modified polyethyleneimine with histidine-lysine short peptides as gene carrier. Cancer Gene Ther *18*, 12–19.

Heyes, J., Palmer, L., Bremner, K., and MacLachlan, I. (2005). Cationic lipid saturation influences intracellular delivery of encapsulated nucleic acids. J Control Release *107*, 276–287.

Hill, N., and Sarvetnick, N. (2002). Cytokines: promoters and dampeners of autoimmunity. Curr Opin Immunol *14*, 791–797.

Hoekstra, D., Rejman, J., Wasungu, L., Shi, F., and Zuhorn, I. (2007). Gene delivery by cationic lipids: in and out of an endosome. Biochem Soc Trans *35*, 68–71.

Hu, F.-Q., Zhao, M.-D., Yuan, H., You, J., Du, Y.-Z., and Zeng, S. (2006). A novel chitosan oligosaccharide-stearic acid micelles for gene delivery: properties and in vitro transfection studies. Int J Pharm *315*, 158–166.

Hu, H.-M., Zhang, X., Zhong, N.-Q., and Pan, S.-R. (2011). Study on Galactose-Poly(Ethylene Glycol)-Poly(l-Lysine) as Novel Gene Vector for Targeting Hepatocytes In Vitro. J Biomater Sci Polym Ed.

Ishii, T., Okahata, Y., and Sato, T. (2001). Mechanism of cell transfection with plasmid/chitosan complexes. Biochim Biophys Acta *1514*, 51–64.

Itaka, K., Osada, K., Morii, K., Kim, P., Yun, S.-H., and Kataoka, K. (2009). Polyplex nanomicelle promotes hydrodynamic gene introduction to skeletal muscle. J Control Release.

Jones, D.S., and Mawhinney, H.J. (2005). Chitosan. In Handbook of Pharmaceutical Excipients, R.C. Rowe, P.J. Sheskey, and S.C. Owen, eds. (Chicago: Pharmaceutical Press and American Pharmacists Association), pp. 159–162.

Kageyama, Y., Koide, Y., Uchijima, M., Nagata, T., Yoshida, A., Taiki, A., Miura, T., Nagafusa, T., and Nagano, A. (2004). Plasmid encoding interleukin-4 in the amelioration of murine collagen-induced arthritis. Arthritis Rheum *50*, 968–975.

Kalyanasundaram, K., and Thomas, J.K. (1977). Environmental effects on vibronic band intensities in pyrene monomer fluorescence and their application in studies of micellar systems. J Am Chem Soc *99*, 2039–2044.

Kasaai, M.R. (2008). A review of several reported procedures to determine the degree of N-acetylation for chitin and chitosan using infrared spectroscopy. Carbohydr Polym *71*, 497–508.

Kawasaki, E., Abiru, N., and Eguchi, K. (2004). Prevention of type 1 diabetes: from the view point of beta cell damage. Diabetes Res Clin Pract *66 Suppl 1*, S27–32.

Kay, M.A., Liu, D., and Hoogerbrugge, P.M. (1997). Gene therapy. Proc Natl Acad Sci U S A *94*, 12744–12746.

Kiang, T., Wen, J., Lim, H.W., and Leong, K.W. (2004). The effect of the degree of chitosan deacetylation on the efficiency of gene transfection. Biomaterials *25*, 5293–5301.

Kim, S., Kim, J.Y., Huh, K.M., Acharya, G., and Park, K. (2008). Hydrotropic polymer micelles containing acrylic acid moieties for oral delivery of paclitaxel. J Control Release *132*, 222–229.

Kim, S.W. (2011). Polymeric Gene Delivery for Diabetic Treatment. Diabetes Metab J *35*, 317–326.

Koch, S., Pohl, P., Cobet, U., and Rainov, N.G. (2000). Ultrasound enhancement of liposome-mediated cell transfection is caused by cavitation effects. Ultrasound Med Biol *26*, 897–903.

Köping-Höggård, M., Tubulekas, I., Guan, H., Edwards, K., Nilsson, M., Vårum, K.M., and Artursson, P. (2001). Chitosan as a nonviral gene delivery system. Structure-property relationships and characteristics compared with polyethylenimine in vitro and after lung administration in vivo. Gene Ther *8*, 1108–1121.

Koynova, R., Tenchov, B., Wang, L., and MacDonald, R.C. (2009). Hydrophobic moiety of cationic lipids strongly modulates their transfection activity. Mol Pharm *6*, 951–958.

Kumar, M.N.V.R., Muzzarelli, R.A.A., Muzzarelli, C., Sashiwa, H., and Domb, A.J. (2004). Chitosan chemistry and pharmaceutical perspectives. Chem Rev *104*, 6017–6084.

Kuo, W., Huang, H., and Huang, Y. (2010). Polymeric micelles comprising stearic acid-grafted polyethyleneimine as nonviral gene carriers. J Nanosci Nanotechnol *10*, 5540–5547.

Kurita, K. (2006). Chitin and chitosan: functional biopolymers from marine crustaceans. Mar Biotechnol *8*, 203–226.

Lappalainen, K., Jääskeläinen, I., Syrjänen, K., Urtti, A., and Syrjänen, S. (1994). Comparison of cell proliferation and toxicity assays using two cationic liposomes. Pharm Res *11*, 1127–1131.

Lawrie, A., Brisken, A.F., Francis, S.E., Wyllie, D., Kiss-Toth, E., Qwarnstrom, E.E., Dower, S.K., Crossman, D.C., and Newman, C.M. (2003). Ultrasound-enhanced transgene expression in vascular cells is not dependent upon cavitation-induced free radicals. Ultrasound Med Biol *29*, 1453–1461.

Lee, M., Ko, K.S., Oh, S., and Kim, S.W. (2003). Prevention of autoimmune insulitis by delivery of a chimeric plasmid encoding interleukin-4 and interleukin-10. J Control Release *88*, 333–342.

Lee, M., Koh, J.J., Han, S.-O., Ko, K.S., and Ki, S.W. (2002a). Prevention of autoimmune insulitis by delivery of interleukin-4 plasmid using a soluble and biodegradable polymeric carrier. Pharm Res *19*, 246–249.

Lee, M.-J., Cho, S.-S., You, J.-R., Lee, Y., Kang, B.-D., Choi, J.S., Park, J.-W., Suh, Y.-L., Kim, J.-A., Kim, D.-K., et al. (2002b). Intraperitoneal gene delivery mediated by a novel cationic liposome in a peritoneal disseminated ovarian cancer model. Gene Ther *9*, 859–866.

Lee, M.-S., Kwon, H.-J., and Kim, H.S. (2012). Macrophages from Nonobese Diabetic Mouse Have a Selective Defect in IFN-γ but Not IFN-α/β Receptor Pathway. J Clin Immunol Epub Ahead of Print.

Lee, S.H., Kim, S.H., and Park, T.G. (2007). Intracellular siRNA delivery system using polyelectrolyte complex micelles prepared from VEGF siRNA-PEG conjugate and cationic fusogenic peptide. Biochem Biophys Res Commun *357*, 511–516.

Li, L., Yi, Z., Tisch, R., and Wang, B. (2008). Immunotherapy of type 1 diabetes. Arch Immunol Ther Exp *56*, 227–236.

Lim, Y.B., Han, S.O., Kong, H.U., Lee, Y., Park, J.S., Jeong, B., and Kim, S.W. (2000). Biodegradable polyester, poly[alpha-(4-aminobutyl)-L-glycolic acid], as a non-toxic gene carrier. Pharm Res *17*, 811–816.

Liu, H., Du, Y., Wang, X., and Sun, L. (2004). Chitosan kills bacteria through cell membrane damage. Int J Food Microbiol *95*, 147–155.

Lu, Q.L., Bou-Gharios, G., and Partridge, T.A. (2003). Non-viral gene delivery in skeletal muscle: a protein factory. Gene Ther *10*, 131–142.

MacLaughlin, F.C., Mumper, R.J., Wang, J., Tagliaferri, J.M., Gill, I., Hinchcliffe, M., and Rolland, A.P. (1998). Chitosan and depolymerized chitosan oligomers as condensing carriers for in vivo plasmid delivery. J Control Release *56*, 259–272.

MacNeil, I.A., Suda, T., Moore, K.W., Mosmann, T.R., and Zlotnik, A. (1990). IL-10, a Novel Growth Cofactor for Mature and Immature T Cells. J Immunol *145*, 4167–4173.

Makadia, H.K., and Siegel, S.J. (2011). Poly Lactic-co-Glycolic Acid (PLGA) as Biodegradable Controlled Drug Delivery Carrier. Polymers *3*, 1377–1397.

Mandke, R., Basarkar, A., and Singh, J. (2012). Nanoparticles, interleukin-10 and autoimmune diabetes. In Nanotechnology and Nanomedicine in Diabetes, L.-A. Le, R.J. Hunter, and V.R. Preedy, eds. (New York: Science Publishers/CRC Press), p. In Press.

Mandke, R., and Singh, J. (2012a). Cationic Nanomicelles for Delivery of Plasmids Encoding Interleukin-4 and Interleukin-10 for Prevention of Autoimmune Diabetes in Mice. Pharm Res *29*, 883–897.

Mandke, R., and Singh, J. (2012b). Effect of acyl chain length and unsaturation on physicochemical properties and transfection efficiency of N-acyl-substituted low-molecular-weight chitosan. J Pharm Sci *101*, 268–282.

Manoharan, C., and Singh, J. (2009). Insulin loaded PLGA microspheres: effect of zinc salts on encapsulation, release, and stability. J Pharm Sci *98*, 529–542.

Mao, S., Shuai, X., Unger, F., Simon, M., Bi, D., and Kissel, T. (2004). The depolymerization of chitosan: effects on physicochemical and biological properties. Int J Pharm *281*, 45–54.

Mao, S., Sun, W., and Kissel, T. (2010). Chitosan-based formulations for delivery of DNA and siRNA. Adv Drug Deliv Rev *62*, 12–27.

Marsich, E., Borgogna, M., Donati, I., Mozetic, P., Strand, B.L., Salvador, S.G., Vittur, F., and Paoletti, S. (2008). Alginate/lactose-modified chitosan hydrogels: a bioactive biomaterial for chondrocyte encapsulation. J Biomed Mater Res A *84*, 364–376.

Martin, A.N. (1993). Colloids. In Physical Pharmacy: Physical Chemical Principles in the Pharmaceutical Sciences, (Baltimore, USA: Lippincott Williams & Wilkins), pp. 393–422.

Masotti, A., and Bordi, F. (2008). A novel method to obtain chitosan/DNA nanospheres and a study of their release properties. Nanotechnology *19*, 055302.

Medi, B.M., and Singh, J. (2003). Electronically facilitated transdermal delivery of human parathyroid hormone (1-34). Int J Pharm *263*, 25–33.

Medi, B.M., and Singh, J. (2008). Delivery of DNA into skin via electroporation. Methods Mol Biol *423*, 225–232.

Miller, A.C., Bershteyn, A., Tan, W., Hammond, P.T., Cohen, R.E., and Irvine, D.J. (2009). Block copolymer micelles as nanocontainers for controlled release of proteins from biocompatible oil phases. Biomacromolecules *10*, 732–741.

Milligan, E.D., Langer, S.J., Sloane, E.M., He, L., Wieseler-Frank, J., O'Connor, K., Martin, D., Forsayeth, J.R., Maier, S.F., Johnson, K., et al. (2005). Controlling pathological pain

by adenovirally driven spinal production of the anti-inflammatory cytokine, interleukin-10. Eur J Neurosci *21*, 2136–2148.

Moghimi, S.M., Symonds, P., Murray, J.C., Hunter, A.C., Debska, G., and Szewczyk, A. (2005). A two-stage poly(ethylenimine)-mediated cytotoxicity: implications for gene transfer/therapy. Mol Ther *11*, 990–995.

Molnar, M.J., Gilbert, R., Lu, Y., Liu, A.-B., Guo, A., Larochelle, N., Orlopp, K., Lochmuller, H., Petrof, B.J., Nalbantoglu, J., et al. (2004). Factors Influencing the Efficacy, Longevity, and Safety of Electroporation-Assisted Plasmid-Based Gene Transfer into Mouse Muscles. Mol Ther *10*, 447–455.

Nafee, N.A., Boraie, M.A., Ismail, F.A., and Mortada, L.M. (2003). Design and characterization of mucoadhesive buccal patches containing cetylpyridinium chloride. Acta Pharm *53*, 199–212.

Nakase, I., Akita, H., Kogure, K., Gräslund, A., Langel, Ü., Harashima, H., and Futaki, S. (2011). Efficient Intracellular Delivery of Nucleic Acid Pharmaceuticals Using Cell-Penetrating Peptides. Acc Chem Res.

Nishikawa, M., Takakura, Y., and Hashida, M. (2005). Pharmacokinetics of Plasmid DNA-Based Non-viral Gene Medicine. In Non-Viral Vectors for Gene Therapy, Second Edition: Part 1, (Academic Press), pp. 47–68.

Nishimura, S., Kohgo, O., Kurita, K., and Kuzuhara, H. (1991). Chemospecific manipulations of a rigid polysaccharide: syntheses of novel chitosan derivatives with excellent solubility in common organic solvents by regioselective chemical modifications. Macromolecules *24*, 4745–4748.

Nunthanid, J., Laungtana-Anan, M., Sriamornsak, P., Limmatvapirat, S., Puttipipatkhachorn, S., Lim, L.Y., and Khor, E. (2004). Characterization of chitosan acetate as a binder for sustained release tablets. J Control Release *99*, 15–26.

Oh, K.T., Oh, Y.T., Oh, N.-M., Kim, K., Lee, D.H., and Lee, E.S. (2009). A smart flower-like polymeric micelle for pH-triggered anticancer drug release. Int J Pharm *375*, 163–169.

Panchagnula, R., Dhanikula, R.S., and Dhanikula, A.B. (2006). An ex vivo characterization of Paclitaxel loaded chitosan films after implantation in mice. Curr Drug Deliv *3*, 287–297.

Pang, S.-W., Park, H.-Y., Jang, Y.-S., Kim, W.-S., and Kim, J.-H. (2002). Effects of charge density and particle size of poly(styrene/(dimethylamino)ethyl methacrylate) nanoparticle for gene delivery in 293 cells. Colloids Surf B Biointerfaces *26*, 213–222.

Panigrahi, L., Pattnaik, S., and Ghosal, S.K. (2004). Design and characterization of mucoadhesive buccal patches of salbutamol sulphate. Acta Pol Pharm *61*, 351–360.

Park, K. (2009). Dendrimer polymeric micelles for enhanced photodynamic cancer treatment. J Control Release *133*, 171.

Peacocke, A.R., and Pritchard, N.J. (1968). The ultrasonic degradation of biological macromolecules under conditions of stable cavitation. II. Degradation of deoxyribonucleic acid. Biopolymers *6*, 605–623.

Pelletier, M., Babin, J., Tremblay, L., and Zhao, Y. (2008). Investigation of a new thermosensitive block copolymer micelle: hydrolysis, disruption, and release. Langmuir *24*, 12664–12670.

Peng, S.-F., Yang, M.-J., Su, C.-J., Chen, H.-L., Lee, P.-W., Wei, M.-C., and Sung, H.-W. (2009). Effects of incorporation of poly(gamma-glutamic acid) in chitosan/DNA complex nanoparticles on cellular uptake and transfection efficiency. Biomaterials *30*, 1797–1808.

Pitt, W.G., Husseini, G.A., and Staples, B.J. (2004). Ultrasonic drug delivery--a general review. Expert Opin Drug Deliv *1*, 37–56.

Prabaharan, M. (2008). Review paper: chitosan derivatives as promising materials for controlled drug delivery. J Biomater Appl *23*, 5–36.

Prabaharan, M., and Mano, J.F. (2005). Chitosan-based particles as controlled drug delivery systems. Drug Deliv *12*, 41–57.

Prochazkova, S., Vårum, K.M., and Ostgaard, K. (1999). Quantitative determination of chitosans by ninhydrin. Carbohydr Polym *38*, 115–122.

Rao, N.M., and Gopal, V. (2006). Cell biological and biophysical aspects of lipid-mediated gene delivery. Biosci Rep *26*, 301–324.

Rastogi, S.K., and Singh, J. (2004). Iontophoretic enhancement of leuprolide acetate by fatty acids, limonene, and depilatory lotions through porcine epidermis. Pharm Dev Technol *9*, 341–348.

Ribeiro, S., Hussain, N., and Florence, A.T. (2005). Release of DNA from dendriplexes encapsulated in PLGA nanoparticles. Int J Pharm *298*, 354–360.

Richardson, S.C., Kolbe, H.V., and Duncan, R. (1999). Potential of low molecular mass chitosan as a DNA delivery system: biocompatibility, body distribution and ability to complex and protect DNA. Int J Pharm *178*, 231–243.

Riesz, P., and Kondo, T. (1992). Free radical formation induced by ultrasound and its biological implications. Free Radic Biol Med *13*, 247–270.

Rinaudo, M. (2006). Chitin and chitosan: Properties and applications. Prog Polym Sci *31*, 603–632.

Robbins, P.D., and Ghivizzani, S.C. (1998). Viral vectors for gene therapy. Pharmacol Ther *80*, 35–47.

Rudzinski, W.E., and Aminabhavi, T.M. (2010). Chitosan as a carrier for targeted delivery of small interfering RNA. Int J Pharm *399*, 1–11.

Ruponen, M., Honkakoski, P., Rönkkö, S., Pelkonen, J., Tammi, M., and Urtti, A. (2003). Extracellular and intracellular barriers in non-viral gene delivery. J Control Release *93*, 213–217.

Sanghvi, Y.S. (2011). A Status Update of Modified Oligonucleotides for Chemotherapeutics Applications. Curr Protoc Nucleic Acid Chem *46*, 4.1.1–4.1.22.

Sanjeevi, C.B., Falorni, A., Kockum, I., Hagopian, W.A., and Lernmark, Å. (1996). HLA and Glutamic Acid Decarboxylase in Human Insulin-dependent Diabetes Mellitus. Diabet Med *13*, 209–217.

Sato, T., Ishii, T., and Okahata, Y. (2001). In vitro gene delivery mediated by chitosan. effect of pH, serum, and molecular mass of chitosan on the transfection efficiency. Biomaterials *22*, 2075–2080.

Sawant, R.M., Hurley, J.P., Salmaso, S., Kale, A., Tolcheva, E., Levchenko, T.S., and Torchilin, V.P. (2006). “SMART” drug delivery systems: double-targeted pH-responsive pharmaceutical nanocarriers. Bioconjug Chem *17*, 943–949.

Schloot, N.C., Hanifi-Moghaddam, P., Goebel, C., Shatavi, S.V., Flohé, S., Kolb, H., and Rothe, H. (2002). Serum IFN-gamma and IL-10 levels are associated with disease progression in non-obese diabetic mice. Diabetes Metab Res Rev *18*, 64–70.

Schmidt, R.E., Dorsey, D.A., Beaudet, L.N., Frederick, K.E., Parvin, C.A., Plurad, S.B., and Levisetti, M.G. (2003). Non-obese diabetic mice rapidly develop dramatic sympathetic neuritic dystrophy: a new experimental model of diabetic autonomic neuropathy. Am J Pathol *163*, 2077–2091.

Shapiro, A.M.J. (2011). Strategies toward single-donor islets of Langerhans transplantation. Curr Opin Organ Transplant *16*, 627–631.

Shiraishi, S., Arahira, M., Imai, T., and Otagiri, M. (1990). Enhancement of dissolution rates of several drugs by low-molecular chitosan and alginate. Chem Pharm Bull *38*, 185–187.

Singh, S., and Singh, J. (1990). Transdermal delivery of drugs by phonophoresis: a review. Drug Des Delivery *5*, 259–265.

Sloane, E.M., Soderquist, R.G., Maier, S.F., Mahoney, M.J., Watkins, L.R., and Milligan, E.D. (2009). Long-term control of neuropathic pain in a non-viral gene therapy paradigm. Gene Ther *16*, 470–475.

Smith, A.E. (1995). Viral Vectors in Gene Therapy. Annu Rev Microbiol *49*, 807–838.

Smith, M.B., and March, J. (2001). March's Advanced Organic Chemistry: Reactions, Mechanisms, and Structure, 5th Edition (Wiley-Interscience).

Summerford, C., and Samulski, R.J. (1998). Membrane-Associated Heparan Sulfate Proteoglycan Is a Receptor for Adeno-Associated Virus Type 2 Virions. J Virol *72*, 1438–1445.

Sun, X., and Zhang, N. (2010). Cationic polymer optimization for efficient gene delivery. Mini Rev Med Chem *10*, 108–125.

Synowiecki, J., and Al-Khateeb, N.A. (2003). Production, properties, and some new applications of chitin and its derivatives. Crit Rev Food Sci Nutr *43*, 145–171.

Tahara, K., Sakai, T., Yamamoto, H., Takeuchi, H., Hirashima, N., and Kawashima, Y. (2011). Improvements in Transfection Efficiency with Chitosan Modified Poly(DL-lactide-co-glycolide) Nanospheres Prepared by the Emulsion Solvent Diffusion Method, for Gene Delivery. Chem Pharm Bull *59*, 298–301.

Tarner, I.H., and Fathman, C.G. (2001). Gene therapy in autoimmune disease. Curr Opin Immunol *13*, 676–682.

The Expert Committee on the Diagnosis and Classification of Diabetes Mellitus (2003). Report of the Expert Committee on the Diagnosis and Classification of Diabetes Mellitus. Diabetes Care *26*, S5–S20.

Thomas, M., Ge, Q., Lu, J.J., Chen, J., and Klibanov, A. (2005). Cross-linked Small Polyethylenimines: While Still Nontoxic, Deliver DNA Efficiently to Mammalian Cells in Vitro and in Vivo. Pharm Res *22*, 373–380.

de la Torre, L.G., Rosada, R.S., Trombone, A.P.F., Frantz, F.G., Coelho-Castelo, A.A.M., Silva, C.L., and Santana, M.H.A. (2009). The synergy between structural stability and DNA-binding controls the antibody production in EPC/DOTAP/DOPE liposomes and DOTAP/DOPE lipoplexes. Colloids Surf B Biointerfaces *73*, 175–184.

Tousignant, J.D., Gates, A.L., Ingram, L.A., Johnson, C.L., Nietupski, J.B., Cheng, S.H., Eastman, S.J., and Scheule, R.K. (2000). Comprehensive analysis of the acute toxicities induced by systemic administration of cationic lipid:plasmid DNA complexes in mice. Hum Gene Ther *11*, 2493–2513.

Tran, V.-T., Karam, J.-P., Garric, X., Coudane, J., Benoît, J.-P., Montero-Menei, C.N., and Venier-Julienne, M.-C. (2012). Protein-loaded PLGA-PEG-PLGA microspheres: A tool for cell therapy. Eur J Pharm Sci *45*, 128–137.

Ubaidulla, U., Sultana, Y., Ahmed, F.J., Khar, R.K., and Panda, A.K. (2007). Chitosan phthalate microspheres for oral delivery of insulin: preparation, characterization, and in vitro evaluation. Drug Deliv *14*, 19–23.

Verma, I.M., and Somia, N. (1997). Gene therapy - promises, problems and prospects. Nature *389*, 239–242.

Vilquin, J.T., Kennel, P.F., Paturneau-Jouas, M., Chapdelaine, P., Boissel, N., Delaère, P., Tremblay, J.P., Scherman, D., Fiszman, M.Y., and Schwartz, K. (2001). Electrotransfer of naked DNA in the skeletal muscles of animal models of muscular dystrophies. Gene Ther *8*, 1097–1107.

Vivès, E. (2005). The XIIth International Symposium on Recent Advances in Drug Delivery Systems. Expert Opin Drug Deliv *2*, 597–601.

Wang, G., and Lu, J. (2010). Retrovirus-mediated delivery of an IL-4 receptor antagonist inhibits allergic responses in a murine model of asthma. Sci China Life Sci *53*, 1215–1220.

Wang, X., Yao, J., Zhou, J.P., Lu, Y., and Wang, W. (2010). Synthesis and evaluation of chitosan-graft-polyethylenimine as a gene vector. Pharmazie *65*, 572–579.

Wang, Y., Wang, L.-S., Goh, S.-H., and Yang, Y.-Y. (2007). Synthesis and characterization of cationic micelles self-assembled from a biodegradable copolymer for gene delivery. Biomacromolecules *8*, 1028–1037.

Wasungu, L., and Hoekstra, D. (2006). Cationic lipids, lipoplexes and intracellular delivery of genes. J Control Release *116*, 255–264.

Wells, D.J. (2009). Electroporation and ultrasound enhanced non-viral gene delivery in vitro and in vivo. Cell Biol Toxicol.

Wen, J., Mao, H.-Q., Li, W., Lin, K.Y., and Leong, K.W. (2004). Biodegradable polyphosphoester micelles for gene delivery. J Pharm Sci *93*, 2142–2157.

Whittaker, G.R. (2003). Virus nuclear import. Adv Drug Deliv Rev *55*, 733–747.

Wiethoff, C.M., and Middaugh, C.R. (2003). Barriers to nonviral gene delivery. J Pharm Sci *92*, 203–217.

World Health Organization Consultation (1999). Definition, Diagnosis and Classification of Diabetes Mellitus and its Complications.

Wu, K.K., and Huan, Y. (2008). Streptozotocin-Induced Diabetic Models in Mice and Rats. Curr Protoc Pharmacol *40*, 5.47.1–5.47.14.

Yao, J., Fan, Y., Du, R., Zhou, J., Lu, Y., Wang, W., Ren, J., and Sun, X. (2010). Amphoteric hyaluronic acid derivative for targeting gene delivery. Biomaterials *31*, 9357–9365.

Ye, Y.-Q., Yang, F.-L., Hu, F.-Q., Du, Y.-Z., Yuan, H., and Yu, H.-Y. (2008). Core-modified chitosan-based polymeric micelles for controlled release of doxorubicin. Int J Pharm *352*, 294–301.

Yi, Y., Jong Noh, M., and Hee Lee, K. (2011). Current Advances in Retroviral Gene Therapy. Curr Gene Ther *11*, 218–228.

Yoksan, R., and Chirachanchai, S. (2008). Amphiphilic chitosan nanosphere: studies on formation, toxicity, and guest molecule incorporation. Bioorg Med Chem *16*, 2687–2696.

You, J., Hu, F.-Q., Du, Y.-Z., and Yuan, H. (2007). Polymeric micelles with glycolipid-like structure and multiple hydrophobic domains for mediating molecular target delivery of paclitaxel. Biomacromolecules *8*, 2450–2456.

Yu, H., Deng, C., Tian, H., Lu, T., Chen, X., and Jing, X. (2011). Chemo-Physical and Biological Evaluation of Poly(L-lysine)-Grafted Chitosan Copolymers Used for Highly Efficient Gene Delivery. Macromol Biosci *11*, 352–361.

Yuan, H., Lu, L.-J., Du, Y.-Z., and Hu, F.-Q. (2011). Stearic acid-g-chitosan polymeric micelle for oral drug delivery: in vitro transport and in vivo absorption. Mol Pharm *8*, 225–238.

Zhang, J., Li, S., and Li, X. (2009a). Polymeric nano-assemblies as emerging delivery carriers for therapeutic applications: a review of recent patents. Recent Pat Nanotechnol *3*, 225–231.

Zhang, L., Nguyen, T.L.U., Bernard, J., Davis, T.P., Barner-Kowollik, C., and Stenzel, M.H. (2007). Shell-cross-linked micelles containing cationic polymers synthesized via the RAFT process: toward a more biocompatible gene delivery system. Biomacromolecules *8*, 2890–2901.

Zhang, S., Xu, Y., Wang, B., Qiao, W., Liu, D., and Li, Z. (2004). Cationic compounds used in lipoplexes and polyplexes for gene delivery. J Control Release *100*, 165–180.

Zhang, X., Oulad-Abdelghani, M., Zelkin, A.N., Wang, Y., Haîkel, Y., Mainard, D., Voegel, J.-C., Caruso, F., and Benkirane-Jessel, N. (2009b). Poly(l-lysine) nanostructured particles for gene delivery and hormone stimulation. Biomaterials.

Zhang, Z.-L., Shen, S.-X., Lin, B., Yu, L.-Y., Zhu, L.-H., Wang, W.-P., Luo, F.-H., and Guo, L.-H. (2003). Intramuscular injection of interleukin-10 plasmid DNA prevented autoimmune diabetes in mice. Acta Pharmacol Sin *24*, 751–756.

Zhu, C., Jung, S., Luo, S., Meng, F., Zhu, X., Park, T.G., and Zhong, Z. (2010). Co-delivery of siRNA and paclitaxel into cancer cells by biodegradable cationic micelles based on PDMAEMA-PCL-PDMAEMA triblock copolymers. Biomaterials *31*, 2408–2416.